

**NTNU Norwegian University of Science and Technology**  
**Faculty of Natural Sciences and Technology**  
**Department of Chemical Engineering**

**MASTER THESIS 2011**

**PROTEIN-NANOPARTICLE CONSTRUCTS  
FOR INTRACELLULAR DELIVERY**

**by**

**Jordi Piella Bagaria**

**Advisor:** Wilhelm Robert Glomm

**Date:** 18<sup>th</sup> February 2011





## MASTER THESIS 2011

<b>Title:</b> Protein-nanoparticle constructs for intracellular delivery	<b>Subject (3-4 words):</b> Chemical Engineering. Colloid and polymer chemistry.
<b>Author:</b> Jordi Piella Bagaria	<b>Carried out through:</b> Ugelstad Laboratory. Colloid and Polymer Chemistry group.
<b>Advisor:</b> Wilhelm Robert Glomm <b>Co-advisors:</b> Sondre Volden and Sina Maria Lystvet <b>External advisor:</b>	<u><b>Number of pages</b></u>  <b>Main report:</b> 85 <b>Appendices:</b> 16
<b>ABSTRACT</b>  <b>Goal of work (key words):</b>  Study of the interaction between proteins and polymer nanoparticles, the understanding of which is essential for a range of applications in medicine, cosmetics, etc. Two kinds of monodisperse anionic polymer nanoparticles, with and without epoxy surface groups, were synthesized by soap free emulsion polymerization. Bovine serum albumin was then immobilized at different pH values. Finally, zeta potential of protein-nanoparticle constructs at various pH, fluorescence spectra, ITC measurements and unfolding studies using urea of immobilized protein were carried out to analyze conformational changes in the protein.  <b>Conclusions and recommendations (key words):</b>  Bovine serum albumin immobilization and degree of unfolding was found to be strongly affected by pH and matching of the global protein and polymer nanoparticle charges. The results suggested that polymer nanoparticles with epoxy groups offered covalent binding with stronger attachment and larger conformational isomerisation than polymer nanoparticles without epoxy groups. A more detailed study is necessary to describe thoroughly the process of Bovine serum albumin adsorption on the surface of a polymer nanoparticle.	
<p style="text-align: center;"><b>I declare that this is an independent work according to the exam regulations of the Norwegian University of Science and Technology</b></p> <p style="text-align: center;"><b>Date and signature:</b> .....</p>	



## Preface

This thesis is the result of six month of research carried out in the Department of Chemical Engineering at the Norwegian University of Science and Technology. Associate Professor Wilhelm Robert Glomm of Colloid and Polymer Chemistry group oversaw the study with the aid of Post doctor Sondre Volden and PhD student Sina Maria Lystvet. The experimental work was performed in the Ugelstad Laboratory between August 2010 and February 2011, and it aims to contribute to research conducted by the group on polymer nanoparticles in aqueous colloidal systems.

Piella Bagaria, Jordi

Norwegian University of Science and Technology, Trondheim

February 2011



## Thanks

I would like to express my appreciation to my supervisor: Dr. Wilhelm Robert Glomm. Thanks for giving me the opportunity to be part of your research group. My gratitude also goes to all people who are working in the Ugelstad Laboratory and Paper and Fibre Research Institute, there are not enough words to describe your excellent work. Special thanks to Sondre Volden and Sina Maria Lystvet for their time, patience and understanding. Thanks for your advice and for acting as a mentor of me. Also thanks to Lisbeth Helene Blekkan Roel, the department is very fortunate to have you. Thanks for all your attentions. Finally, my appreciation to Thomas Tichelkamp for continuing my research.





## Abstract

Proteins are essential parts of organisms and participate in virtually every process within cells. Being able to control them, deliver them to specific locations or give them desired functionalities and properties pave the way to numerous applications, including use as biosensors, within biocatalysis and biomedical devices. Thus, protein monitoring is extremely relevant and one of the most important challenges in biotechnology. One way to protein monitoring could be related to understanding and controlling their tertiary structure. It is known that the properties and functions of proteins are determined by their conformation. Therefore being able to induce conformational changes in proteins may be a possible way to control them.

In the present study, a series of experiments with Bovine serum albumin (BSA) were performed, analyzed and described to understand the adsorption, unfolding behaviour and conformational changes in tertiary structure of this protein when it was attached and spread on the surface of different types of polymer nanoparticles. BSA was selected since it is well-studied protein, the most abundant protein in plasma and one of the most used model protein. Three kinds of negatively charged monodisperse polymer nanoparticles were elaborated by soap free emulsion polymerization: two different size polymer nanoparticles with epoxy groups and one type of polymer nanoparticles without epoxy groups. Finally, size and zeta potential measurements of corresponding BSA-polymer nanoparticle constructs, fluorescence spectroscopy, isothermal titration calorimetry (ITC) and unfolding studies with urea were carried out to study BSA conformational isomerisation in immobilized polymer nanoparticle systems. All experiments were done at three different pH conditions; 3.8, 7.4 and 9, corresponding to conditions below and above the isoelectric point (pI) of BSA.

BSA immobilization and degree of unfolding was found to be strongly affected by pH and matching of the global protein and polymer nanoparticle charges. The results suggested that polymer nanoparticles with epoxy groups offered covalent binding with stronger attachment and larger conformational isomerisation than polymer nanoparticles without epoxy groups. These changes occurred to the largest degree at pH 7.4. This may be due to a high number of epoxy groups conjugated with amino groups of the protein. At pH 3.8 it seemed that the attachment of BSA was highest but without relevant structural alterations while at pH 9 it was in an intermediate level of adsorption and structural changes. Finally, there were no appreciable discrepancies between different size polymer nanoparticles.



# Index

<b>PREFACE</b>	<b>1</b>
<b>THANKS</b>	<b>3</b>
<b>ABSTRACT</b>	<b>5</b>
<b>INDEX</b>	<b>7</b>
<b>ABBREVIATIONS</b>	<b>9</b>
<b>1. INTRODUCTION</b>	<b>11</b>
<b>2. ADSORPTION OF PROTEINS ON THE SURFACE OF POLYMER NANOPARTICLES</b>	<b>15</b>
2.1. Polymer nanoparticles.....	15
2.2. Proteins .....	16
2.2.1. Protein stability.....	17
2.2.2. BSA protein.....	18
2.3. Adsorption of protein on nanoparticles with associated structural changes .....	21
<b>3. CHARACTERIZATION TECHNIQUES</b>	<b>23</b>
3.1. Dynamic light scattering .....	23
3.1.1. Dynamic light scattering as a particle size determination tool.....	24
3.1.2. Laser Doppler electrophoresis as a zeta potential determination tool .....	26
3.2. Fluorescence spectroscopy .....	29
3.2.1. Intrinsic fluorescence of proteins .....	31
3.2.2. ANS: fluorescent probe for the characterization of proteins .....	32
3.3. Isothermal titration calorimetry .....	34
<b>4. EXPERIMENTAL PROCEDURE</b>	<b>37</b>
4.1. Polymer nanoparticles synthesized by soap free emulsion polymerization .....	37
4.1.1. Polymer nanoparticles with epoxy groups on the surface.....	37
4.1.2. Polymer nanoparticles without epoxy groups on the surface.....	38
4.1.3. Concentration of polymer nanoparticles .....	38
4.1.4. Characterization of polymer nanoparticles.....	39
4.2. BSA immobilization on polymer nanoparticles.....	39
4.2.1. Characterization of BSA-polymer nanoparticle constructs.....	39

4.3. Unfolding of immobilized BSA using urea in combination with ANS.....	40
4.4. Isothermal titration calorimetry.....	40
<b>5. RESULTS AND DISCUSSION</b> .....	<b>41</b>
5.1. Synthesis and characterization of monodisperse polymer nanoparticles ...	41
5.1.1. Polymer nanoparticles with epoxy groups .....	41
5.1.2. Polymer nanoparticle without epoxy groups .....	47
5.2. BSA immobilization on monodisperse polymer nanoparticles. Zeta potential titration measurements. ....	49
5.2.1. Zeta potential titration measurements of BSA-polymer nanoparticle constructs .....	50
5.3. Fluorescence spectroscopy of BSA-polymer nanoparticle constructs.....	54
5.3.1. Intrinsic and extrinsic fluorescence of polymer nanoparticles.....	54
5.3.2. Intrinsic and extrinsic fluorescence of BSA.....	57
5.3.3. Intrinsic and extrinsic fluorescence of BSA-polymer nanoparticle constructs. Particles size comparison. ....	59
5.3.4. Intrinsic and extrinsic fluorescence of BSA-polymer nanoparticle constructs. Surface group comparison. ....	66
5.4. Unfolding studies of immobilized BSA using urea in combination with ANS .....	70
5.4.1. Extrinsic fluorescence of BSA-polymer nanoparticle constructs in urea solution .....	70
5.5. Studies of immobilized BSA by isothermal titration calorimetry .....	73
<b>CONCLUSIONS</b> .....	<b>77</b>
<b>BIBLIOGRAPHY</b> .....	<b>79</b>
Bibliographic referencing.....	79
<b>APPENDICES</b> .....	

## Abbreviations

Ammonium persulfate	AMS
Bovine Serum Albumin	BSA
Derjaguin-Landau-Verwey-Overbeek theory	DLVO
Divinyl benzene	DVB
Double Layer theory	DL
Dynamic Light Scattering	DLS
Electrical Double Layer theory	EDL
Electrophoresis Light Scattering	ELS
Glycidyl methacrylate	GMA
Human $\alpha$ -lactalbumin made lethal to tumor cells	HAMLET
Isothermal Titration Calorimetry	ITC
Light Scattering	LS
Molten globule	MG
Photon Correlation Spectroscopy	PCS
Polymer nanoparticle	PP
Quasi-elastic Light Scattering	QELS
Styrene monomer	St
$\alpha$ -lactalbumin	$\alpha$ -La
8-anilino-1-naphthalenesulfonic acid	ANS



# 1. Introduction

*The principles of physics, as far as I can see, do not speak against the possibility of manoeuvring things atom by atom. It is not attempt the violate any laws; It is something, in principle, that can be done; but in practice, it has not been done because we are too big.*

*Richard Feynman, 1959.*

Nanotechnology can be understood as the capacity to control and manipulation of matter at an atomic scale [1]. The idea of nanotechnology was first presented by Richard Feynman in 1959 in a lecture “There is Plenty Room at the Bottom” [2] and nowadays molecular nanotechnology lead us to creating molecules individually atom by atom. Some scientists have speculated that the fabrication of a single working assembler, so-called bottom-up approach, would explode to fill every need and utterly changes our way of live [3]. Bottom-up fabrication may in the future offer rather important advantages in comparison than the top-down category current used. Fabrication of nanostructures fall without exception into this focusing as the construction principle mimics biological systems by using the order factors that are innate in the system [4]. A precondition for nanostructure preparation by self-assembly way is the availability of sufficiently stable building blocks, which have to be well characterized and uniform with respect to size and shape. They should ideally also be chemically versatile enough to undergo a range of reaction, allowing them to fulfil various structural and/or functional roles within the final system. The capacity of three-dimensional assembly, simplicity in the experimental atomic scale and the potential for economical and environmentally friendly mass assembly are some of the prospective points in nanotechnology. Unfortunately, assemblers based on mechanosynthesis currently remain in the beginning, and there are also some mentions of potentially huge problems with these assemblers, sometimes referring to the catastrophic end result as the *Grey goo problem*<sup>1</sup>.

---

<sup>1</sup> The term was first used by nanotechnology pioneer Eric Drexler in his book *Nanotechnology: the rise of the machines created* (Engines of Creation, 1986). It refers to a hypothetical end of the world that involves molecular nanotechnology in which out-of-control self-replicating robots consume all matter on Earth while building more of themselves.

Another new concept that in the last half century has acquired an important role in the new development science is biotechnology introduced by Karl Ereki in 1919 [5]. Biotechnology uses the ready-made assemblers available in living cells to build thousands of custom-designed molecules to atomic specifications, including the construct of new assemblers [6]. This has led to innumerable applications, including commercial production of drugs, elegant methods for diagnosing and curing infections as genetic diseases, and engineering of organisms for specialized tasks such as bioremediation and disease resistance. However, the biological functioning is based on cells and their components, which are to be found in an atomic scale size. For this reason biotechnology and nanotechnology are two branches of science that need inevitably to advance in parallel. In this sense the term of bionanotechnology is a key factor [7][8][9]. Today, individual bionanomachines are being designed and created to perform specific nanoscale tasks, such as the targeting of cancer cells or the solution of a simple computational task. As bionanotechnology matures, it is possible to redesign the bimolecular machinery of the cell to perform large-scale tasks for human health and technology.

Protein is the most versatile of natural biomolecules and one of the most important macromolecules in bionanotechnology [8]. Powerful methods for creating custom proteins are available but the major current limitation is basic knowledge. Among other interesting qualities, it is known that changes in protein conformation, interpreted in general terms, regulate their function, such as specific interaction with other molecules, catalytic activity, and signal transduction [10]-[13]. We need to understand and be able to predict the process by which proteins fold into stable, globular structures and how its conformational changes are related to their functionality. Protein conformation and the folding and unfolding mechanisms could lead us to monitoring protein functions and use this knowledge to find out the cause of some diseases and diseases cure. Alzheimer's, Parkinson's, Huntington's are related to protein misfolding and are some of many medical areas in which proteins play an important role. It is well known that conformational changes can be induced by protein association to a surface, whether the surface is a membrane or other entity such as a nanoparticle [14]-[18]. Nowadays the use of nanoparticles paves the way to understand chemical and physical governing protein factors [19]. Nanoparticles small size allows interacting with proteins (Figure 1.1) [20]-[23]. The set of themes deals with how reduced dimensionality of proteins by adsorption to a surface of nanoparticles can be used as folding templates for polypeptides [24].





been successfully used such as ANS, intrinsic fluorescence or probes covalently bound to study it **[34 and bibliography]**.

The objective of the project is to develop a stable support for BSA immobilization, as well as evaluate conformational changes of immobilized proteins in buffered aqueous media at different pH. Herein, two kinds of negatively charged monodisperse polymer nanoparticles, with and without epoxy surface groups, at different sizes were synthesized by soap free emulsion polymerization. BSA was then immobilized at different protein concentrations and pH values. Finally, zeta potential of protein-polymer nanoparticle constructs at various pH, fluorescence spectra, isothermal titration calorimetry (ITC) measurements of immobilized protein (section 3 *Characterization techniques*) and unfolding urea studies were performed to analyze conformation changes of BSA protein.

## 2. Adsorption of proteins on the surface of polymer nanoparticles

The present section aims to provide the necessary information to understand protein-nanoparticle interactions and thus to give a coherent explanation for the results obtained during the project BSA-polymer nanoparticle constructs. The study of proteins and the use of nanoparticles is not a coincidence; both have a specific molecular structure and determined features that allowing them to be compatible with each other. Nanoparticles can induce conformational change to proteins which is really important as already been mentioned. Therefore it is first necessary to know the properties and behaviour of these two molecules.

### 2.1. Polymer nanoparticles

A nanoparticle is defined as a small body with a definite mass having one or more dimensions the order of some hundred nanometers or less that behaves as a whole unit in terms of its transport and properties<sup>1</sup>. Nanoparticles may or may not exhibit size-related properties that differ significantly from those observed in fine particles or bulk materials [19]. The use of nanoparticles has gained popularity in recent years, and the numbers of applications is increasing dramatically as science progress, especially in medicine [35][36]. Despite the need to understand the response of biological systems to these particles, for the moment there are few overall conceptual frameworks and remains unclear the mechanisms that govern biological processes at nanoscale [37]. Nanoparticles, when entering the body become coated with proteins, which means that there exist some interactive capability and this may have several effects on the proteins. [20]-[24] [38]-[40]. The proteins might become partially unfolded upon adsorption, producing conformational alterations with subsequent changes in function, activity, etc [37][38][40].

---

<sup>1</sup> Rigorously a nanoparticle can not have any dimension greater than 100 nm. In contrast, the term "polymer particles" usually is associated with particles larger than a micron. As the particles used in the present project fall between the two categories in terms of size, but largely behave like nano-species moreso than micro-species, they are defined as nanoparticles.

Nanoparticles are usually found as a colloid suspension, where the dispersed solid phase is regarded as the internal phase and the continuous phase as the external phase. So stability nanoparticles are subjected to colloidal systems laws<sup>1</sup>. Gold nanoparticles, silver nanoparticles, nanoclusters or polymer nanoparticles are some types of nanoparticles with interesting properties [20]-[23].

In the present project only one type of polymer nanoparticles were used, composed predominantly by styrene (St) and glycidyl methacrylate (GMA). Since the pioneer synthetic method of hollow polymer particles, made of latex, was patented in 1981 [41], there has been an exhaustive research and development effort to extend the synthetic techniques and application areas [42]-[45]. Because in some cases the diameter of such polymer particles have to be less than 1  $\mu\text{m}$  to become useful in bionanotechnology, interfacial polymerization, dispersion and suspension processes leading to voided morphology were eliminated and only emulsion polymerization was left [46]. A surfactant-free heterogeneous polymerization in water solvent is soap-free emulsion polymerization, which is usually applied to the production of sub-micrometer-sized polymer particles, as in the present case [47]-[49]. The application of this polymerization method to the synthesis of sub-micrometer-sized particles can overcome the problems of the conventional methods [47][48]. Using soap free emulsion polymerization, it is possible to synthesize monodisperse polymer nanoparticles with different diameters (100 nm-800 nm) and some reacting groups can be introduced on the surface in order to functionalize the polymer nanoparticles [50].

## 2.2. Proteins

Proteins are biological macromolecules made up by linear chains called polypeptides, which in turn are formed by 20 different types of amino acids combined in different order. Amino acids are linked together through a peptide bond; a covalent binding between amino group of one amino acid and carboxylic group of another. The sequence and type of amino acids describe the primary structure of proteins. The peptide chain is then folded up on itself to make secondary structure, where the most common models are  $\alpha$ -helix and  $\beta$ -sheet. When

---

<sup>1</sup> Detailed information on the stability of nanoparticles in colloidal systems can be found in (Glomm *et al.* 2005) where it is explained the forces presents in the suspension and the mechanism regulating the stability, successfully defined by DLVO theory. In the present case it is not the aim of the project but it is a necessary background.

dissolved in water, the secondary structure bends and fold in such a way that the hydrophobic groups are buried inside the core of the protein, away from water, while the hydrophilic groups turn outwards giving the spatial form of the structure. This last one is called tertiary structure and among other things decides the function of proteins [10]-[13] [51]-[53]. The tertiary structure of proteins is stabilized by disulfide bonds between cysteines, hydrogen bonds between side chains, ionic interactions between side chains, van der Waals interactions between side chains and the hydrophobic effect. Finally, some proteins are composed for more than one polypeptide and the spatial arrangement of these several polypeptides forms the quaternary structure.

Almost always proteins are surrounding by hydrophilic atmosphere like water. In this situation, the interior of proteins consist mostly of non-polar amino acids, where there are in contact with other non-polar moities, while the polar side chains are forced away from the core to the surface, allowing a lower free energy by interactions and giving stability. This bipolarity in the structure is one of the most important properties of proteins.

### 2.2.1. Protein stability

Protein stability is quantitatively described by the standard Gibbs energy change, involved in unfolding the unique from three dimensional structure to randomly coiled polypeptide chains [54]. Native state is the functional shape that posses a minimum of free energy and is related to how tertiary structure is folded. In this state proteins coil up to compact rigid structure and play an important role in a wide range of bioprocess. Instead denatured state is free and flexible, results in an entropic loss with vital changes in its features and unfavourable functional capacity.

The assumption is that protein can not only exists as either as set of folded conformation or set of unfolded conformations, which are separate by energy barriers [55]-[58]. From refolding studies, the existence of intermediates has been experimentally established and the intermediate conformations have been called the molten globule (MG) states [59]-[61]. Molten globules are partially folded states of proteins which are generally believed to mimic structures formed during the folding process [61]. MG state conserves native-like secondary structure content but without the tightly packed protein interior which leads an enormous flexibility and range of motion, keeping almost intact functional capacity [62]. Conformational change between the native form and the MG state is reversible [63]. Its properties are intermediate between those of native and unfolded protein molecules: it is compact and has a number of important features of the native secondary structure and of the native overall architecture but has only traces of the detailed native tertiary structure [63]. Stable MG state gives the possibility to use interfaces as two-dimensional folding template for proteins because of their greater flexibility [14]-[18]. Thus elucidate the

structure and the interactions which stabilize molten globule states is a key issue in protein folding. The mechanism and pathway of conformational change depend on the amino acid sequence of the protein, solvation of hydrophobic side chains, steric hindrance, interaction with other amino acid residues or other organic compounds, hydrogen bonding, covalent disulfide bonding, and the folding behaviour of helix and sheet microdomains [50]. Unfortunately, their dynamic nature, conformational heterogeneity and sometimes limited solubility make direct structural studies extremely difficult [64].

In case of BSA numerous studies have been done to determine its structure, its properties and even reversible conformational isomerisation with changes in pH (section 2.2.2 *BSA protein*). These studies allow us to ensure that the nanoparticles might be a good tool to monitor BSA conformations and features [14].

### 2.2.2. BSA protein

Bovine serum albumin (BSA) is a serum albumin protein and one of the most widely studied proteins [65]-[70]. BSA is commonly used in different biochemical applications because of its stability, its lack of effect in many biochemical reactions, and its low cost, since large quantities of it can be readily purified from bovine blood, a subproduct of the cattle industry [32].  $\alpha$ -La have similar pI to that of BSA (pI 4.8), but with a much smaller molecular mass (14,200 Daltons) than BSA (67,000 Daltons) [71]. Maybe  $\alpha$ -La is the most well-situated protein that could cause apoptosis in tumoral cells in combination with nanoparticles but it is quite expensive. Therefore BSA is selected as model protein, although the number of surface lysines and the conformations of each protein could be different.

Table 2.1. Physical properties of BSA [72].

Number of amino acids residues	585
Molecular weight	66.776 Da
Isoelectric point in water at 25 °C	4.8
Dimensions	140 X 40 X 40 Å <sup>3</sup> (prolate ellipsoid where a = b < c)

BSA, as all albumins, is characterized by a low content of tryptophan and methionine and a high content of cystine and the charged amino acids, aspartic and glutamic acids, lysine, and arginine. The glycine and isoleucine content of BSA are lower than in the average protein [73]. Albumins structure is predominantly  $\alpha$ -helical with the remaining polypeptide occurring in turns and extended or flexible regions between subdomains with no beta-sheets [74]. The global structure of BSA is made up of three homologous areas (I, II and III) which can be divided into 9 loops by 17 disulphide bonds (Figure 2.1). Domains I and II and domains II and III are connected through helical extensions, creating the two longest helices in albumin.

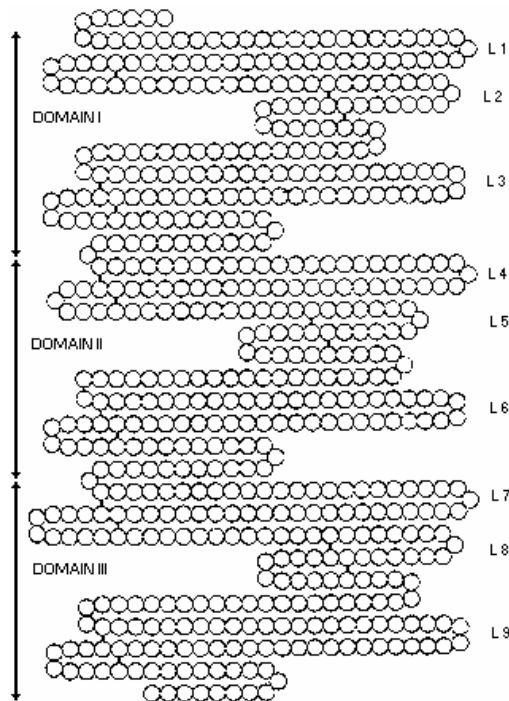


Figure 2.1. BSA domains. Adapted from [70]; <<http://www.friedli.com/research/PhD/chapter5a.html>> [15/01/11].

None of the disulphide bonds was accessible to reducing agents in the pH range 5-7, but became progressively available as the pH was raised or lowered. Therefore, the disulphides in albumin were protected at neutral pH from reducing agents [75]. This is also apparent in the structure, which shows that the majority of disulphides are well protected and most are not readily accessible to solvent. During unfolding, the conformation of some of the disulphide bonds changes. The albumin molecule is not uniformly charged within the primary structure, although the tertiary structure seems fairly uniform [74].

BSA undergoes reversible conformational isomerisation with changes in pH [33][76]. Table 2.2 and Figure 2.2 shows the conformations and its respectively transitions.

Table 2.2. Relationship of isomeric forms of bovine serum albumin [33].

	<b>E form</b>	trans	<b>F form</b>	trans	<b>N form</b>	trans	<b>B form</b>	trans	<b>A form</b>
pH		2.7		4.3		8		10	
Name	Expanded		Fast		Normal		Basic		Aged
% $\alpha$ -helix	35		45		55		48		48

The N-F transition involves the unfolding of domain III. The F form is characterized by a dramatic increase in viscosity, much lower solubility, and a significant loss in helical content. At pH values lower than 4, albumin undergoes another expansion with a loss of the helical extension between domains. This expanded form is known as the (E) form which has an increased intrinsic viscosity, and a rise in the hydrodynamic axial ratio from about 4 to 9. At pH 9, albumin changes conformation to the basic form (B). If solutions of albumin are

maintained at pH 9 and low ionic strength at 3°C for 3 to 4 days, another isomerisation occurs which is known as the (A) form.

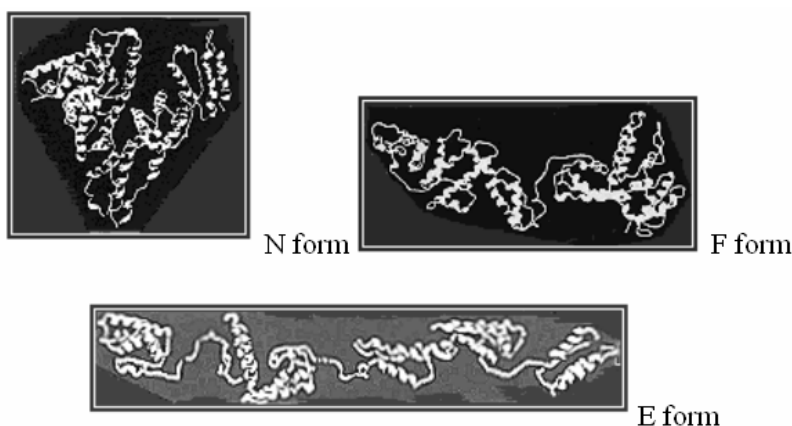


Figure 2.2. BSA domains [70]. Adapted from [74]; <<http://www.friedli.com/research/PhD/chapter5a.html>> [15/01/11].

BSA has two tryptophan residues that possess (Figure 2.3) intrinsic fluorescence [77]. Trp-134 in the first domain and Trp-212 in the second domain. Trp-212 is located within a hydrophobic binding pocket of the protein and Trp-134 is located on the surface of the molecule.

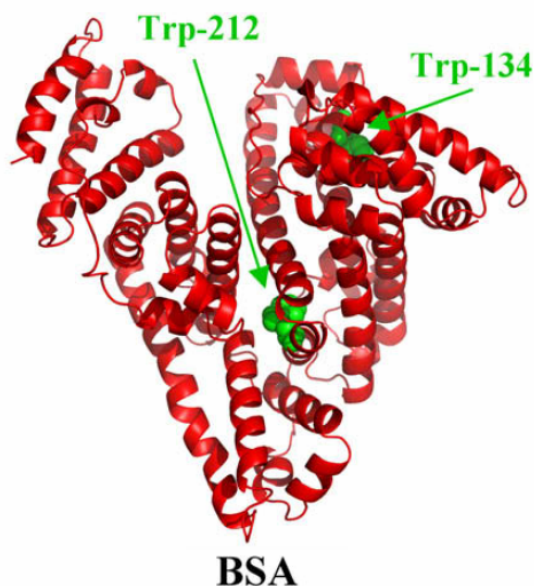


Figure 2.3. Three-dimensional structures of BSA with tryptophan residues in green colour. Adapted from [78].

BSA binds free fatty acids, other lipids and flavour compounds, which can alter the denaturation of the protein. Isolated BSA has been reported to be a very functional protein. Perhaps, the most outstanding property of albumin is its ability to bind reversibly an incredible variety of ligands [32].



## 2.3. Adsorption of protein on nanoparticles with associated structural changes

Protein adsorption (Figure 2.4) is an interesting but complicated process [79]. Perhaps the most intriguing and at the same time the most evasive question is the extent to which the molecule undergoes structural alterations. Additional involved subprocess are the incorporation (or exclusion) of protons and other ions, dehydration of (parts of) the surface and the protein molecule, and the assessment of van der Waals and electrostatic interactions among many others [80][81].

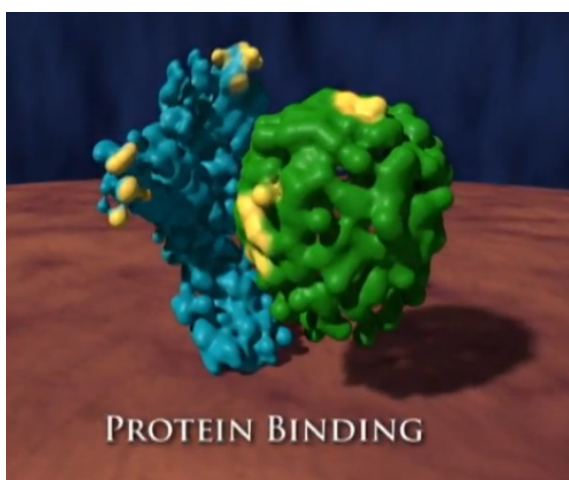


Figure. 2.4. BSA-nanoparticle construct. BSA is represented in blue and nanoparticle in green. Adapted from <<http://www.tainstruments.com/main.aspx?siteid=11&id=263&n=1>> [17/01/11].

Adsorption of protein at the interface is assumed to pass for three steps: diffusion process towards the surface (1), attachment on the surface (2) and spreading on the surface (3) [20]. Depending on protein-nanoparticle interaction, it can reach the last step or simply stay in the first (attached with partial unfolding, attached or not attached). If the conditions are favourable, the adsorption on nanoparticle might affect the tertiary structure of protein, and thereby also the function, but without completely denaturation [13][82]. For this reason how interaction with interfaces affect the tertiary structure is a relevant factor to study protein-nanoparticle interaction, in the concrete case of this project BSA-polymer nanoparticle interaction.

In addition to van der Waals and dispersive forces, when a protein attaches to a surface of any kind two of the most important adhesion source are: electrostatic bonding and covalent bonding [83][84]. The electrostatic bonding is due to attractive/repulsive forces between the electrostatic charges of the surface groups of the protein (pH-dependent) and the oppositely charge of surface nanoparticles groups. Depending on the charge density and the sign of each charge the attachment can be stronger or weaker. On the other hand, if nanoparticles

are functionalized with some specific groups it is enable protein immobilization through covalent bonding. Lysine, arginine and histidine residues are often used as covalent junction points. The advantageous of covalent bound is a much firmer immobilization, but by contrast chemical reactions undergoes concomitant structural alterations. In any case it is necessary keep a reasonable dichotomy between retaining a desired functions and securing sufficient immobilization without denaturation [85]. The spreading of a protein involves the exposure of hydrophobic groups to the surface and forces some functional groups away from the core of protein so that they can interact with the surface causing partly denaturation [20]. The final solution is to find a balance between the two types of attachment, electrostatic and covalent.

While surface charge and surface groups of polymer nanoparticles define the source of attachment, the size is also an important parameter. The curvature of the immobilizing agent can influence how much the protein unfolds on the surface. To choose a correct type of nanoparticles according to the protein is a key success factor.

### 3. Characterization techniques

This section seeks to highlight some of the most used analytical techniques in the characterization of nanoparticles and protein-nanoparticle construct, in particular those that have been used in this work. However, the purpose is not to give a detailed description of each one, but only the background needed to understand the methods. In cases where further information is required, some important bibliography sources are cited.

The main analytical techniques to study the features of nanoparticles are: light scattering techniques for the hydrodynamic diameter and zeta potential; fluorescence spectroscopy respect to conformational changes in proteins; and isothermal titration calorimetry to study the reaction kinetics (enthalpy, stoichiometry, equilibrium constant) of protein adsorption.

#### 3.1. Dynamic light scattering

The microstructure of colloidal suspension is commonly studied by scattering experiments. A considerable amount of theoretical background is needed to extract information about the microstructure from the measured scattered intensity, Doppler shifts in the frequency, Raman effect in scattered light and to understand such microstructure in terms of properties of the suspended particles and the solvent [86][87].

Scattering (Figure 3.1) is a general physical process in which some forms of radiation changes its direction and, on occasion, also its frequency after interacting with the medium. In light scattering (LS) process when a light beam incises in a determinate frame the total number of photons is unaltered, but the number going in forward direction decreases due to redirection of light from scattering interaction. In other words, when light impinges on matter, the electric field of the light induces an oscillating polarization of electrons in the molecules and these molecules provide a secondary source of light and subsequently scattering light. The frequency shifts, the angular distribution, the polarization and the intensity of scattered light are determined by the size, shape and molecular interaction in the scattering material [88].

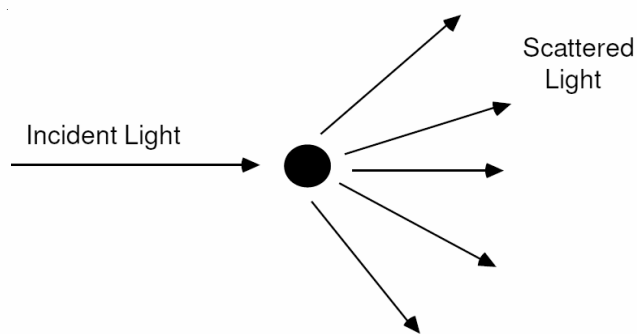


Figure 3.1. Light scattering phenomena. Adapted from [89].

With the aid of electrodynamics and theory dependent of statistical mechanics, light scattering give information about the structure and molecular dynamics of the scattering medium through the light scattering characteristics of the system<sup>1</sup> [88].

Analytical techniques mentioned below, which were used in the present project are based on quasi-elastic light scattering [90]. Zetasizer Nano ZS (Malvern) was the machine employed in the project.

### 3.1.1. Dynamic light scattering as a particle size determination tool

Dynamic light scattering (DLS), Photon correlation spectroscopy (PCS) or Quasi-elastic light scattering (QELS) is one of the most used methods to determinate the size of particles [91][92]. DLS uses the principles of Brownian motion, Rayleigh theory and Mie theory to determine the size and molecular weight of particles in a suspension.

Colloidal sized particles<sup>2</sup> in a liquid undergo random motion, also called Brownian motion, owing to multiple collisions with the thermally driven molecules of the liquid. In DLS, the

---

<sup>1</sup> Classical light elastic scattering theory was derived by Lord Rayleigh (Rayleigh *et al.* 1881). New theories have been developed to apply a correction for size effect. Rayleigh-Gans-Debye theory and Mie theory (Jennings *et al.* 1965) involves extrapolation terms and they are an important tools for analysing results in colloid solutions and the fundament of different analytical techniques.

<sup>2</sup> A colloid is a substance in the range of nm- $\mu$ m dispersed evenly throughout another substance. A colloidal system consists of two separate phases: a *dispersed phase* (or *internal phase*), which is usually solid, and a *continuous phase* (or *dispersion medium*), which is usually liquid.

speed at which the particles are diffusing due to Brownian motion is measured. This is done by measuring (Figure 3.2) the rate at which the intensity of the scattered light fluctuates when it is detected using a suitable optical arrangement. DLS measures Brownian motion and relates this to the size of the particles due to the bombardment by the solvent molecules that surrounded them.

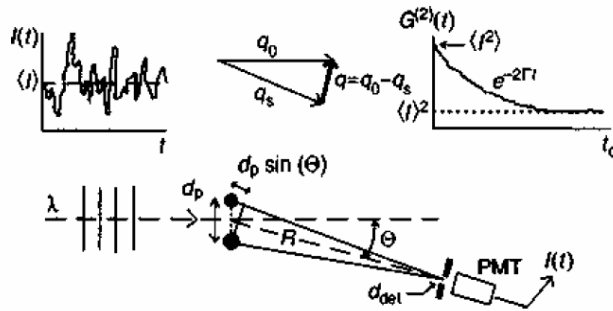


Figure 3.2. The basis of DLS:  $q$  is the scattering vector,  $\lambda$  the wavelength of beam,  $d_p$  the particle distance,  $\theta$  the angle between light beam and detected scattered light, and  $G$  the correlation equation. Adapted from [91].

The relative positions and orientations of the particles undergo Gaussian random changes in time (Brownian motion). The result is a total intensity (Figure 3.3) which fluctuates in time from zero to double the single particle scattered intensity.

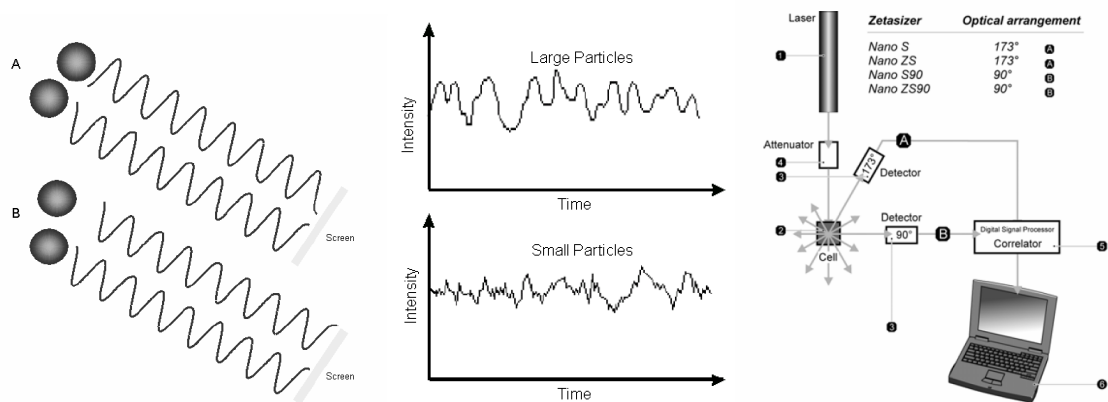


Figure 3.3. On the left side, the observed signal depends on the phase addition of the scattered light falling on the detector. Adapted from [93]. On the middle, fluctuation in the intensity detected from the scattering light in different size particle solutions. Adapted from [93]. On the right side, optical configurations of the Zetasizer Nano series for dynamic light scattering measurements. Adapted from [93].

In a real experiment there are perhaps  $10^{10}$  particles in the scattering volume, and the total intensity is the result from the interference between the scattered fields from all of these. As a consequence, the intensity  $I(t, q)$ , as seen by the detector, will be a randomly fluctuating signal as shown. The small particles cause the intensity to fluctuate more rapidly than the large ones [91][92].

Radiating a monochromatic light beam, such as a laser, onto a solution with spherical particles in Brownian motion causes a fluctuation in the intensity of the light. This change is related to the size of the particle, hence it is possible to compute the sphere size distribution and give a description of the particle's motion. Note that the diameter that is measured in DLS is value that refers to how a particle diffuses within a fluid so it is referred to as a hydrodynamic diameter. The diameter that is obtained by this technique is the diameter of a sphere that has the same transitorial diffusion coefficient as the particle [92].

### 3.1.2. Laser Doppler electrophoresis as a zeta potential determination tool

Surface charge of particles [94] is one of the most important parameters in the characterization of colloid solutions and can be understood as the electric charge present in the interface between two media. Among other things, surface charge of particles in a colloid solution determinates the electrostatic force interaction between particles and between a particle with its environment, affect the stability of the colloidal system determined by Derjaguin-Landau-Verwey-Overbeek theory (DLVO) and it is a essential monitoring tool (bonding, attachment, modification, delivery...) of any substance in aqueous colloidal systems.

The most important reference about the surface charge of particles in a colloidal solution is the zeta potential value, which can be measured using different techniques, and it is an approximation of the real surface charge, as this parameter is not possible to measure. More specifically zeta potential is the electrostatic potential that exists between the separations of layers surrounding the particle [95]. Colloidal stability in aqueous system is related with zeta potential. DLVO theory proposes that the stability of aqueous colloidal system in aqueous media is determined by the sum of these electrical repulsive and van der Waals attractive forces that exist between particles as they approach each other due to the Brownian motion they are undergoing [96][97]. This theory suggests that an energy barrier resulting from the repulsive force prevents two particles approaching one another and adhering together. But if the particles collide with sufficient energy to overcome that barrier, the attractive force will pull them into contact where they adhere strongly and irreversibly together. The zeta potential indicates the degree of repulsion between adjacent, similarly charged particles in a dispersion. For molecules and particles that are small enough, a high zeta potential will confer stability and the solution or dispersion will resist aggregation. When the potential is low, attraction exceeds repulsion and the dispersion will break and flocculate.

#### 1.1.1.1. Double layer theory (DL) and Zeta potential

The model of the double layer (DL), also called electrical double layer (EDL), is used to describe the ionic atmosphere around a charged colloid in an aqueous media and explain how electrical repulsion forces (induced by ions-counterions interaction in the system)

operate as a function of distance from the surface of the colloid [95]. It is possible to understand this model as a sequence of steps that occurs around negatively charged colloid, when the ions that neutralize its charge are attracted to it (Figure 3.4). Theory about DL is reviewed in J. Lyklema's *Fundamentals of Interface and Colloid Science IV*, which uses the fundamentals of the earliest DL model developed for Helmholtz (Helmoltz *et al.* 1853) in combination with Gouy-Chapman-Stern improvements [98]. Necessary background that it is needed to understand the fundamentals of theory can be found in [94][95][99]. The potential drop and the distance from the colloid is an indicator of the repulsive force between the colloids as a function of the distance to which these forces come into play.

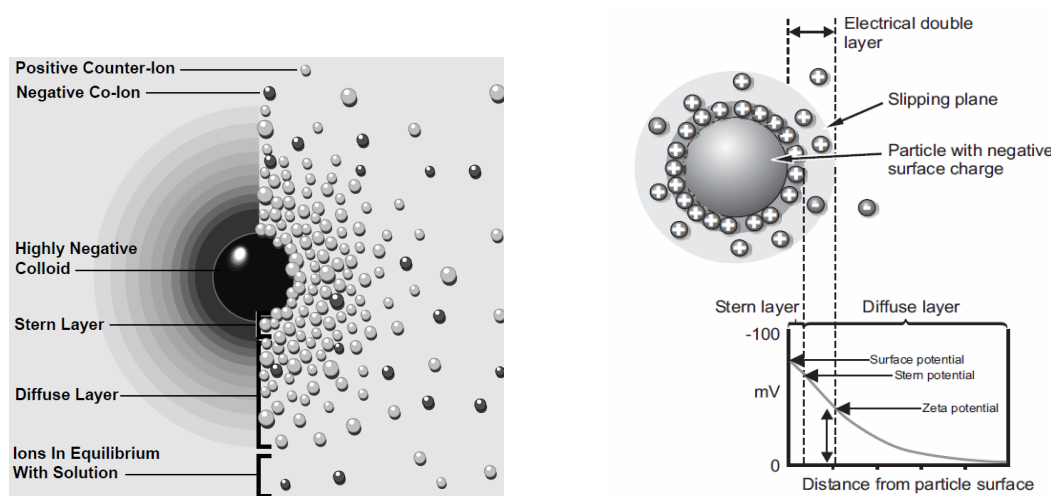


Figure 3.4. On the left side, two ways to visualize the Double Layer. The left view shows the change in charge density around the colloid. The right shows the distribution of positive and negative ions around the charged colloid. Adapted from [102]. On the right side, representation of zeta potential. Adapted from [102].

A point of particular interest is the potential that brings together the diffuse and Stern layers. This potential is known as the zeta potential, which is important because it can be measured in a very simple, while the surface charge and potential can not be measured, and it is a good approximation of its. The zeta potential is an effective way to control the behaviour of the colloid as it indicates changes in the surface potential and the repulsive forces between colloids.

#### 1.1.1.2. Electrophoresis and Doppler Effect

Electrophoresis [95] is the movement of charged colloidal particles, immersed in a liquid, under the influence of an external electric field. The electrophoretic velocity is the velocity during electrophoresis. The electrophoretic mobility is the magnitude of the velocity divided by the magnitude of the electric field strength and is direct function of zeta potential. [100]. The mobility is counted positive if the particles move towards lower potential (negative electrode) and negative in the opposite case. For uniform and not very strong electric field,

a linear relationship exists between electrophoretic velocity and the applied field<sup>1</sup> (equation 3.1 and 3.2).

$$v_e = u_e(\zeta) \cdot E \quad (\text{equation 3.1})$$

$$u_e = \frac{\varepsilon_{rs} \cdot \varepsilon_0}{\eta} \cdot \zeta \quad (\text{equation 3.2})$$

Where  $v_e$  is the electrophoretic velocity [ $\text{m s}^{-1}$ ];  $u_e$  is the electrophoretic mobility [ $\text{m}^2 \text{s}^{-1} \text{V}^{-1}$ ];  $E$  is the electric field strength [V];  $\zeta$  is the zeta potential [V];  $\varepsilon_{rs}$  is the relative permittivity of the dispersion medium;  $\varepsilon_0$  is the electric permittivity of vacuum [ $\text{F m}^{-1}$ ];  $\eta$  is the dynamic viscosity [Pa s]. In case of Brownian motion, particles do not maintain a steady velocity, leading to a broadened spectrum centred on the original laser frequency, the degree of broadening begin related to the diffusion coefficient of the species of particles involved. In laser Doppler electrophoresis (LDE), the scattering centres are illuminated by a laser whilst being subjected to an electrical field. The electrophoretic velocity of the scatterings particles is determined by measuring the Doppler shift in the frequency of scattered light (equation 3.3), described by Ware and Flygare (1971) [101].

$$\Delta\omega = K \cdot v_e \quad (\text{equation 3.3})$$

Where  $K$  is the magnitude of scattering vector [ $\text{m}^{-1}$ ]. So in this case the important parameter is the Doppler shift and not the intensity as in DL [100]. Zeta potential is then calculated from electrophoretic velocity. Figure 3.5 illustrates the two techniques.

---

<sup>1</sup> Electrophoretic velocity is direct function of zeta potential, deduced from Helmholtz-Smoluchowski equation (equation. 3.1) respect to electrophoresis. It is not apply in all conditions, Henry's treatment or Obraian-whit can be used in some conditions (Sattelle *et al.* 1988).



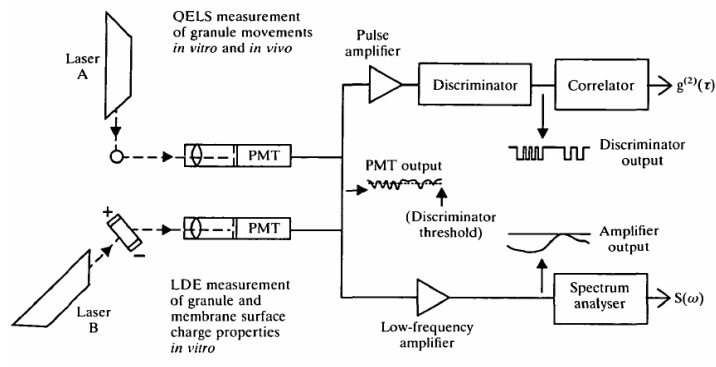
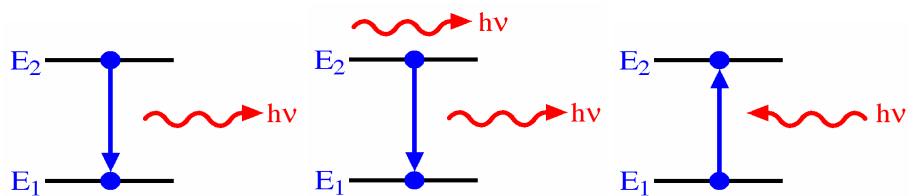


Figure 3.5. Schematic representation of experiments designed to monitor secretory granule movements *in vitro* and *in vivo*. Laser A illuminates suspended secretory granules or isolated nerve terminals. Light scattered at a given angle is focused on to the photomultiplier (PMT). This configuration permits quasi-elastic laser light-scattering (QELS) measurements. Laser B illuminates an electrophoresis cell. Movements of membrane-bound particles subjected to an electric field are detected. Scattered light is focused onto the surface of the photomultiplier. In this way laser Doppler electrophoresis (LDE) measurements of membrane surface charge properties are obtained from secretory granules and plasma membranes. Adapted from [102].

### 3.2. Fluorescence spectroscopy

One of the most important applications of nanoparticles in bionanotechnology, as previously reported, is to use them for protein monitoring. Nanoparticles can apply changes to protein conformation and, thus, it is possible to alter its functions. The most used technique to study these conformational changes in proteins is fluorescence spectroscopy, as some structural groups are fluorophores and their fluorescence features depend on protein conformation.

Fluorescence is a type of luminescence based on the emission of light, according to the excited states of atoms, when a specific substance is exposed to light or other electromagnetic waves [104]. Fluorescence spectroscopy is primarily concerned with electronic and vibrational states (Figure 3.6). First the sample is excited by absorbing a photon of light, from baseline to an excited electronic state with vibrational state. The molecule then drops back to one of several vibrational levels of basal electronic state, emitting a photon in the process (Figure 3.7). Since molecules can fall to any of the different levels of vibration in the basal state, the emitted photons have different energies and, therefore, frequencies. The emission spectroscopy record these frequencies and intensities (Figure 3.8).



$$\left(\frac{dn_1}{dt}\right)_{A_{21}} = A_{21} \cdot n_2 \qquad \left(\frac{dn_1}{dt}\right)_{B_{21}} = B_{21} \cdot n_2 \cdot \rho(\nu) \qquad \left(\frac{dn_1}{dt}\right)_{B_{12}} = -B_{12} \cdot n_1 \cdot \rho(\nu)$$

Figure 3.6. The Einstein coefficients [103].  $A_{21}$  ( $s^{-1}$ ) gives the probability per unit time that an electron in state 2 with energy  $E_2$  will decay spontaneously to state 1 with energy  $E_1$ , emitting a photon ( $E_2 - E_1 = h\nu$ );  $B_{21}$  ( $sr \cdot m^{-2} \cdot Hz \cdot W^{-1} \cdot s^{-1} = sr \cdot m^{-2} \cdot J^{-1} \cdot s^{-1}$ ) gives the probability per unit time per unit spectral radiance of the radiation field that an electron in state 2 with energy  $E_2$  will decay to state 1 with energy  $E_1$ , emitting a photon;  $B_{12}$  ( $sr \cdot m^{-2} \cdot Hz \cdot W^{-1} \cdot s^{-1} = sr \cdot m^{-2} \cdot J^{-1} \cdot s^{-1}$ ) gives the probability per unit time per unit spectral radiance of the radiation field that an electron in state 1 with energy  $E_1$  will absorb a photon and jump to state 2 with energy  $E_2$ .  $n_i$  is the number density of atoms in state  $i$ ;  $\rho(\nu)$  is the radiation density of the radiation field at the frequency of the transition.

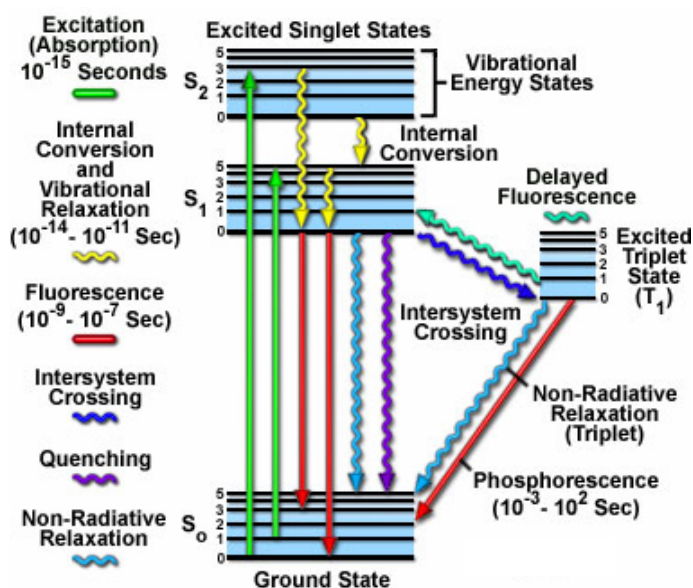


Figure 3.7. Jablonski Energy Diagram. Adapted from <<http://www.olympusmicro.com/primer/java/jablonski/jabintro/index.html>> [4/2/2010].

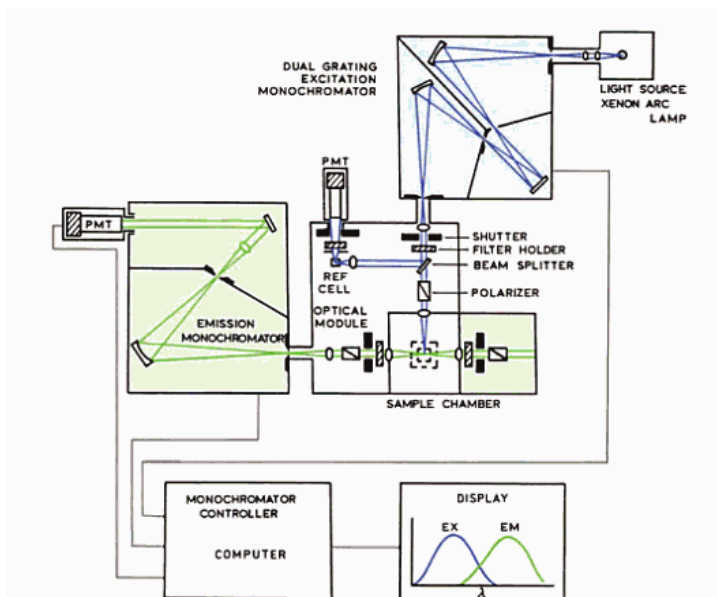


Figure 3.8. Schematic representation of fluorescence spectrometer. Adapted from [104].

In the present work, Fluorolog-3 (Horiba Jobin Yvon, Paris, France) was used to study the interaction between BSA and polymer nanoparticles.

### 3.2.1. Intrinsic fluorescence of proteins

Fluorescence is divided into intrinsic (occurs naturally), and extrinsic (added). Proteins contain three aromatic amino acid residues (tryptophan, tyrosine, phenylalanine) which may contribute to their intrinsic fluorescence [104][105]. These three amino acids have a common sequence in that they all contain aromatic ring in their structure that absorbs UV-light for excitation. The fluorescence of a folded protein is a mixture of the fluorescence from individual aromatic residues (Figure 3.9).

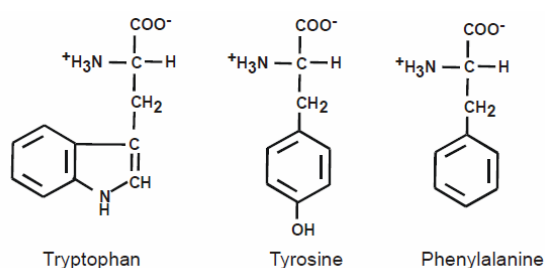


Figure 3.9. Amino acids with fluorescent features. Adapted from [105].

Tryptophan is much more fluorescent than either tyrosine or phenylalanine. Due to this greater absorptivity, higher quantum yield, and resonance energy transfer, the fluorescence spectrum of a protein containing the three amino acids usually resembles that of tryptophan (Table 3.1).

Table 3.1. Fluorescent Characterization of the aromatic amino acids [105].

Amino acid	Absorption		Fluorescence	
	Wavelength [nm]	Molar absorptivity	Wavelength [nm]	Quantum Yield
Tryptophan	280	5.600	348	0.20
Tyrosine	274	1.400	303	0.14
Phenylalanine	247	200	382	0.04

However, the fluorescent properties of tryptophan are solvent dependent. As the polarity of the solvent decreases, the spectrum shifts to shorter wavelengths and increases in intensity. For this reason this method is useful to study the interaction between nanoparticles and proteins. If a protein is in folded conformation, tryptophan amino acids are in a hydrophobic environment in the core of protein but if the protein is in partially unfold form, tryptophan residues are exposed to a more hydrophilic environment in the solvent. Tryptophan residues that are exposed to water, have maximal fluorescence at a wavelength of about 340-350 nm, whereas totally buried residues fluoresce at about 330 nm. In fluorescence spectroscopy, protein is generally excited at 280 nm or at longer wavelengths, usually at 295 nm to avoid contribution from tyrosine, and with polarization to avoid water Raman signal.

Intrinsic fluorescence of BSA has been also studied [106] and tryptophan is a good reference to understand the unfolding state of this protein.

### 3.2.2. ANS: fluorescent probe for the characterization of proteins

Frequently the molecules of interest are not fluorescent or the intrinsic fluorescence is not useful for the desired research. In these cases functional fluorescence is obtained by labelling molecules with extrinsic probes [104]. For protein it is frequently desirable to label them with fluorophores with longer excitation and emission wavelength than the aromatic amino acids. Then the labelled protein can be studied in the presence of other unlabeled proteins.

8-anilino-1-naphthalenesulfonic acid (ANS) showed in Figure 3.10 is an extensively utilized fluorescent probe for the characterization of protein binding sites (Figure 3.11 and 3.12) [107]-[111].

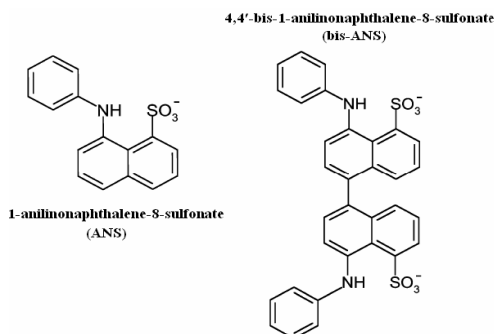


Figure 3.10. Chemical structure of ANS and bis-ANS. Adapted from [107].

ANS is a sulfonated naphthalene with aniline group [107]. The naphthalene group and aniline ring are hydrophobic, but sulfonate group has negative charge. Also, amide at the aniline ring can provide electrons for hydrogen bond formation with a protein. Therefore ANS has both polarity and hydrophobicity. Using the sulfonate group, ANS can interact with the positively charged amino acids such lysine, arginine and histidine. In addition, aromatic rings of ANS stabilize the binding with apolar sides of protein. The complementary interaction of both polar groups and apolar groups is the key component used in the protein folding study. In general, native conformation tend to hide their hydrophobic residues inside them and, except for some ligand binding sites, proteins have hydrophilic or polar amino acids on the surface. The beauty of ANS is that the binding of these molecules with proteins requires both the ionic interaction of sulfonate with positively charged amino acids and the hydrophobic interaction of aromatic rings with hydrophobic residues in an orientated manner. If a protein is denatured, it does not have any organized structure of having both charged region and hydrophobic region in a complementary manner. In this scenario, ANS bind unstably with the protein by just one form of interaction which leads an easy detachment of the dye from the freely moving protein.

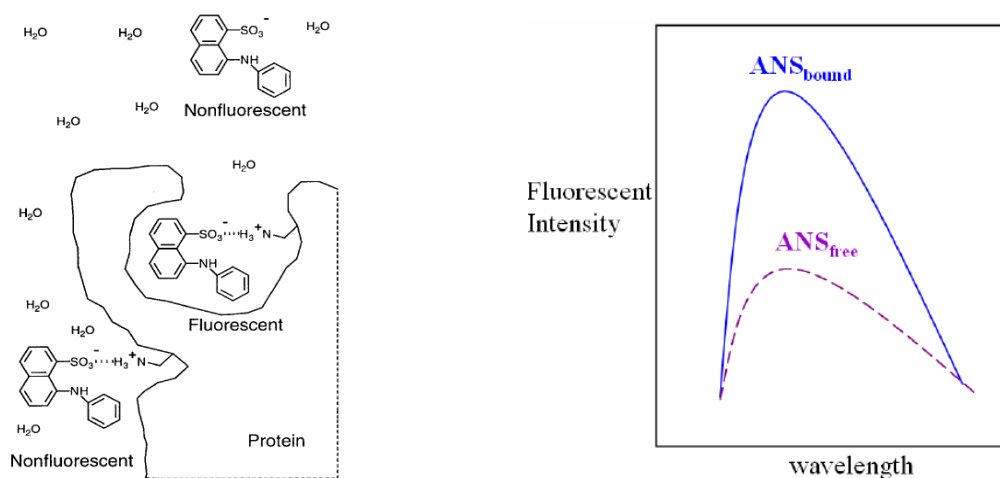


Figure 3.11. On the right side, anion binding of ANS to proteins. Adapted from [109]. On the right side, possible fluorescence spectra of ANS. Adapted from [107].

Aromatic rings (aniline and naphthalene) are fluorescent with the energy transfer within the molecular electrons. The excitation of ANS is 350-380 nm and the emission maximum in water is 500 nm. Interestingly, when ANS binds to protein hydrophobes the emission maximum is shifted to blue wavelength range 470 nm approximately and it always come along with the huge increase of emission intensity.

Serum albumins are the most multifunctional proteins known to date and their most outstanding property is their ability to reversibly bind an incredible variety of ligands [108].

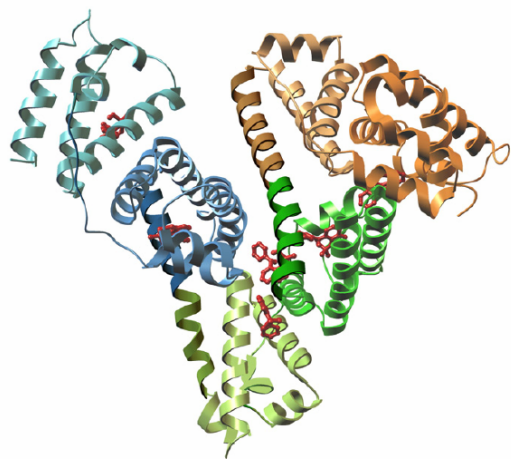


Figure 3.12. Molecular docking between ANS and BSA. BSA structure was obtained by homology modeling using HAS (1BM0) as a template. The domains are colour-coded as follows: I, orange; II, green, and III, blue. The subdomains are depicted by different colour values, dark (A) and light (B). The ANS molecules successfully docked to BSA are shown in a ball and stick representation coloured red. Adapted from [107].

### 3.3. Isothermal titration calorimetry

Calorimetric methods have been an individual tool for understanding the forces that stabilize the folded conformations of proteins and has long been used to accurately measure ligand-binding properties. Isothermal titration calorimetry (ITC) is a versatile and sensitive technique that allows for the simultaneous determination of binding affinity, enthalpy and stoichiometry of an interaction. ITC can quickly determine the thermodynamics of an interaction under native conditions, without the use of tags or labels that may otherwise interfere with binding [112].

An ITC instrument (Figure 3.13) consist of two identical cells composed of a highly efficient thermal conducting material surrounded by an adiabatic jacket [113][114]. Sensitive thermopile/thermocouple circuits detect temperature differences between the two cells and between the cells and the jacket. Heaters located on both cells and the jacket are activated when necessary to maintain identical temperatures between all components. In an ITC experiment, the macromolecule solution is placed in the sample cell. The reference cell contains buffer or water minus the macromolecule. Prior to the injection of the titrant, a

constant power (<1 mW) is applied to the reference cell. This signal directs the feedback circuit to activate the heater located on the sample cell. This represents the baseline signal. The direct observable measured in an ITC experiment is the time-dependent input of power required to maintain equal temperatures in the sample and reference cell. During the injection of the titrant into the sample cell, heat is taken up or evolved depending on whether the macromolecular association reaction is endothermic or exothermic. For an exothermic reaction, the temperature in the sample cell will increase, and the feedback power will be deactivated to maintain equal temperatures between the two cells. For endothermic reactions, the reverse will occur, meaning the feedback circuit will increase power to the sample cell to maintain the temperature. From several repeat injections, a binding curve can be obtained, and the affinity, stoichiometry, and enthalpy change upon binding can be derived.

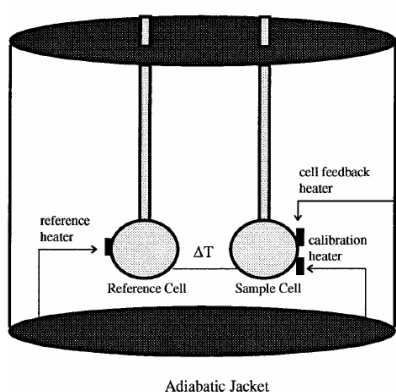


Figure 3.13. ITC mechanism. Adapted from [113].

Stoichiometry of the reaction, equilibrium constant and enthalpy of the reaction are the three main parameters that can be calculated using ITC [115]. As in case of fluorescence is determined the folding or unfolding state of BSA, here it is determined the amount of BSA that react and the thermodynamic parameters of the reaction. In the present work Nano ITC single injection (TA instruments, Hedehusene, Denmark) has been used to study the unfolding of BSA at the surface of polymer nanoparticles.





## 4. Experimental procedure

This section deals in the procedure followed to study BSA-polymer nanoparticle construct. All steps are described in chronological order: synthesis of polymer nanoparticles, characterization of polymer nanoparticles, adsorption of BSA on the nanoparticles and characterization of native BSA and BSA-polymer nanoparticle constructs.

### 4.1. Polymer nanoparticles synthesized by soap free emulsion polymerization

The procedure followed was the same as that used by Yasudas *et al.* [50]. In the present project, two types of negatively charged monodisperse polymer nanoparticles having epoxy groups and one type having no epoxy groups were synthesized by soap free emulsion copolymerization of glycidyl methacrylate (GMA), styrene (St), divinyl benzene (DVB) and ammonium persulfate (APS). Glycidyl methacrylate and styrene were the monomers involved in the copolymerization process; divinyl benzene was the cross linker agent; and ammonium persulfate was the initiator. In order to introduce epoxy groups and negative surface charge on the polymer nanoparticles, glycidyl methacrylate was added to the reaction mixture at 2 h from the start of the reaction. Thus the possibility of hydrophobic interaction with the core of BSA, which would induce most likely irreversible conformational changes, was removed. The epoxy groups of the polymer nanoparticles were opened using strong acid to obtain polymer nanoparticles without epoxy groups.

#### 4.1.1. Polymer nanoparticles with epoxy groups on the surface

Polymer nanoparticles for protein immobilization support were synthesized by soap-free emulsion polymerization [50]. First, GMA<sup>1</sup> (1.8 g, 12.28 mmoles), DVB<sup>2</sup> (0.04 g, 0.25 mmoles), St<sup>3</sup> monomer (1.2 g, 11.41 mmoles) and 95 ml of mili Q-water were added to a

---

<sup>1</sup> Glycidyl methacrylate, 97%

<sup>2</sup> Divinylbenzene technical grade, 80%

<sup>3</sup> Styrene, RegeantPlus, >=99%

300 ml five-neck reaction flask. Plastic pipettes were used for introducing reagents. The reaction vessel was immersed in an oil bath at 70 °C and the reaction mixture was stirred between 50 rpm and 100 rpm, depending on the particle size desired, for 15 minutes. When the temperature in the reaction mixture reached 70 °C, APS<sup>1</sup> (0.06 g, 0.26 mmoles) dissolved in 5 ml of milli-Q water was added to initiate the reaction. 2 h after addition of aqueous initiator solution (check the disappearance monomer on the surface), GMA (2.04 mmoles) was added to the reaction mixture. The reaction mixture was heated for 16 hours after addition of aqueous initiator solution. The final solution was white with the intensity of the colour proportional to the total amount of polymer nanoparticles. Following polymerization, the reaction mixture was centrifuged at 11000 rpm for 30 min, and the precipitate polymer nanoparticles were suspended in distiller water. Centrifugation, discarding supernatant and resuspending polymer nanoparticles with distiller water (particles washing) was repeated three times. After that polymer nanoparticles were resuspended in 80 ml milli-Q water and stocked at 4 °C approximately.

#### 4.1.2. Polymer nanoparticles without epoxy groups on the surface

Polymer nanoparticles with epoxy groups were kept in an aqueous system, 0.2 M of HCl or NaOH, for 1 h at 60 °C in order to open the epoxy groups. After reaction, polymer nanoparticles were washed by ammonium hydroxide 0.2 M to exchange counter ions of  $SO_3^-$ . Finally, centrifugation (11000 rpm 30 min), discarding supernatant and resuspending polymer nanoparticles with distiller water (particles washing) was repeated three times.

#### 4.1.3. Concentration of polymer nanoparticles

Polymer nanoparticles concentration was measured by gravimetry. A small portion of particles suspension (200 µl) was added to aluminium cup and then it was stored in dry oven (60°C) for 90 min. The difference between cup weight with dry portion of particles and cup weight empty gave the amount of nanoparticles in a known volume. The total amount of polymer nanoparticles was then calculated by multiplying the concentration by total sample volume.

---

<sup>1</sup> Ammonium persulfate, 98+%, A.C.S. reagent

#### 4.1.4. Characterization of polymer nanoparticles

Polymer nanoparticle size and its distribution were measured using a Zetasizer Nano ZS (Malvern). A portion polymer nanoparticles solution was loaded into 1 cm x 1 cm poly(styrene) cell and automatically measured by the machine. High concentrations of polymer nanoparticles showed wrong results since the scattering was affected by the interaction of a lot of particles; in that case the sample was diluted (<10 mg/ml). The zeta potentials of the polymer nanoparticles were measured using also a Zetasizer Nano ZS (Malvern). Here, 15 ml of polymer nanoparticles 3.75 mg/ml adjusted with mili-Q water 10 mM NaCl was prepared and loaded into the pH titration unit (MPT-2, Malvern). pH of the sample solution was varied from 10 to 3 using 0.25 M of hydrochloric acid or 0.25 M of sodium hydroxide. Additional volume was considered neglectable. The pH adjusted sample solution was circulated in the Zetasizer and zeta potentials at various pH were automatically measured.

## 4.2. BSA immobilization on polymer nanoparticles

BSA protein was immobilized on polymer nanoparticles by preparing different solutions of BSA 3.6  $\mu$ M and polymer nanoparticles 3.75 mg/ml. The volume of the sample was adjusted using mili-Q water 10 mM NaCl for zeta potential measurements or buffer solutions at different pH for fluorescence measurements. The pH of the samples solutions was regulated using either sodium acetate (pH 3.8), potassium phosphate (pH 7.4), or sodium borate (pH 9.0). It was necessary to wait at least three hours after mixing for equilibrium to be reached.

### 4.2.1. Characterization of BSA-polymer nanoparticle constructs

The zeta potentials of BSA and BSA-polymer nanoparticle constructs were measured using also Zetasizer Nano ZS (Malvern). In that case 15 ml of sample mixture adjusted with mili-Q water 10 mM NaCl were loaded into the pH titration unit (MPT-2, Malvern). Isoelectric point was also reported.

Fluorescence emission spectra were measured using a Fluorolog-3 (Horiba Jobin Yvon, Paris, France). Protein solution, or a mixture of protein and particle, in a buffer solution was added to 1 cm x 1 cm quartz cell and the detector was placed in the 90° direction against excitation beam. All samples containing ANS 17  $\mu$ M were measured from 385 nm to 700 nm with 370 nm as excitation wavelength and slit 1. All samples with no ANS were measured from 310 nm to 500 nm at 295 nm and slit 5. The set up with 295 nm was with polarization and at 370 nm was without polarization. The reason was that at 295 nm water fluorescence could affect the results due to water Raman peak. For calibration, fluorescence emission

spectra of the particle suspension in various buffer solutions were also measured. In the case of immobilized protein, fluorescence emission spectra included particle contribution for fluorescence emission spectra. To obtain fluorescence emission spectra of immobilized protein, measured fluorescence emission spectra were numerically extracted from the fluorescence emission spectra of particle.

### **4.3. Unfolding of immobilized BSA using urea in combination with ANS**

BSA-polymer nanoparticle constructs were also studied by fluorimetry in a different denaturation conditions. Urea was used as a denaturation agent to induce the protein unfolding [116].

Different samples BSA 3.6  $\mu\text{M}$ , polymer nanoparticles 3.75 mg/ml and ANS 17  $\mu\text{M}$  in a buffer solution with urea were prepared. The concentration of urea varied from 0 M to 8 M. Finally, fluorescence spectroscopy was carried out ten minutes after the addition of urea to the samples. Protein-polymer nanoparticle solution was loaded into 1 cm x 1 cm quartz cell and the detector was placed in the  $90^\circ$  direction against excitation beam. Fluorescence was measured with 370 nm as excitation wavelength, slit 1 and without polarization using a Fluorolog-3 (Horiba Jobin Yvon, Paris, France).

### **4.4. Isothermal titration calorimetry**

Adsorption of BSA on the surface of polymer nanoparticles was finally studied by isothermal titration calorimetry (ITC) using a Nano Isothermal Titration Calorimeter (TA instruments, Hedehusene, Denmark). The experiments were performed at different conditions and in all cases BSA was titrated to a sample cell containing polymer nanoparticles. Finally the amount of heat derived from the reaction at each titration was recorded by the instrument and the enthalpy, the stoichiometry and the equilibrium constant of the reaction were automatically calculated.

Different samples of polymer nanoparticles 3.75 mg/ml in a buffer solution were loaded in a 943  $\mu\text{l}$  sample cell. The titration was carried out using a 100  $\mu\text{l}$  syringe filled with BSA 36  $\mu\text{M}$ . 25 titrations of 4  $\mu\text{l}$  every 500 seconds constituted one experiment.

## 5. Results and discussion

The present section report the results obtained after followed the previous procedure. The aim of this is to give a coherent explanation to the results concerning the interaction between BSA protein and polymer nanoparticle.

### 5.1. Synthesis and characterization of monodisperse polymer nanoparticles

Three different types of monodisperse anionic polymer nanoparticles were synthesized by soap free emulsion polymerization: two different size of polymer nanoparticles functionalized with epoxy groups and one type of polymer nanoparticles without epoxy groups.

#### 5.1.1. Polymer nanoparticles with epoxy groups

In order to determine the effect of the agitation speed during the soap free emulsion polymerization process in polymer nanoparticles size, four experiments were carried out in a batch reactor by soap free emulsion polymerization, two at low stirring rate and two at high stirring rate. The two first experiments were at 50 rpm which gives laminar flow during the polymerization, while the two last experiments were at 100 rpm, resulting in more turbulent flow. Table 5.1 and Figure 5.1 and 5.2 show the average result of each experiment.

Table 5.1. Average size distribution of monodisperse polymer nanoparticles.

Stirring 50 rpm*							
Exp.	Z-Ave		Pdl		Pk 1 Mean Int		Pk 1 Area Int
	d.nm	$\sigma$	$\sigma$		d.nm	$\sigma$	%
1	227	0.85	0.033	0.025	231	2.43	100
2	212	2.71	0.052	0.017	216	6.37	100
Stirring 100 rpm*							
Exp.	Z-Ave		Pdl		Pk 1 Mean Int		Pk 1 Area Int
	d.nm	$\sigma$	$\sigma$		d.nm	$\sigma$	%
1	153	0.146	0.056	0.004	160	3.1	0
2	139	0.73	0.062	0.017	146	1.06	0

\*Each sample was recorded 3 times and the results are the average of all.

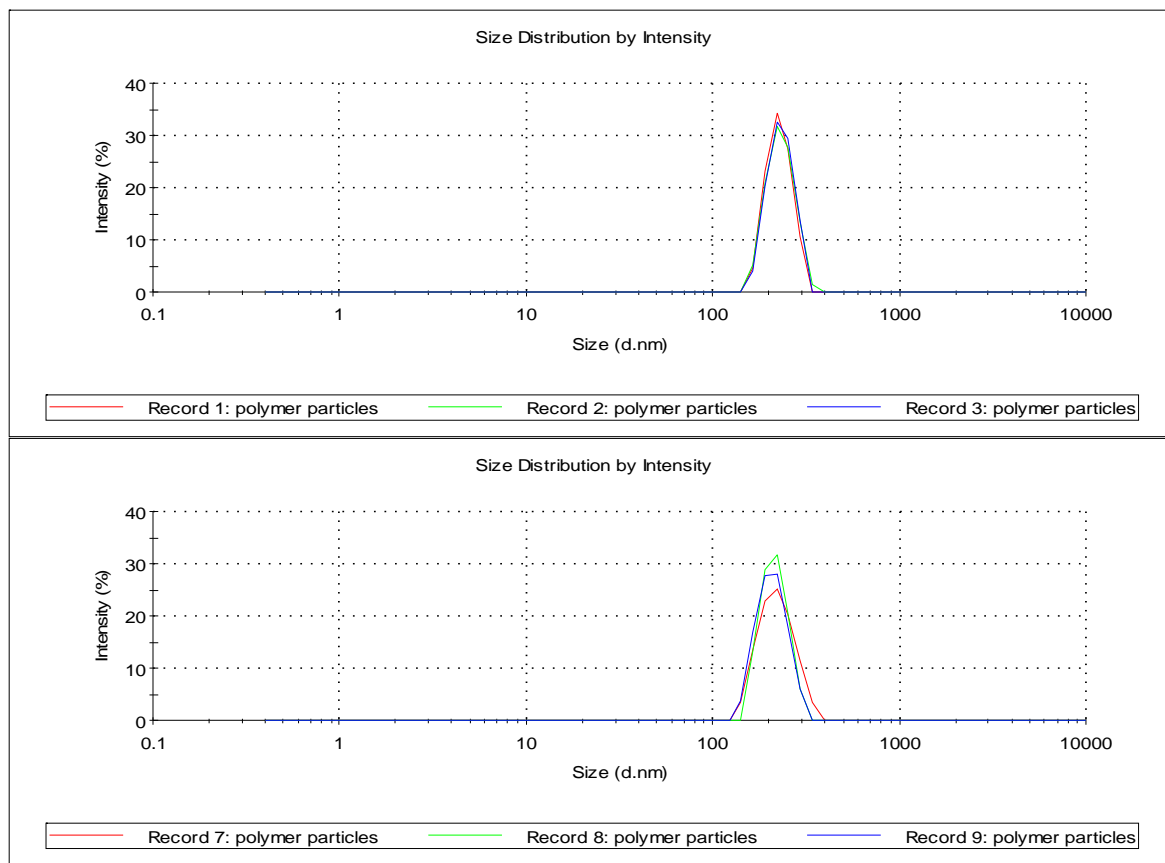


Figure 5.1. Size distribution by intensity of monodisperse polymer nanoparticles at 50 rpm. The first one shows the results of experiment 1 and the second one the results of experiment 2 from table 5.1.

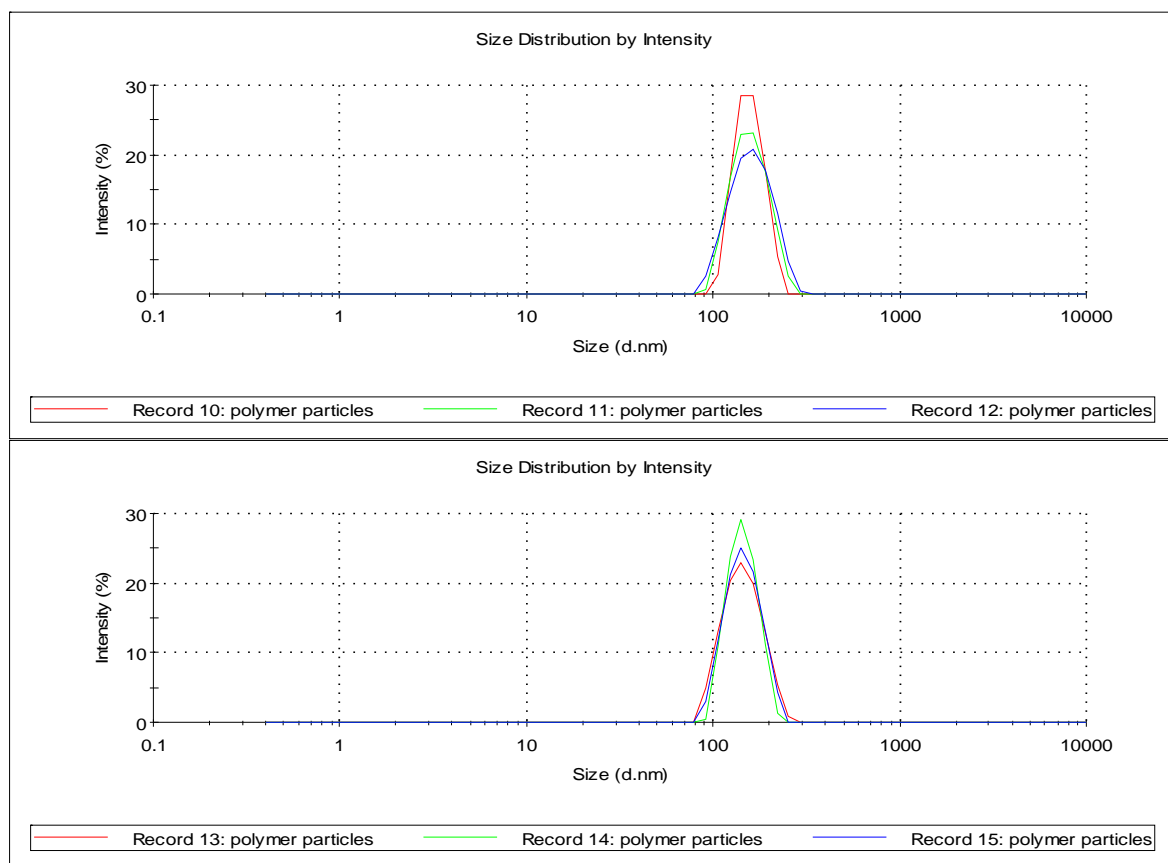


Figure 5.2. Size distribution by intensity of monodisperse polymer nanoparticles 100 rpm. The first one shows the results of experiment 1 and the second one the results of experiment 2 from Table 5.1.

Both experiments, 50 rpm and 100 rpm, showed a very narrow monodisperse size distribution. Furthermore really interesting differences could be found. At low stirring the diameter of nanoparticles<sup>1</sup> were around 227 nm, whereas with increasing the agitation speed of the sample the diameter decreased around 153 nm. Therefore by controlling this parameter it might be possible to synthesize polymer nanoparticles in a different range of diameters. High stirring means more turbulent flow in the batch reactor and more polydispersity. In the range of work this is not a problem, but must be considered when working in more drastic conditions. Finally the reproducibility is quite high. When the same parameters are used, the results varied with less than 10%.

<sup>1</sup> The particle size measured by dynamic light scattering is the hydrodynamic diameter, which can exceed the physical diameter for strongly charged particles. Compare the size measured using dynamic light scattering and another method like microphotography would be recommended.

Process efficiency is also an important parameter. Polymer nanoparticles concentration was measured by gravimetry (section 4.1.3 *Concentration of polymer nanoparticles*). The results (Table 5.2) reported that as the size of nanoparticles increases, also the total amount obtained.

Table 5.2. Obtained amount of polymer nanoparticles by soap free emulsion polymerization.

Diameter [nm]	Concentration [mg/ml]	Quantity [g]
		$\sigma$
227	33.5	0.6
153	15.2	0.8
		$\sigma$
		0.051
		0.066

\*The amount of substances used in the experiment is reported in the section 4.1 *Polymer nanoparticles synthesized by soap free emulsion polymerization*. Each experiment was repeated three times and the results are the average of all.

The total mass was reduced 54% in polymer nanoparticles 153 nm when it was compared with polymer nanoparticles 227 nm. The main cause of this fact could be explained by a lower efficiency in the procedure of centrifugation due to the lower mass of each individual particle. Higher speed and/or more time centrifugation should help to obtain more quantity, although it affects the polydispersity of the particles.

Determination of zeta potential of polymer nanoparticles in a wide range of pH using Nano ZS Malvern was done in combination with acid-base titration process. The concentration of polymer nanoparticles in the sample was adjusted to 3.75 mg/ml. Zeta potential of polymer nanoparticles 227 nm and 153 nm was then measured (Table 5.3, Figure 5.3). Finally, in order to determine the distribution of zeta potential in the particles, zeta deviation was checked (Table 5.3, Figure 5.4).

Table 5.3. Zeta potential of polymer nanoparticles at different pH.

Sample polymer nanoparticles 227 nm 3.75 mg/ml						
Record	T °C	Zeta potential mV	Zeta deviation mV	Mobility $\mu\text{mcm/Vs}$	Conductivity mS/cm	pH
1	25	-27.8	7.55	-2.18	1.44	8.91
2	25	-27.2	7.77	-2.13	1.42	8.83
3	25	-27.5	7.14	-2.16	1.42	8.75
4	25	-26.7	6.02	-2.1	1.43	7.81
5	25	-26.5	7.9	-2.08	1.42	7.75
6	25	-27.5	7.5	-2.16	1.42	7.72
7	25	-25.1	6.2	-1.96	1.43	6.63
8	25	-25.0	7.16	-1.96	1.42	6.68
9	25	-25.6	7.59	-2.01	1.42	6.71
10	25	-26.2	6.04	-2.05	1.43	6.10
11	25	-24.8	7.28	-1.95	1.42	6.15
12	25	-25.7	6.44	-2.02	1.42	6.19
13	25	-23.5	6.88	-1.84	1.43	4.99
14	25	-24.6	7.28	-1.93	1.43	5.06



15	25	-23.1	6.82	-1.81	1.43	5.10
16	25	-24.6	4.77	-1.93	1.45	4.19
17	25	-25.1	4.73	-1.96	1.45	4.20
18	25	-24.1	4.62	-1.89	1.45	4.22
19	25	-24.2	6.17	-1.89	1.87	3.08
20	25	-22.8	5.43	-1.78	1.87	3.08
21	25	-23.0	6.9	-1.80	1.86	3.09
22	25	-14.7	14	-1.15	8.60	2.06
23	25	-13.1	16.9	-1.03	8.78	2.06
24	25	-16.0	13.3	-1.26	8.76	2.06

**Sample polymer nanoparticles 153 nm 3.75 mg/ml**

Record	T °C	Zeta potential mV	Zeta deviation mV	Mobility µmcm/Vs	Conductivity mS/cm	pH
1	25	-23.2	8.75	-1.82	1.42	9.13
2	25	-24.5	9.72	-1.92	1.41	9.09
3	25	-22.6	8.97	-1.77	1.41	9.06
4	25	-23.6	8.98	-1.85	1.42	8.06
5	25	-23.9	10	-1.88	1.41	8.01
6	25	-23.4	8.52	-1.83	1.41	7.95
7	25	-22.3	8.41	-1.75	1.42	6.59
8	25	-22.3	8.36	-1.75	1.41	6.66
9	25	-20.9	9.26	-1.64	1.41	6.71
10	25	-21.5	8.83	-1.68	1.43	5.17
11	25	-21.1	8.82	-1.65	1.42	5.32
12	25	-21.5	9.01	-1.68	1.42	5.40
13	25	-20.2	8.31	-1.59	1.43	5.03
14	25	-20.7	8.93	-1.62	1.42	5.08
15	25	-21.4	7.68	-1.68	1.43	5.12
16	25	-19.2	5.92	-1.51	1.46	4.14
17	25	-18.4	7.28	-1.45	1.46	4.15
18	25	-18.6	6.4	-1.46	1.46	4.16
19	25	-17.8	5.05	-1.39	1.86	3.12
20	25	-17.3	6.24	-1.36	1.86	3.11
21	25	-17.8	6.37	-1.40	1.86	3.11
22	25	-11.1	16	-0.87	10.2	2.25
23	25	-10.8	16.6	-0.843	10.5	2.28
24	25	-10.7	13.6	-0.836	10.4	2.26

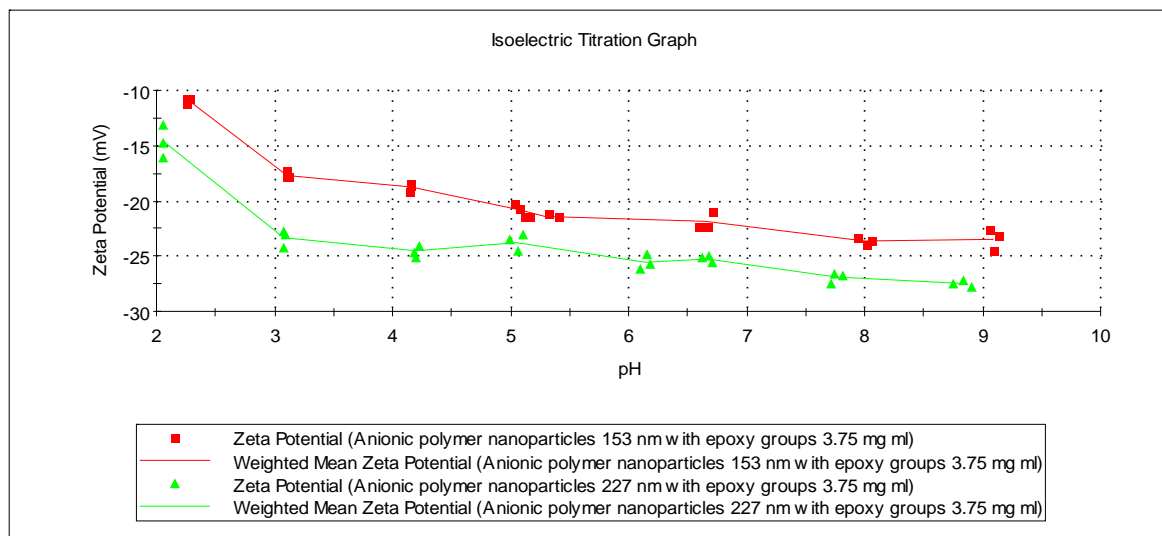


Figure 5.3. Isoelectric titration graph. Zeta potential at different pH of two samples of polymer nanoparticles. Green line refers to diameter 227 nm while red line refers to 153 nm.

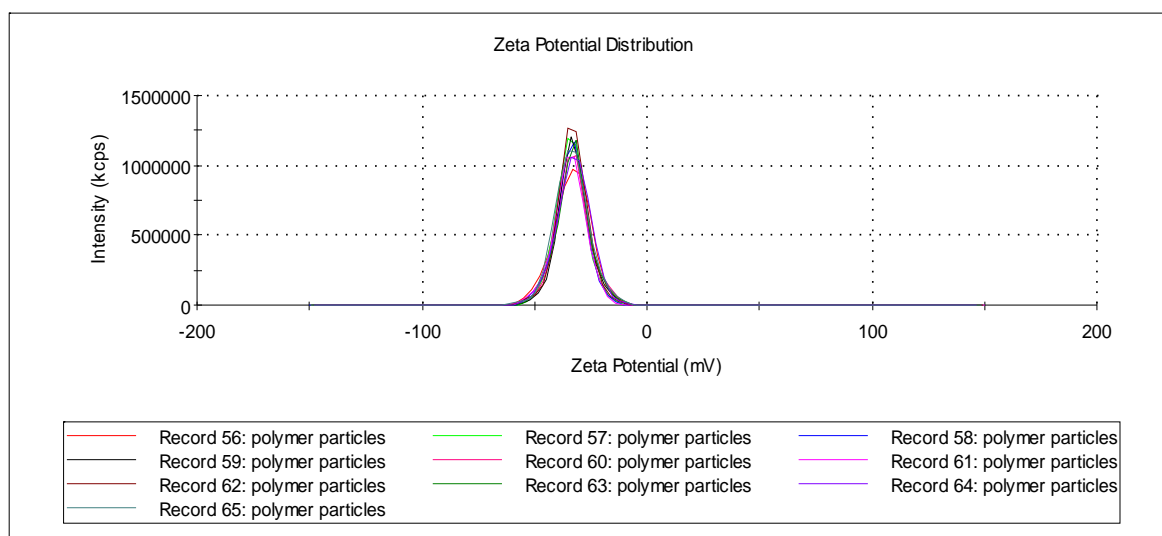


Figure 5.4. Zeta potential distribution. Zeta potential at pH 7 of 227 nm polymer nanoparticles.

The polymer nanoparticles with epoxy groups remained negatively charged throughout the entire pH region studied here, with the value of zeta potential decreasing by increasing pH values as it was expected. The zeta potential distribution of the samples at a specific pH was also quite narrow, which means that all particles had the same charge as shown in Figure 5.4. There was no isoelectric point and the polymer nanoparticles did not show amphoteric conduct. At pH below three they became useless and the results were far from the trend line. Thus, surface charge could be considered homogeneous in polymer nanoparticles and it was possible to use them in non-extreme pH conditions. Zeta potential of polymer nanoparticles 227 nm was slightly more negatively than polymer nanoparticles 153 nm. Large particles give room for more negative groups at the surface. In any case both polymer nanoparticles could be used as a stable support for protein immobilization. It is

important to note that the negative charge is a combination of the charges brought by the epoxy surface groups plus other surface anionic groups, especially provided by oxygen atoms from glycidyl methacrylate.

### 5.1.2. Polymer nanoparticle without epoxy groups

Epoxy groups were removed from polymer nanoparticles 227 nm, as described in section 4.1.2 *Polymer nanoparticles without epoxy groups on the surface*. Thereby it was possible to produce negatively charged nanoparticles that allowed a purely electrostatic interaction with BSA protein since covalent links had been removed. Table 5.4 and Figure 5.5 show the results of the polymer nanoparticles before and after the removal process.

Table 5.4. Average size distribution of monodisperse polymer nanoparticles before and after removing the epoxy groups.

Sample polymer nanoparticles 227 nm*							
	Z-Ave		Pdl		Pk 1 Mean Int		Pk 1 Area Int
	d.nm	$\sigma$		$\sigma$	d.nm	$\sigma$	%
Before	227	0.85	0.033	0.025	231	2.43	100
After	224	1.73	0.036	0.025	227	3.95	100

\*Each sample was recorded 3 times and the results are the average of all.

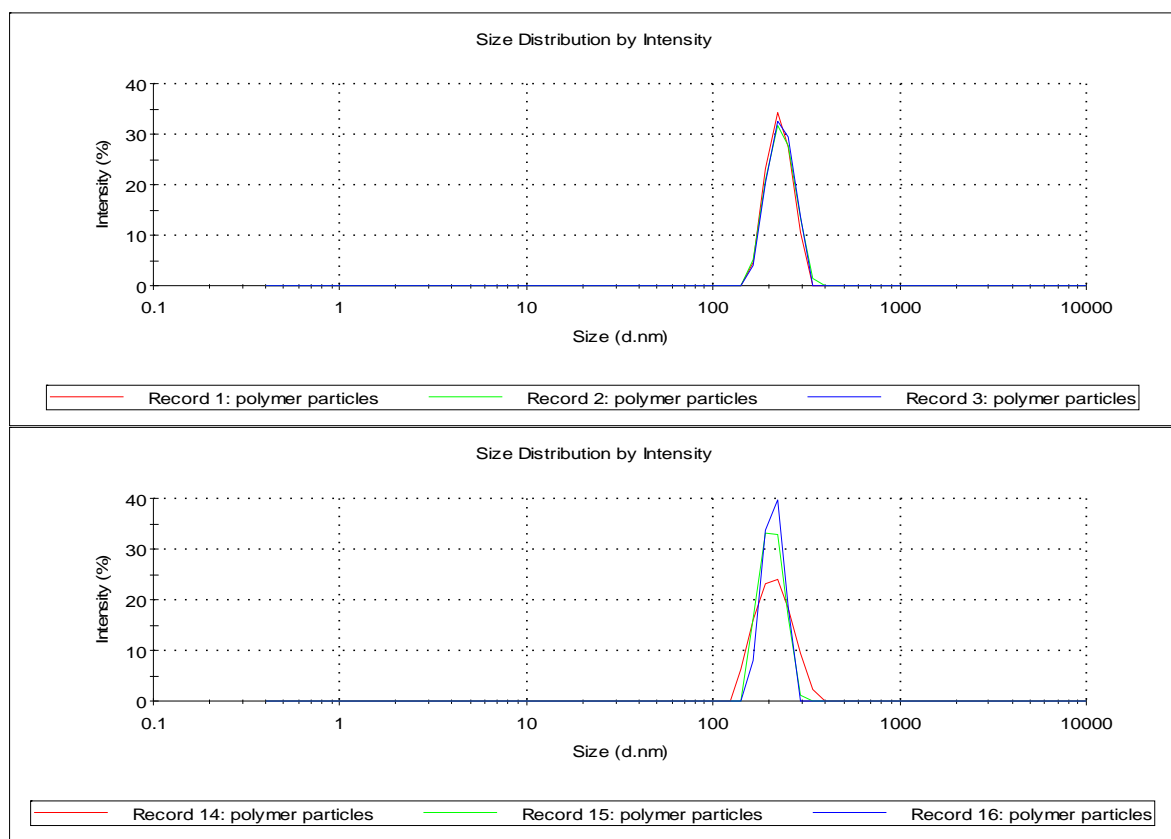


Figure 5.5. Size distribution by intensity of monodisperse polymer nanoparticles before and after removing the epoxy groups.

The sample remained practically unchanged. Opening of epoxy rings in a strongly acidic medium (0.2 M HCl) and subsequent washing with ammonium hydroxide (0.2 M NH<sub>4</sub>OH) and mili-Q water did not affect particles size as showed the results. Therefore it was possible to create particles with and without epoxy groups alike. However, it is necessary to clarify that a significant amount of particles, the order of 26 %, was lost in the re-washing process of these after opening the epoxy groups. Higher speed centrifugation should be studied.

Zeta potential was determined following the same technique as for the previous case. But in this case pH was adjusted manually and not by acid-base titration machine, which implying some differences in the exact points of measurement. This does however not affect the results. Table 5.5 shows zeta potential of 227 nm polymer nanoparticles without epoxy groups and Figure 5.6 compares the three different particles.

Table 5.5. Zeta potential of polymer nanoparticles without epoxy groups at different pH.

Sample polymer nanoparticles 227 nm without epoxy groups 3.75 mg/ml						
Record	T °C	Zeta potential mV	Zeta deviation mv	Mobility µmcm/Vs	Conductivity mS/cm	pH
1	25	-26	7.21	-2.04	1.83	9.13
2	25	-27.4	5.95	-2.14	1.98	9.13
3	25	-28	7.3	-2.2	2.01	9.13
4	25	-25.3	7	-1.99	3.24	7.38
5	25	-25.6	7.1	-2.01	1.75	7.01
6	25	-25.5	8.4	-2.00	1.90	7.01
7	25	-24.1	8.16	-1.89	1.80	5.94
8	25	-22.5	5.87	-1.76	1.81	5.02
9	25	-19.6	9.26	-1.54	2.29	3.22
10	25	-19.6	9.89	-1.54	2.29	3.22
11	25	-18.5	8.93	-1.45	2.49	2.62
12	25	-19.8	7.12	-1.55	2.52	2.62
13	25	-19.3	13.6	-1.52	4.08	2.21
14	25	-20.3	10.1	-1.59	4.16	2.21

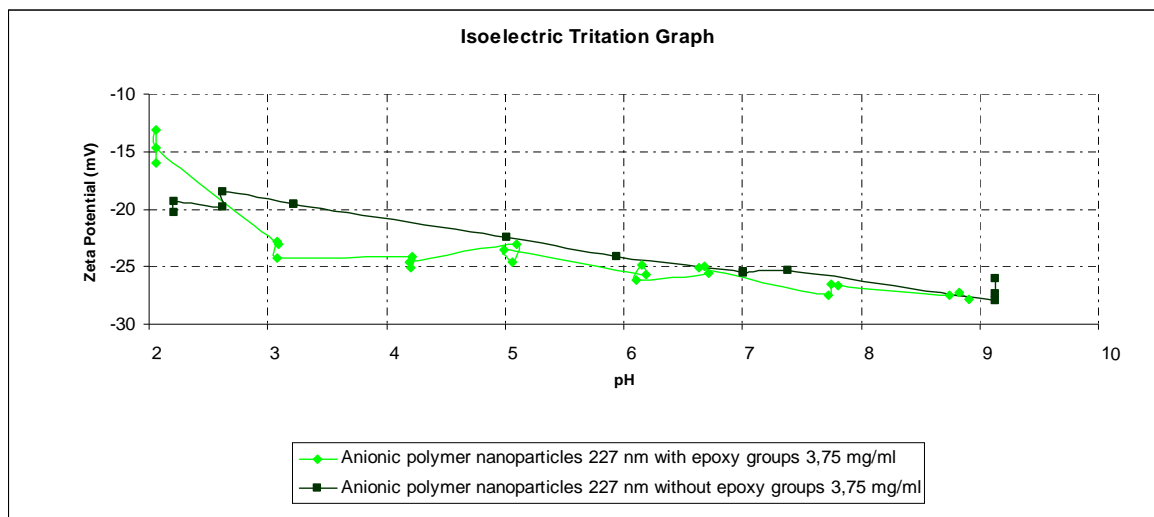


Figure 5.6. Isoelectric titration graph. Zeta potential at different pH of two samples of polymer nanoparticles. Green line refers to diameter 227 nm with epoxy groups while dark green line refers to 227 nm without epoxy groups.

Polymer nanoparticles still had negative surface charge after the process, which means that this fact was not caused only by epoxy groups. From titration graphic (Figure 5.6), it could also observe that there were not so many differences between polymer nanoparticles with epoxy groups and without epoxy groups. Small changes indicated that the particles actually had experienced alteration, supposedly caused by the removal of these surface groups. Trend line of zeta potential value when pH decreases was much more linear and at extreme pH conditions seemed that polymer nanoparticles without epoxy groups were less altered. For this reason it was possible to synthesize polymer nanoparticles that could interact with BSA protein just by electrostatic force.

Hence, it is possible to make polymer nanoparticles with diverse sizes and different interaction forces. Changes in the diameter of nanoparticles provide different curvature and unfolding states in BSA protein. Also depending on the type of bonding, covalent or electrostatic, BSA protein can be just adsorbed, adsorbed and unfolded or not adsorbed. Variety in nanoparticles means variety in tools we have and more likely to find one that satisfy the needs required.

## 5.2. BSA immobilization on monodisperse polymer nanoparticles. Zeta potential titration measurements.

Proteins can interact with polymer nanoparticles in different ways. In case of BSA protein attached on polymer nanoparticles electrostatic bonding is the main probably hypothesis (section 2.3 *Adsorption of protein on nanoparticles with associated structural changes*). The attraction between positively charge surface residues of protein, which are pH-dependent,

and the oppositely charges passivation ligands on polymer nanoparticles are responsible for this phenomena. If polymer nanoparticles are also functionalized with epoxy groups, which can react with amino groups such as lysine, histidine or arginine on the protein surface, then the attachment is complemented with covalent bonding and the interaction is stronger, with a greater importance in the structural modification of BSA protein. Under different pH conditions, BSA experiment reversibly conformational isomerisation (section 2.2.2 *BSA protein*). Finally BSA is a well documented protein and therefore a valid tool in the study protein-polymer nanoparticle study (section 2.2.2 *BSA protein*).

From global charge it is expected that polymer nanoparticles are more efficient at immobilizing BSA below pI as in this environment electrostatic attraction is favourable. In addition among all nanoparticles those with big size and epoxy groups should show better results for its stronger attachment. Here different experiments at different pH and concentrations have been done.

### 5.2.1. Zeta potential titration measurements of BSA-polymer nanoparticle constructs

Zeta potential of BSA-polymer nanoparticle constructs was measured in different pH using Nano ZS Malvern in combination with acid-base titration process. Four samples of 15 ml were measured. The first one contained 3.6  $\mu\text{M}$  of BSA protein. The remaining three contained, in addition to protein, 3.75 mg/ml of three different polymer nanoparticles: polymer nanoparticles 227 nm with epoxy groups, polymer nanoparticles 153 nm with epoxy groups and polymer nanoparticles 227 nm without epoxy groups. Table 5.6 shows zeta potential results, Figure 5.7 compare the behaviour at different polymer nanoparticles size and Figure 5.8 between polymer nanoparticles with and without epoxy groups.

Table 5.6. Zeta potential of BSA--polymer nanoparticle constructs. Polymer nanoparticles 227 nm and polymer nanoparticles 153 nm.

Sample BSA 3.6 $\mu\text{M}$						
Record	T	Zeta potential	Zeta deviation	Mobility	Conductivity	pH
	$^{\circ}\text{C}$	mV	mV	$\mu\text{mcm/Vs}$	mS/cm	
1	25	-34.3	8.81	-2.69	1.36	8.99
2	25	-34.6	7.8	-2.71	1.35	8.92
3	25	-33.6	8.2	-2.63	1.35	8.84
4	25	-34.6	9.83	-2.71	1.36	7.72
5	25	-31	7.17	-2.43	1.35	7.68
6	25	-32.1	6.55	-2.52	1.35	7.64
7	25	-31.5	6.93	-2.47	1.36	7.06
8	25	-29.4	7	-2.3	1.35	7.06
9	25	-29.8	6.85	-2.34	1.35	7.07
10	25	-21.7	4.98	-1.7	1.36	6.1

11	25	-21.8	5.18	-1.71	1.36	6.17
12	25	-21.3	5.19	-1.67	1.36	6.21
13	25	-9.73	4.15	-0.763	1.37	5.21
14	25	-8.84	4.44	-0.693	1.37	5.24
15	25	-8.87	4.11	-0.695	1.37	5.26
16	25	16.3	3.85	1.27	1.41	4.13
17	25	16.5	4.03	1.29	1.4	4.14
18	25	16.5	4.36	1.29	1.41	4.14
19	25	26.5	4.77	2.08	1.8	3.07
20	25	27.2	4.86	2.13	1.81	3.07
21	25	26.4	4.48	2.07	1.81	3.07
22	25	24.2	11.6	1.89	7.99	2.04
23	25	23.7	11	1.85	8.06	2.03
24	25	25.2	9.32	1.98	8.06	2.02
<b>Sample BSA 3.6 <math>\mu</math>M and polymer nanoparticles 227 nm with epoxy groups 3.75 mg/ml</b>						
Record	T	Zeta potential	Zeta deviation	Mobility	Conductivity	pH
	$^{\circ}$ C	mV	mV	$\mu$ mcm/Vs	mS/cm	
1	25	-26.5	5.61	-2.08	1.25	9.38
2	25	-26	6.8	-2.04	1.23	9.33
3	25	-26.6	7.37	-2.09	1.24	9.29
4	25	-26.7	6.83	-2.1	1.26	7.76
5	25	-26.7	6.47	-2.09	1.26	7.73
6	25	-25.9	7.37	-2.03	1.26	7.69
7	25	-25.7	6.53	-2.01	1.28	6.8
8	25	-25.5	6.08	-2	1.27	6.82
9	25	-25.2	6.65	-1.98	1.27	6.83
10	25	-24.8	7.25	-1.94	1.29	6.01
11	25	-25.3	7.02	-1.99	1.28	6.04
12	25	-22.7	7.15	-1.78	1.28	6.06
13	25	-22.5	5.92	-1.77	1.3	5.17
14	25	-19.9	5.46	-1.56	1.29	5.19
15	25	-19.2	5.78	-1.5	1.29	5.2
16	25	8.88	5.99	0.696	1.35	4.02
17	25	9.97	5.79	0.781	1.34	4.03
18	25	10.1	6.33	0.792	1.34	4.04
19	25	22.8	12.3	1.79	1.75	3.07
20	25	22.7	12.3	1.78	1.75	3.07
21	25	22.1	12.9	1.73	1.75	3.07
22	25	22.8	18.5	1.79	8.73	2.06
23	25	23.9	19.1	1.88	8.77	2.05
24	25	21.5	19.8	1.69	8.76	2.05
<b>Sample BSA 3.6 <math>\mu</math>M and polymer nanoparticles 153 nm with epoxy groups 3.75 mg/ml</b>						
Record	T	Zeta potential	Zeta deviation	Mobility	Conductivity	pH
	$^{\circ}$ C	mV	mV	$\mu$ mcm/Vs	mS/cm	
1	25	-24	8.32	-1.88	1.31	8.89
2	25	-24.2	8.85	-1.89	1.3	8.84
3	25	-25.1	10.4	-1.97	1.3	8.78

4	25	-23.8	7.7	-1.86	1.32	7.69
5	25	-24.2	8.85	-1.9	1.31	7.66
6	25	-23	9.98	-1.8	1.32	7.63
7	25	-21.9	9.05	-1.71	1.33	6.8
8	25	-22.6	8.92	-1.77	1.32	6.83
9	25	-22.9	8.69	-1.79	1.33	6.84
10	25	-21.5	8.22	-1.68	1.34	5.96
11	25	-20.8	8.98	-1.63	1.33	6.01
12	25	-20.7	8.25	-1.62	1.33	6.04
13	25	-18.1	7.3	-1.42	1.34	5.11
14	25	-17.9	6.44	-1.4	1.34	5.14
15	25	-17.4	7.13	-1.36	1.34	5.16
16	25	4.95	5.18	0.388	1.39	4.06
17	25	5.89	5.57	0.462	1.38	4.07
18	25	5.82	4.86	0.456	1.38	4.08
19	25	20.5	14.4	1.61	1.81	3.1
20	25	19.4	16.3	1.52	1.8	3.1
21	25	19.3	15.9	1.51	1.8	3.1
22	25	18.4	17.9	1.44	9.88	2.08
23	25	20.4	21	1.6	9.92	2.08
24	25	18	22.8	1.41	9.92	2.11

**Sample BSA 3.6  $\mu$ M and polymer nanoparticles 227 nm without epoxy groups 3.75 mg/ml**

Record	T °C	Zeta potential mV	Zeta deviation mV	Mobility $\mu$ mcm/Vs	Conductivity mS/cm	pH
1	25	-26.1	8.2	-2.05	1.65	9.56
2	25	-26.5	7.05	-2.08	1.78	9.56
3	25	-27.8	6.26	-2.18	1.4	8.4
4	25	-28	7.01	-2.2	1.51	8.4
5	25	-26.8	7.74	-2.1	1.43	6.54
6	25	-26.9	6.44	-2.11	1.52	6.54
7	25	-24	7.83	-1.88	1.35	6.05
8	25	-19.8	6.42	-1.55	1.39	4.91
9	25	-12.3	6.89	-0.968	1.38	4.55
10	25	21.2	9.42	1.67	1.61	3.05
11	25	21.3	10.6	1.67	1.67	3.05
12	25	26.2	8.89	2.05	2.53	2.48
13	25	26.3	7.95	2.06	2.58	2.48
14	25	26.4	14.1	2.07	2.49	2.48
15	25	24.5	8.32	1.92	2.38	2.48
16	25	24.4	10.3	1.92	2.27	2.48



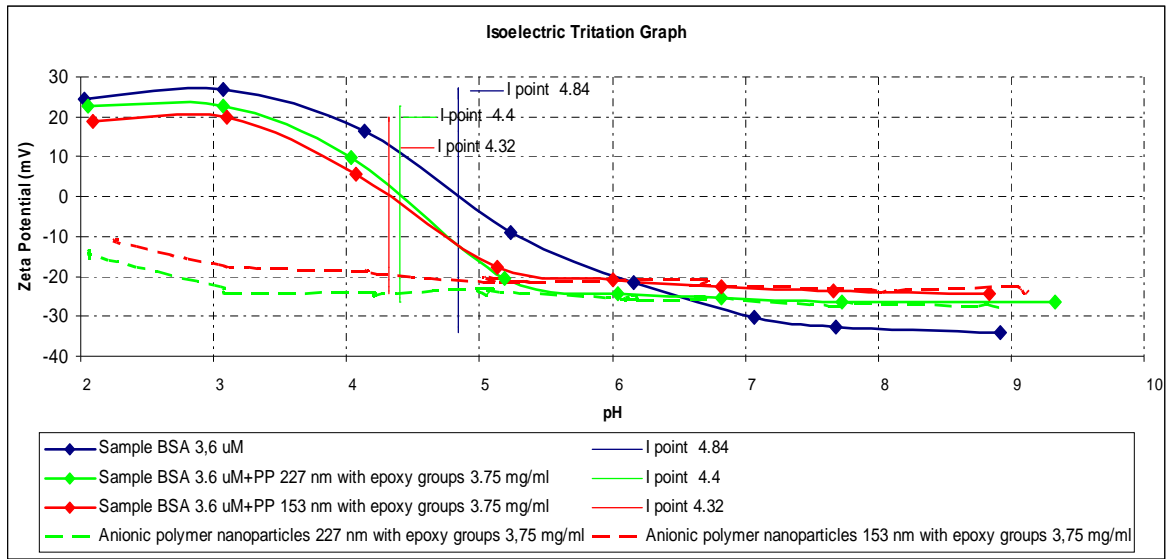


Figure 5.7. Isoelectric titration graph. Zeta potential at different pH of three samples of BSA+PP with epoxy groups. Size comparison. Blue line refers to BSA, green line to BSA+PP 227 nm and red line BSA+PP 153 nm.

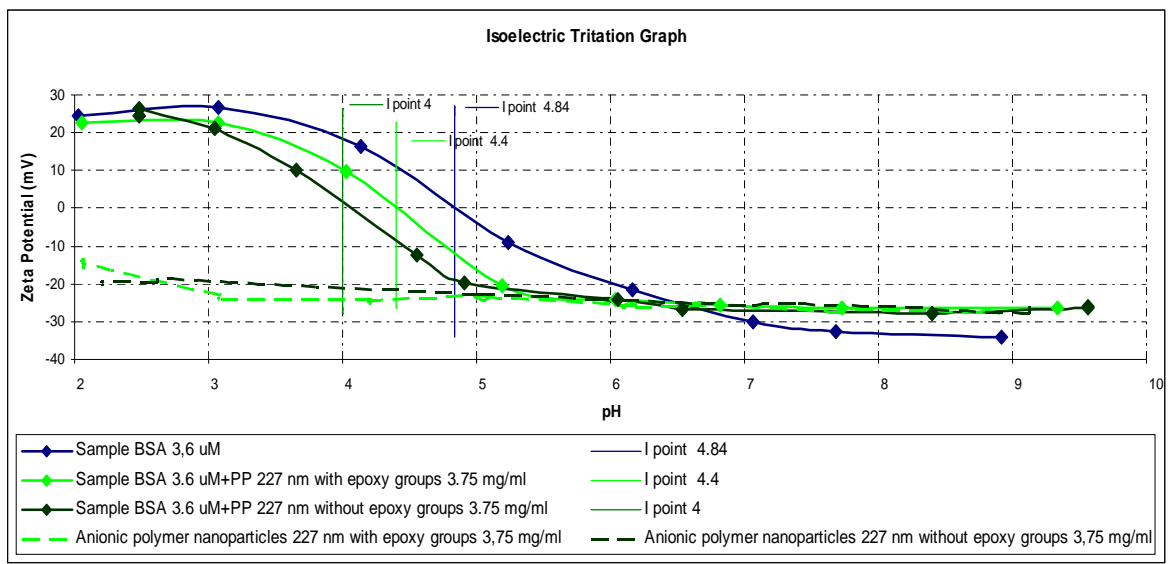


Figure 5.8. Isoelectric titration graph. Zeta potential at different pH of three samples of BSA+PP 227 nm. Surface groups comparison. Blue line refers to BSA, green line to BSA+PP with epoxy groups and dark green line BSA+PP without epoxy groups.

BSA protein had isoelectric point at  $4.84(\pm 0.05)$ . The value reduced until  $4.40(\pm 0.10)$ ,  $4.32(\pm 0.15)$  and  $4.00(\pm 0.10)$  when immobilized on polymer nanoparticles 227 nm with epoxy groups, 153 nm with epoxy groups and 227 nm without epoxy groups respectively. The changes in pI indicated that BSA protein suffered an alteration due to the interaction with anionic polymeric surface of nanoparticles. Unfortunately the grade of interaction can not be related to the sizes of nanoparticles since the shifts were almost the same and the results overlapped if the uncertainties were accounted (Figure 5.7). In contrast there existed some variation between polymer particles with epoxy groups and polymer particles without epoxy

groups (Figure 5.8). Polymer nanoparticles without epoxy groups seemed to alter the pI of the sample more. This fact reveals differences in the attachment of BSA on the polymer nanoparticles according to the surface groups. Thus the conclusion which derives is that exist some interaction between polymer nanoparticles and BSA protein and some differences in this interaction depending on the type of nanoparticles.

To further detail this information it is also requested to know the degree of conformational changes and the amount of protein attached. Fluorescence spectroscopy (section 5.3 *Fluorescence spectroscopy of BSA-polymer nanoparticle constructs*) and ITC (section 5.5 *Studies of immobilized BSA by isothermal titration calorimetry*) measurements are two tools used to obtain more detailed information.

### **5.3. Fluorescence spectroscopy of BSA-polymer nanoparticle constructs**

Fluorescence spectroscopy is regarded as a good system to evaluate conformational changes in BSA protein. BSA has two tryptophan (Trp) residues responsible for the fluorescence as it has been already mentioned: one embedded in the hydrophobic environment in the core and one which is present on the surface (section 2.2.2 *BSA protein*). Unfolding grade of BSA induces changes in the microenvironment surrounding these residues and result in a shift in the intrinsic fluorescence emission of the protein. The same occurs when a probe like ANS is used in extrinsic fluorescence. Here some tests were done with polymer nanoparticles at various pH. To prevent pH changes attributed to the counter ions of the ionic polymer nanoparticles, three kinds of buffer solutions were used; at pH 3.8 (sodium acetate buffer), 7.4 (potassium phosphate buffer), and 9.0 (sodium borate buffer). When BSA was immobilized on polymer nanoparticles in sodium acetate buffer (pH 3.8), the polymer nanoparticles precipitated slowly in the course of few minutes. This indicates that the protein-nanoparticle constructs formed by the polymer nanoparticles softly aggregated, with the positive charge of immobilized BSA acting as a bridge between negatively charged particles [50].

#### **5.3.1. Intrinsic and extrinsic fluorescence of polymer nanoparticles**

Fluorescence emission spectra of polymer nanoparticles 3.75 mg/ml were measured at three different pH (3.6, 7.4 and 9). Figure 5.9 show the results of intrinsic fluorescence and Figure 5.10, 5.11 and 5.12 the results of extrinsic ANS fluorescence.

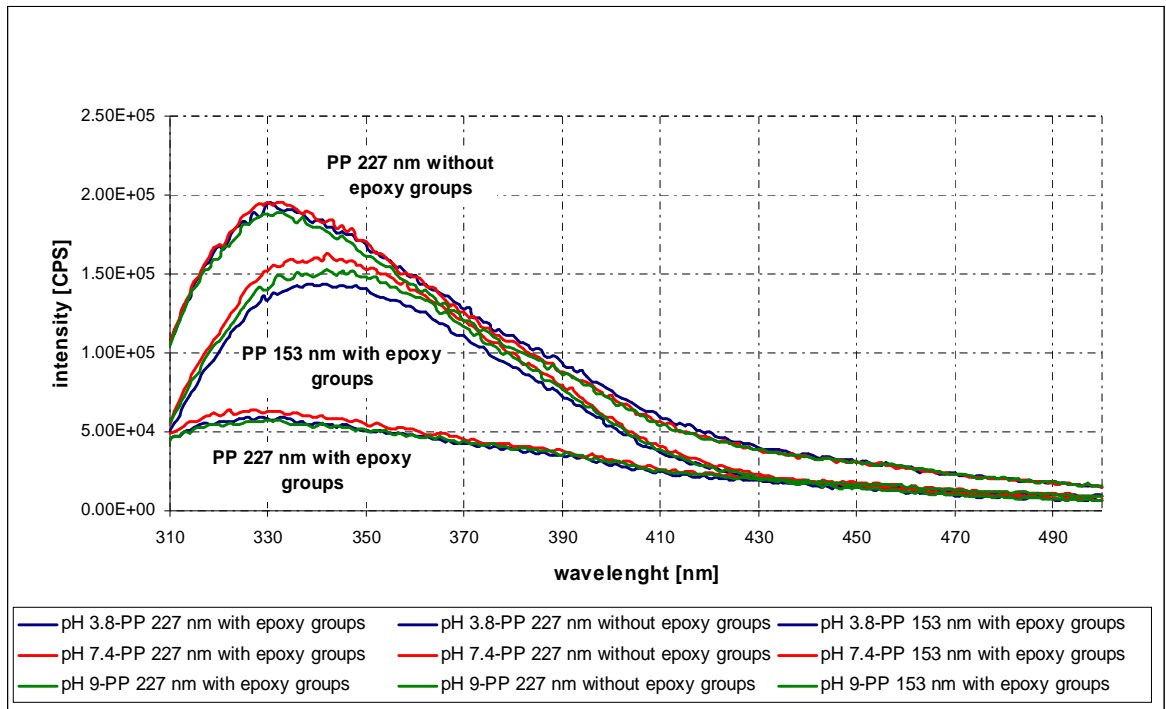


Figure 5.9. Intrinsic fluorescence emission spectra of polymer nanoparticles at different pH. The concentrations used were: polymer nanoparticles 3.75 mg/ml, ANS 0  $\mu$ M. Excitation wavelength 295 nm, slit 5, polarization 90°.

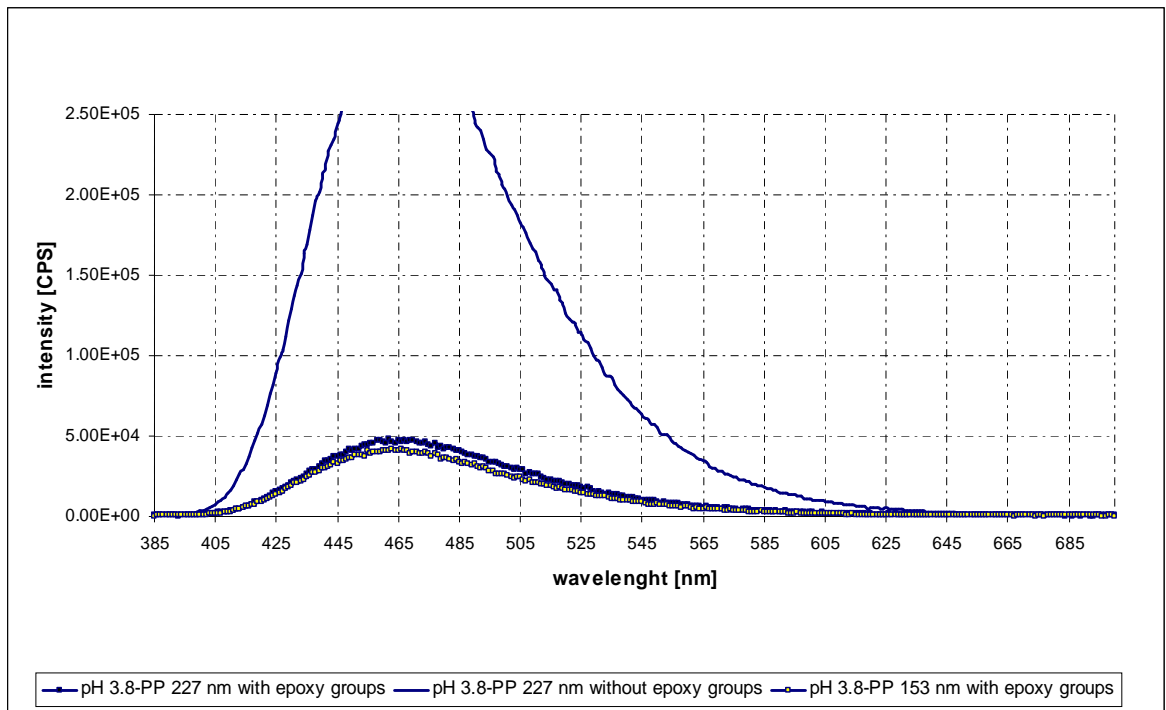


Figure 5.11. Extrinsic ANS fluorescence emission spectra of polymer nanoparticles at pH 3.8. The concentrations used were: polymer nanoparticles 3.75 mg/ml, ANS 17  $\mu$ M. Excitation wavelength 370 nm, slit 1, without polarization.

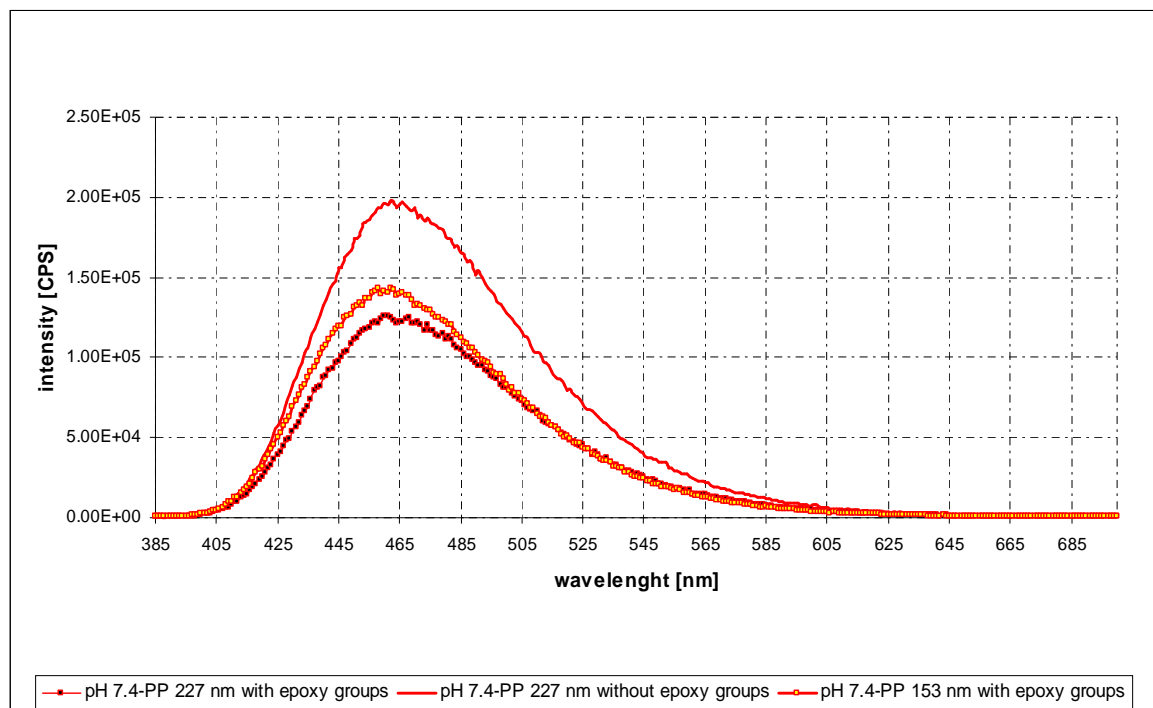


Figure 5.11. Extrinsic ANS fluorescence emission spectra of polymer nanoparticles at pH 7.4. The concentrations used were: polymer nanoparticles 3.75 mg/ml, ANS 17  $\mu$ M. Excitation wavelength 370 nm, slit 1, without polarization.

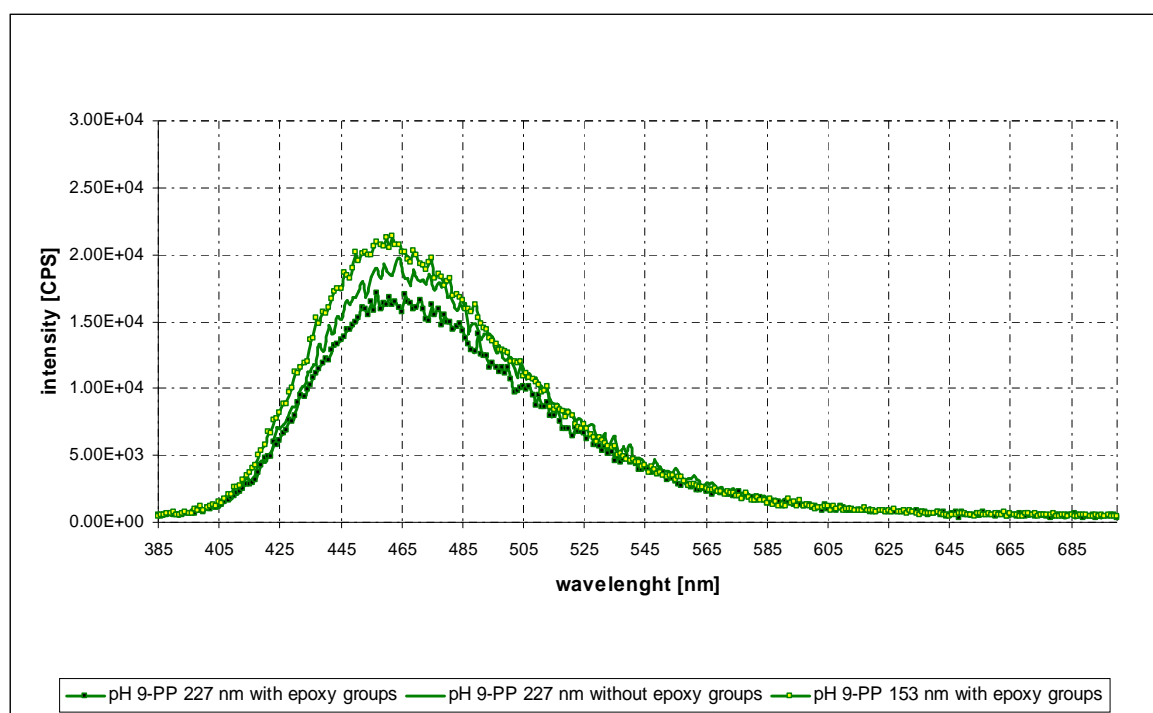


Figure 5.12. Extrinsic ANS fluorescence emission spectra of polymer nanoparticles at pH 9. The concentrations used were: polymer nanoparticles 3.75 mg/ml, ANS 17  $\mu$ M. Excitation wavelength 370 nm, slit 1, without polarization.

Intrinsic fluorescence of polymer nanoparticles did not depend on pH. In this case spectra only changed if polymer nanoparticles were different and not with respect of pH at which the samples was as it can be seen in Figure 5.9. This fact indicates that polymer nanoparticles were stable throughout the pH-range. Wavelength of maximum intensity increased 15-20 nm by decreasing the size of nanoparticles. In the case of nanoparticles with the same size those without epoxy groups presented more intensity in the emission spectra without changing the wavelength of maximum emission. In reference to extrinsic fluorescence opposite happens. Fluorescence was pH-dependent, highest at pH 7.4 and minimum at pH 9, and it did not depend on polymer nanoparticles size with the wavelength at maximum intensity around 465 nm in all cases. Polymer nanoparticles were not porous [50] but it could be possible that ANS bound on the surface in such a way that the fluorescence emission increased, allegedly with greater intensity at pH 7.4, or it could also be an effect of using different buffers. Unlike the previous case, polymer nanoparticles without epoxy groups presented bigger discrepancy by decreasing pH, with higher emission intensity (Figure 5.11). The reason could be that in polymer nanoparticles without epoxy groups charge changed more with pH due to protonation/deprotonation. This could affect possible bindingsites for ANS. Epoxy groups are not that dependent of pH, so ANS no matter which pH at least be able to bind to the epoxy groups.

The most interesting information is the fluorescence of BSA protein and not the fluorescence of polymer nanoparticles. However, it is necessary to know this last one to eliminate the interference of polymer nanoparticles and to study only changes in BSA protein.

### 5.3.2. Intrinsic and extrinsic fluorescence of BSA

BSA Trp fluorescence and BSA extrinsic ANS fluorescence emission spectra were studied at pH 3.8, 7.4 and 9. Three samples BSA 3.6  $\mu\text{M}$  at each pH were done and measured. Figure 5.13 show obtained results in intrinsic fluorescence and Figure 5.14 results in extrinsic fluorescence.

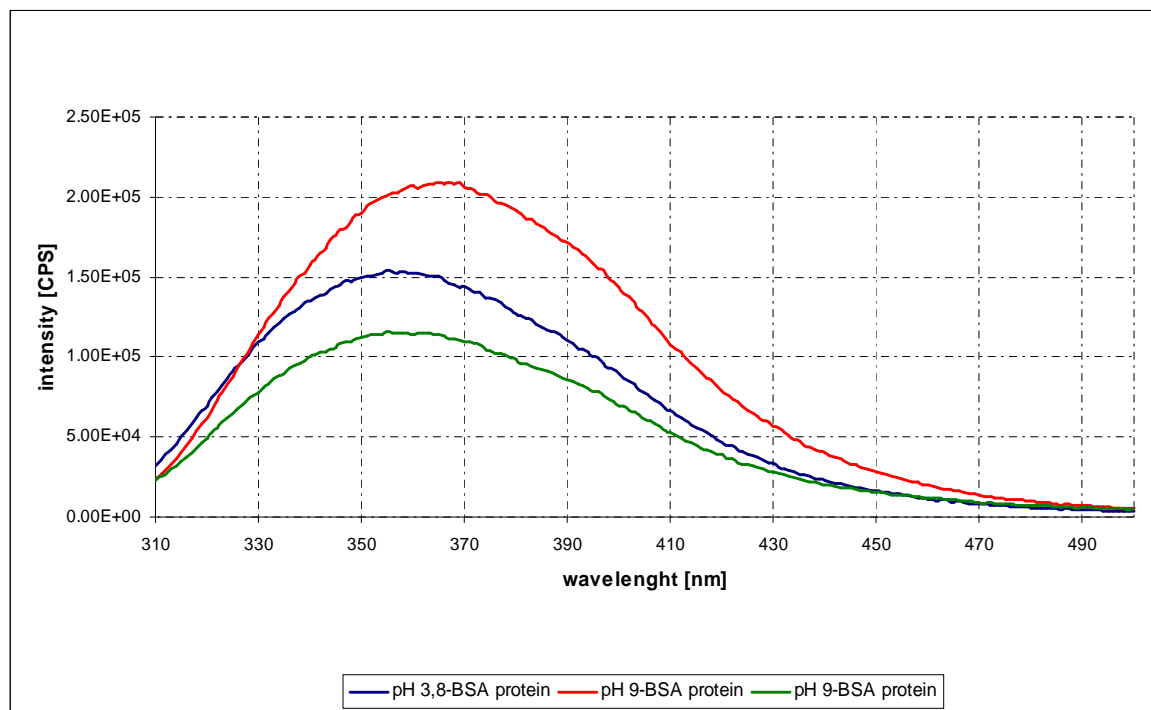


Figure. 5.13. Intrinsic fluorescence emission spectra of BSA at different pH. The concentrations used were: BSA 3.6  $\mu$ M, ANS 0  $\mu$ M. Excitation wavelength 295 nm, slit 5, polarization 90°.

Li *et al.* 2007 [65] have reported BSA Trp fluorescence spectra in phosphate buffer at the same pH noted above, where it was found that fluorescence intensity was inversely correlated to pH value, with the intensity at pH 9 being the lowest. However, Yasuda *et al.* [50] found that BSA fluorescence intensity was at a maximum at pH 7.4 and attributed the discrepancy to differences in buffer systems used between studies. In the present work the buffer solutions that were used were the same as Yasudas *et al.* [50] work for this reason the maximum intensity was at pH 7.4 and the minimum at pH 9, being at pH 3.8 in an intermediate level. The maximum emission peak positions at pH 3.8, 7.4, and 9 were 358, 366, 358 nm, respectively. It was around 10 nm higher than expected [65][50] but the parameter that gives us information is the difference and not the value, so this fact does not alter the conclusions. Finally, it should be mentioned that variation in BSA emission maxima at different pH could be related to conformational isomerisation induced by the conditions in which the protein was subjected. At pH 7.4 BSA was in native form and the emission intensity was maximum. At pH 3.8 and pH 9 it was in partially unfolded conformations, F form and B form respectively, and the fluorescence intensity decreased (section 2.2.2 *BSA protein*).

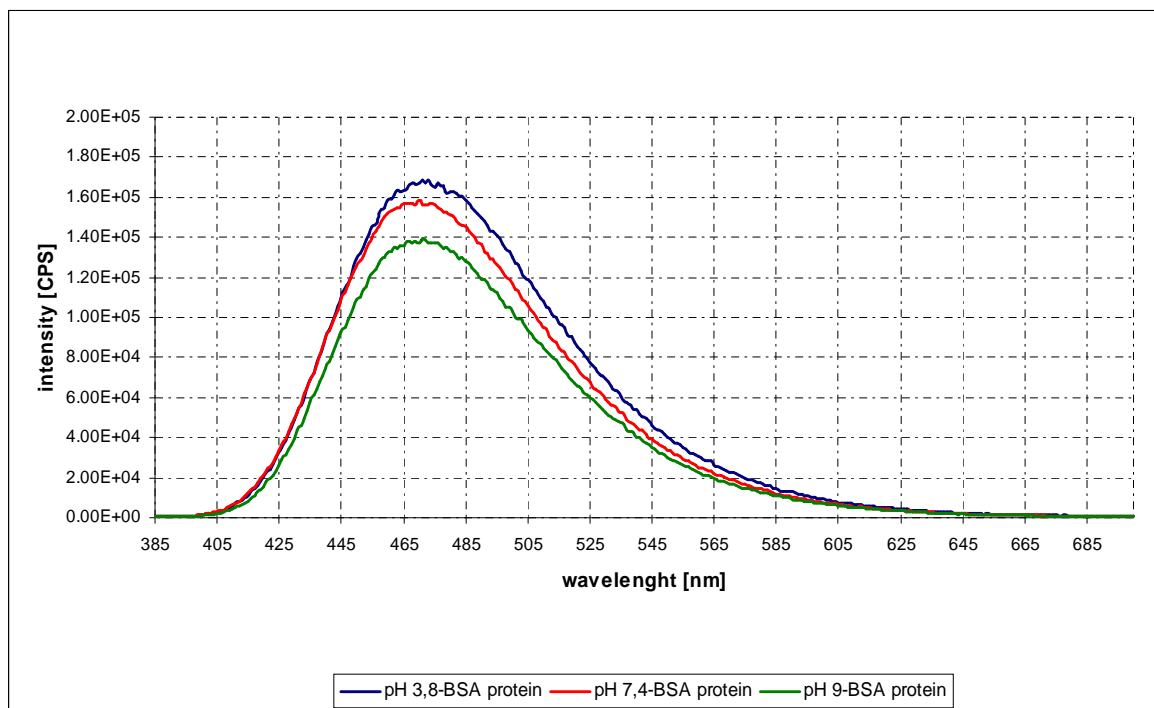


Figure 5.14. Extrinsic ANS fluorescence emission spectra of BSA at different pH. The concentrations used were: BSA 3.6  $\mu\text{M}$ , ANS 0  $\mu\text{M}$ . Excitation wavelength 295 nm, slit 5, polarization 90°.

BSA extrinsic fluorescence emission spectra (Figure 5.14) did not change significantly with the pH and just to clarify that at high pH the intensity decreased. It is known that ANS buried by hydrophilic environment has its maximum emission at 500 nm while if it is in hydrophobic atmosphere the value shifts to shorter wavelength. In all cases the maximum was around 470 nm and therefore BSA protein was not unfolded and ANS surrounded by non-polar groups. We expect that BSA-polymer nanoparticles constructs show a low increase in the corresponding wavelength.

All modifications produced by mixing BSA protein with the particles are studied in later sections.

### 5.3.3. Intrinsic and extrinsic fluorescence of BSA-polymer nanoparticle constructs. Particles size comparison.

Different BSA-polymer nanoparticle construct were done in order to elucidate the effect of polymer nanoparticles in BSA protein conformation. Two different types of polymer nanoparticles with epoxy groups were chosen; polymer nanoparticles 227 nm and polymer nanoparticles 153 nm. It is expected a covalent binding with lysine, histidine and arginine residues on the protein. Table 5.7 shows all the samples and its composition.

Table 5.7. BSA-polymer nanoparticle constructs. Polymer nanoparticles 3.75 mg/ml, BSA 3.6  $\mu\text{M}$ . Size comparison.

Sample	pH	Polymer nanoparticles type
1	3.8	Polymer nanoparticles 227 nm with epoxy groups
2	7.4	Polymer nanoparticles 227 nm with epoxy groups
3	9	Polymer nanoparticles 227 nm with epoxy groups
4	3.8	Polymer nanoparticles 153 nm with epoxy groups
5	7.4	Polymer nanoparticles 153 nm with epoxy groups
6	9	Polymer nanoparticles 153 nm with epoxy groups

Each sample was divided in two and half mixed with ANS 17  $\mu\text{M}$ . Finally fluorescence emission spectroscopy was completed and the results compared with the spectra of BSA obtained in the previous section. Constant spectra of polymer nanoparticles were subtracted from the diminished spectra of the protein. Figure 5.15 shows the results of intrinsic fluorescence and Figure 5.16 the result of extrinsic fluorescence.

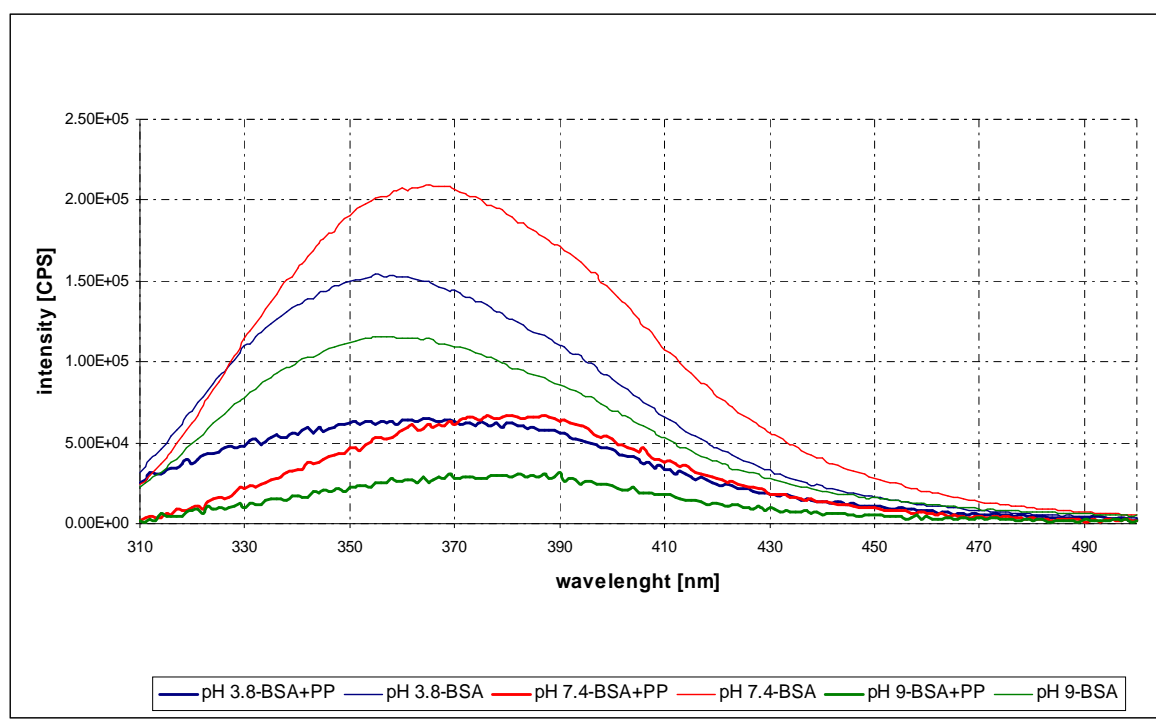


Figure 5.15. Intrinsic fluorescence emission spectra of BSA in the presence and absence of polymer nanoparticles at different pH. The concentrations used were: polymer nanoparticles 227 nm with epoxy groups 3.75 mg/ml (if it corresponds), BSA 3.6  $\mu\text{M}$ , ANS 0  $\mu\text{M}$ . Excitation wavelength 295 nm, slit 5, polarization 90°. Constant spectra of polymer nanoparticles were subtracted from the diminished spectra of the protein.



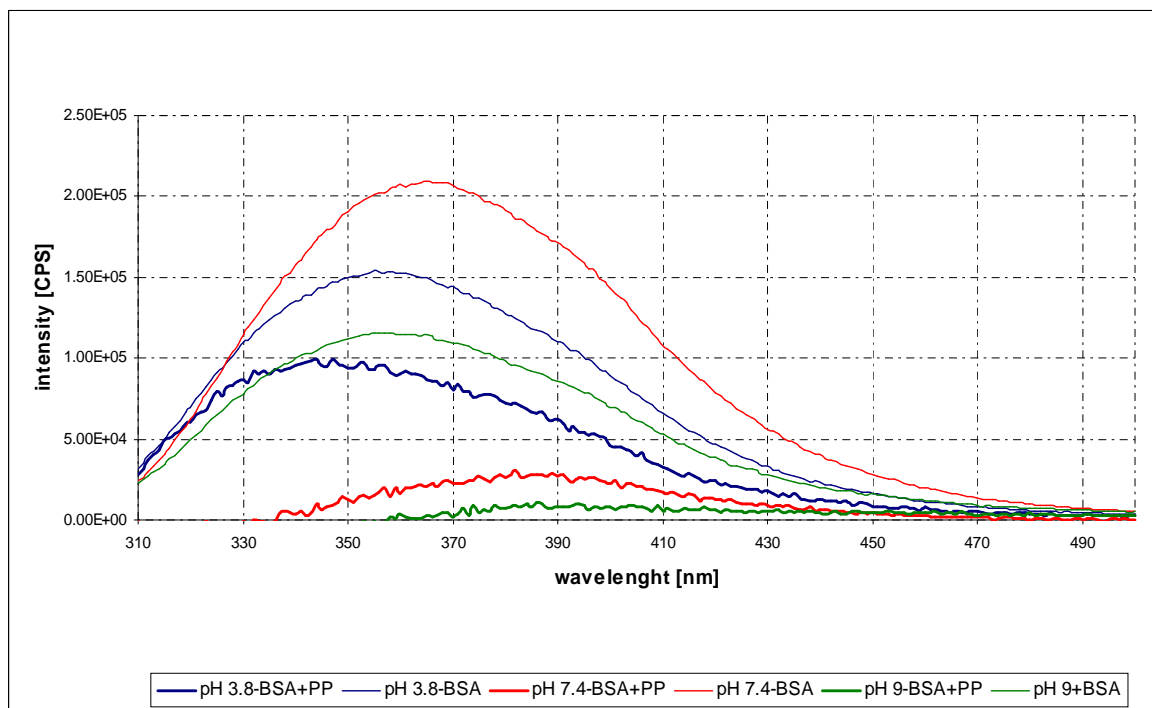


Figure 5.16 Intrinsic fluorescence emission spectra of BSA in the presence and absence of polymer nanoparticles at different pH. The concentrations used were: polymer nanoparticles 153 nm with epoxy groups 3.75 mg/ml (if it corresponds), BSA 3.6  $\mu$ M, ANS 0  $\mu$ M. Excitation wavelength 295 nm, slit 5, polarization 90°. Constant spectra of polymer nanoparticles were subtracted from the diminished spectra of the protein.

Concerning the intrinsic fluorescence, all samples with only BSA showed more intensity at all pH, regardless of the size of nanoparticles. This is a signal which could confirm that Trp residues of BSA protein were exposed to more hydrophilic environment when interacted with nanoparticles. However, polymer nanoparticles can act as a quencher, as well as they provide scattering which might reduce the signal. The emission wavelength also experienced changes. With the exception of acidic pH, which did not shift the emission maxima, the wavelength of maximum intensity increased until approximately 385 nm in pH 7.4 and pH 9 with respect to the signals of free BSA at these pH. The red shift of the maximum emission could mean a hydrophilic shift in the microenvironment surrounding the Trp residues of immobilized BSA, which might be attributed to partial unfolding of the protein [65]. Using these techniques it was not possible to determine the total amount of free or attached BSA protein but the method confirmed that conformational changes exist. It seems that the most important alterations occurred at pH 7.4, followed by pH 9, and finally at pH 3.8 it was quite more difficult to find any pattern and BSA could be only attached and not unfolding. Regarding the results between polymer nanoparticles 227 nm and polymer nanoparticles 153 nm, no significant changes were observed. Induced modifications in BSA proteins were more or less equivalent as there were no differences in wavelengths. The signal strength was weaker in small particles than in large particles. It could be related to the number of attached protein and not to conformational changes. With the same amount of

polymer nanoparticles the number and the surface area of small particles should be higher than the number and the surface area of large polymer nanoparticles.

It can be concluded that polymer nanoparticles with epoxy groups induce pH-dependent alterations in BSA proteins, beforehand with greater impairment at pH 7.4 and these changes can not be related to the size of the particles in the range of study.

Below the results of ANS fluorescence are shown (Figure 5.17 and 5.18). In contrast to the previous case, here the emission spectra are presented in two graphics; one with the constant spectra of polymer nanoparticles subtracted from the diminished spectra of the protein and another without any subtraction.

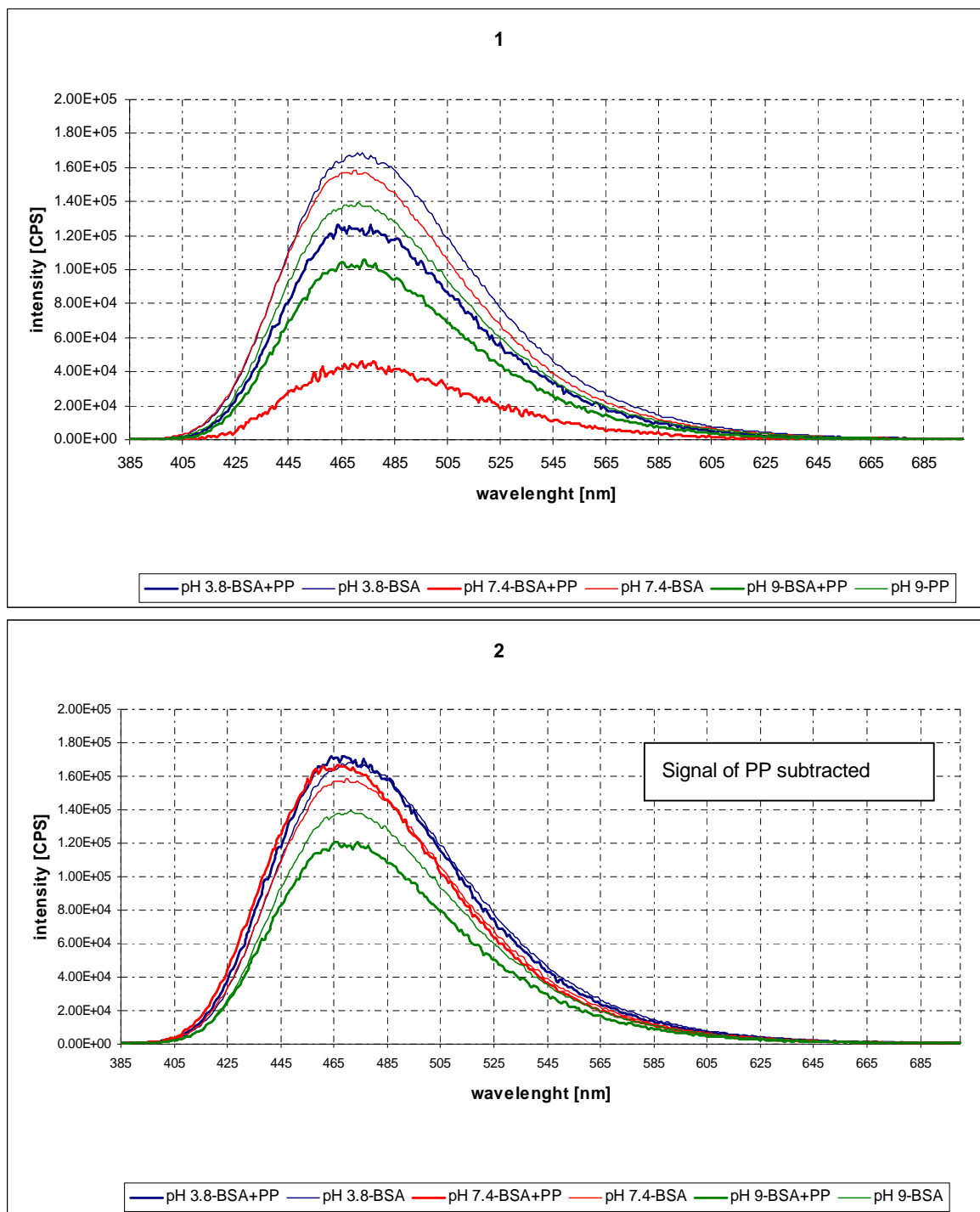


Figure 5.17. Extrinsic ANS fluorescence emission spectra of BSA in the presence and absence of polymer nanoparticles at different pH. The concentrations used were: polymer nanoparticles 227 nm with epoxy groups 3.75 mg/ml (if it corresponds), BSA 3.6  $\mu$ M, ANS 17  $\mu$ M. Excitation wavelength 370 nm, slit 1, without polarization. Graphic 1 show the results with the constant spectra of polymer nanoparticles subtracted from the diminished spectra of the protein. Graphic 2 show the results without the constant spectra of polymer nanoparticles subtracted from the diminished spectra of the protein.

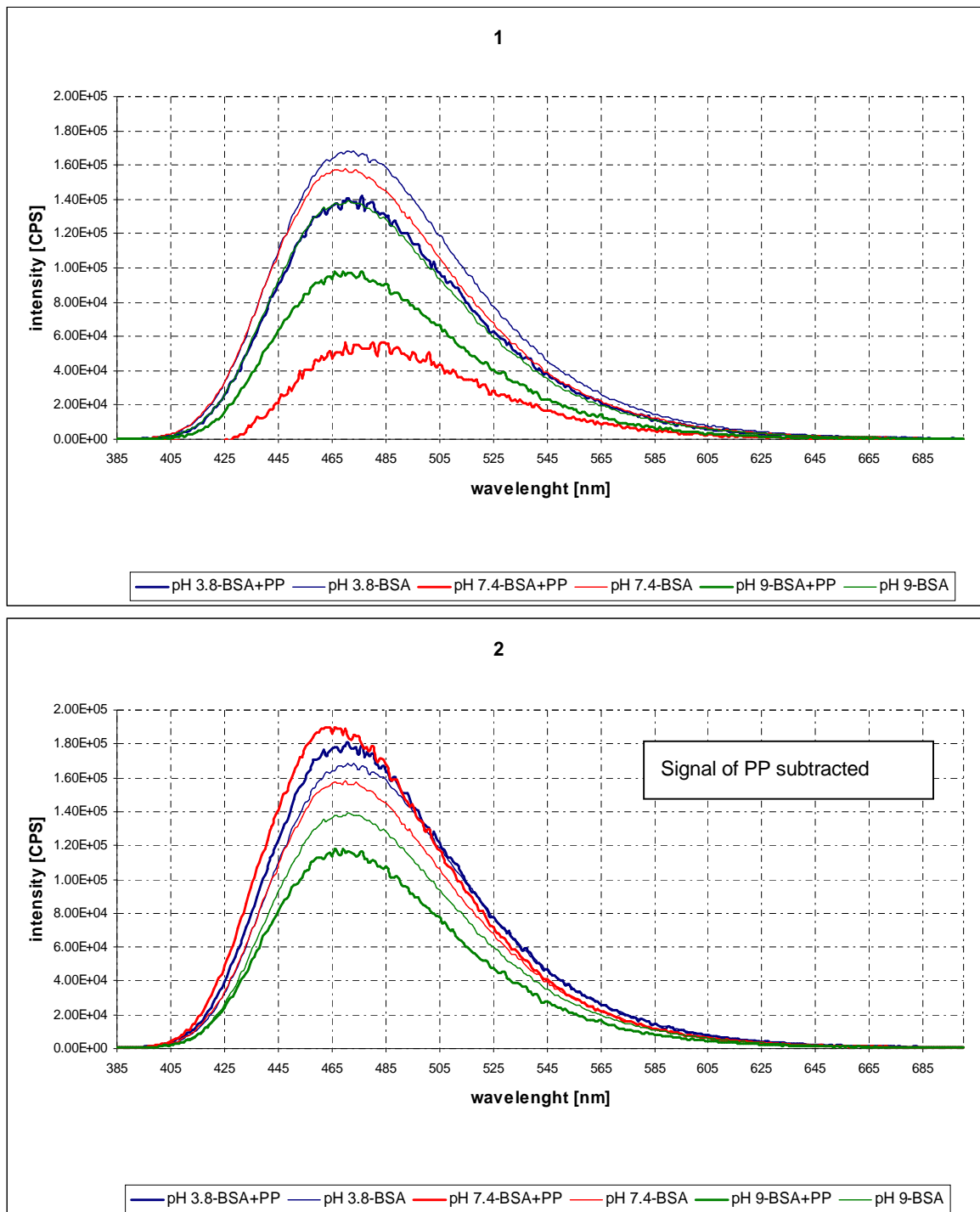


Figure. 5.18 Extrinsic ANS fluorescence emission spectra of BSA in the presence and absence of polymer nanoparticles at different pH. The concentrations used were: polymer nanoparticles 153 nm with epoxy groups 3.75 mg/ml (if it corresponds), BSA 3.6  $\mu$ M, ANS 17  $\mu$ M. Excitation wavelength 370 nm, slit 1, without polarization. Graphic 1 show the results with the constant spectra of polymer nanoparticles subtracted from the diminished spectra of the protein. Graphic 2 show the results without the constant spectra of polymer nanoparticles subtracted from the diminished spectra of the protein.

Given only the graphics with the constant signal of polymer nanoparticles subtracted, it was possible to observe that the intensity of BSA-polymer nanoparticle constructs were always weaker than the intensity with only BSA protein. This fact indicated that ANS resides in a more polar environment when polymer nanoparticles were present in the sample. The main difference was at pH 7.4, followed by pH 9, which matches what was reported before. The maximum emission peaks almost did not change and it was possible only see a slight increase at pH 7.4 from 470 nm to 480 nm. Concerning the results of two types of nanoparticles size, no important variations were appreciated and the conduct was similar. However, it would not be entirely correct to compare only the results of the samples with the signal of the particles removed. ANS fluorescence is affected for BSA and polymer nanoparticles at the same time. For this reason, now it makes reference to the other two graphics (graphic 2 of Figure 5.17 and 5.18) with no polymer nanoparticles signal subtracted. Spectra at pH 3.8 almost did not change, spectra at pH 7.4 increase its intensity in relation to the sample of BSA and at pH 9 spectra decrease. Finally in all cases the wavelength of maximum emission shifted slightly to lower value, from 470 to 465 approximately. Although it might seem meaningless it is not the case. The decrease in the wavelength could be explained because ANS-BSA were closer packed on the particle surface and thus more protected from solvent. Referring to the signal with and without polymer nanoparticles interference, more differences were at pH 7.4 which means that the total amount of ANS attached on the polymer nanoparticles was higher than the other two in this value. At pH 3.8 and 9 ANS was not affected for the polymer nanoparticles and there are not so many changes before and after to remove polymer nanoparticles signal. Thus it is possible to conclude the same has been said so far, but should it be clarify that at pH 7.4 spectra is interfered by polymer nanoparticles.

Herein, it seems that the most favourable condition for partial unfolding of BSA was at pH 7.4. In the study reported by Yasudas *et al.* [50] the immobilized amount of BSA on anionic polymer nanoparticles at pH 3.8 was highest of all tested in that study and concluded that this could be explained either by dimer formation onto epoxy-coated polymer nanoparticles below the pI of BSA, or by optimized packing of the protein layer under these conditions. However, at or close to complete surface coverage, the protein was tightly packed and more likely to retain its native structure, whereas low fractional surface coverage in that case enabled multipoint conjugation with available epoxy groups. This might explain the results which demonstrate that highest degree of conformational changes were at neutral and high pH instead at low pH.

#### 5.3.4. Intrinsic and extrinsic fluorescence of BSA-polymer nanoparticle constructs. Surface group comparison.

Two different types of polymer nanoparticles with the same size was used, one with epoxy groups and one without epoxy groups, and the fluorescence spectra of BSA-polymer nanoparticle were compared. The polymer nanoparticle with epoxy groups was the same as the previous point. It is expected electrostatic attachment and covalent binding with lysine, histidine and arginine residues on the polymer nanoparticles with epoxy groups and just electrostatic attachment in polymer nanoparticles without epoxy groups. Table 5.8 shows all the samples and its composition.

Table 5.8. BSA-polymer nanoparticle constructs. Polymer nanoparticles 3.75 mg/ml, BSA 3.6  $\mu$ M. Surface group comparison.

Sample	pH	Polymer nanoparticles type
7	3.8	Polymer nanoparticles 227 nm without epoxy groups
8	7.4	Polymer nanoparticles 227 nm without epoxy groups
9	9	Polymer nanoparticles 227 nm without epoxy groups

Each sample was divided in two, then one half was mixed with ANS 17  $\mu$ M as in the previous section. Finally fluorescence emission spectroscopy was completed and the results compared with the spectra of BSA. Polymer nanoparticles fluorescence spectra were also remove from the signal. Figure 5.19 shows the results of intrinsic fluorescence and Figure 5.20 the result of extrinsic fluorescence.

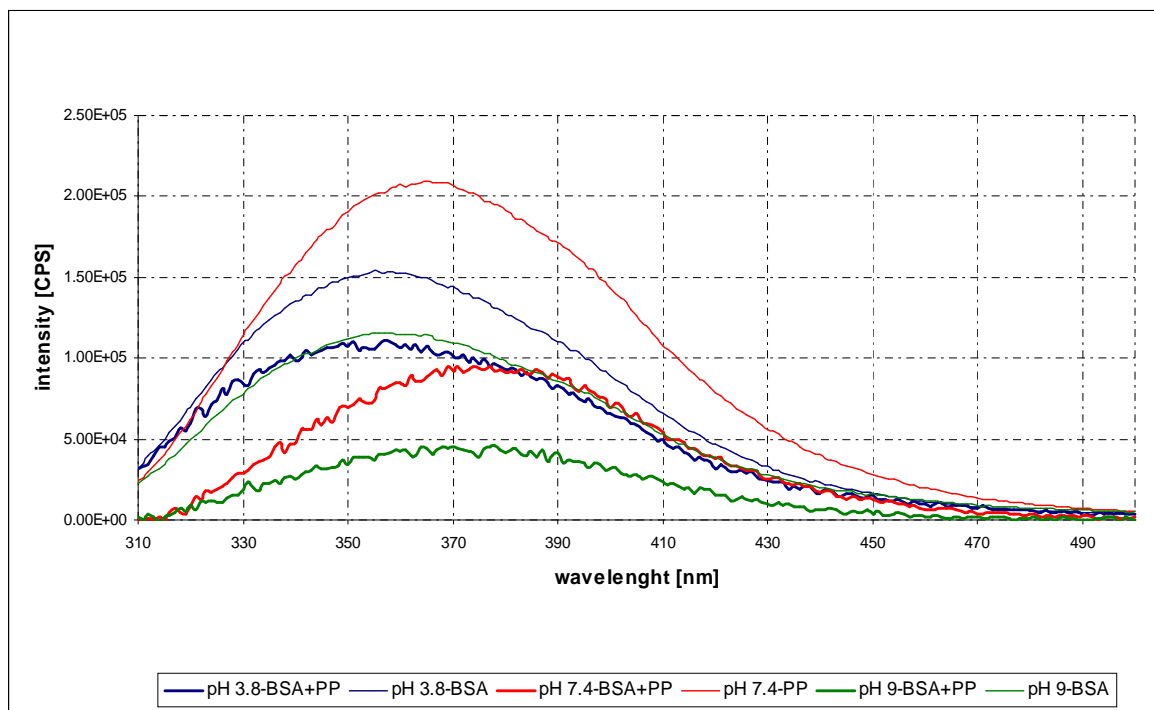


Figure. 5.19. Intrinsic fluorescence emission spectra of BSA in the presence and absence of polymer nanoparticles at different pH. The concentrations used were: polymer nanoparticles 227 nm without epoxy groups 3.75 mg/ml (if it corresponds), BSA 3.6  $\mu$ M, ANS 0  $\mu$ M. Excitation wavelength 295 nm, slit 5, polarization 90°. Constant spectra of polymer nanoparticles were subtracted from the diminished spectra of the protein.

The results of polymer nanoparticles without epoxy groups were in accordance with the others; all samples with polymer nanoparticles had less intensity, higher wavelength of maximum emission and it was difficult to find any meaning at pH 3.8. However, some important differences could be observed. The intensity of samples containing polymer nanoparticles without epoxy groups was a bit higher than in the other samples and this is an evidently indication which verify that Trp residues were buried for more hydrophobic environment and BSA protein less unfolded. The red shift of the maximum emission peak was not as pronounced as in particles with epoxy groups, 380 nm at pH 7.4 and 375 nm at pH 9 instead of 385 nm as the other cases. Thus it could be possible that polymer nanoparticles without epoxy groups, independently of the total amount of attached BSA, induced less conformational changes in the protein.

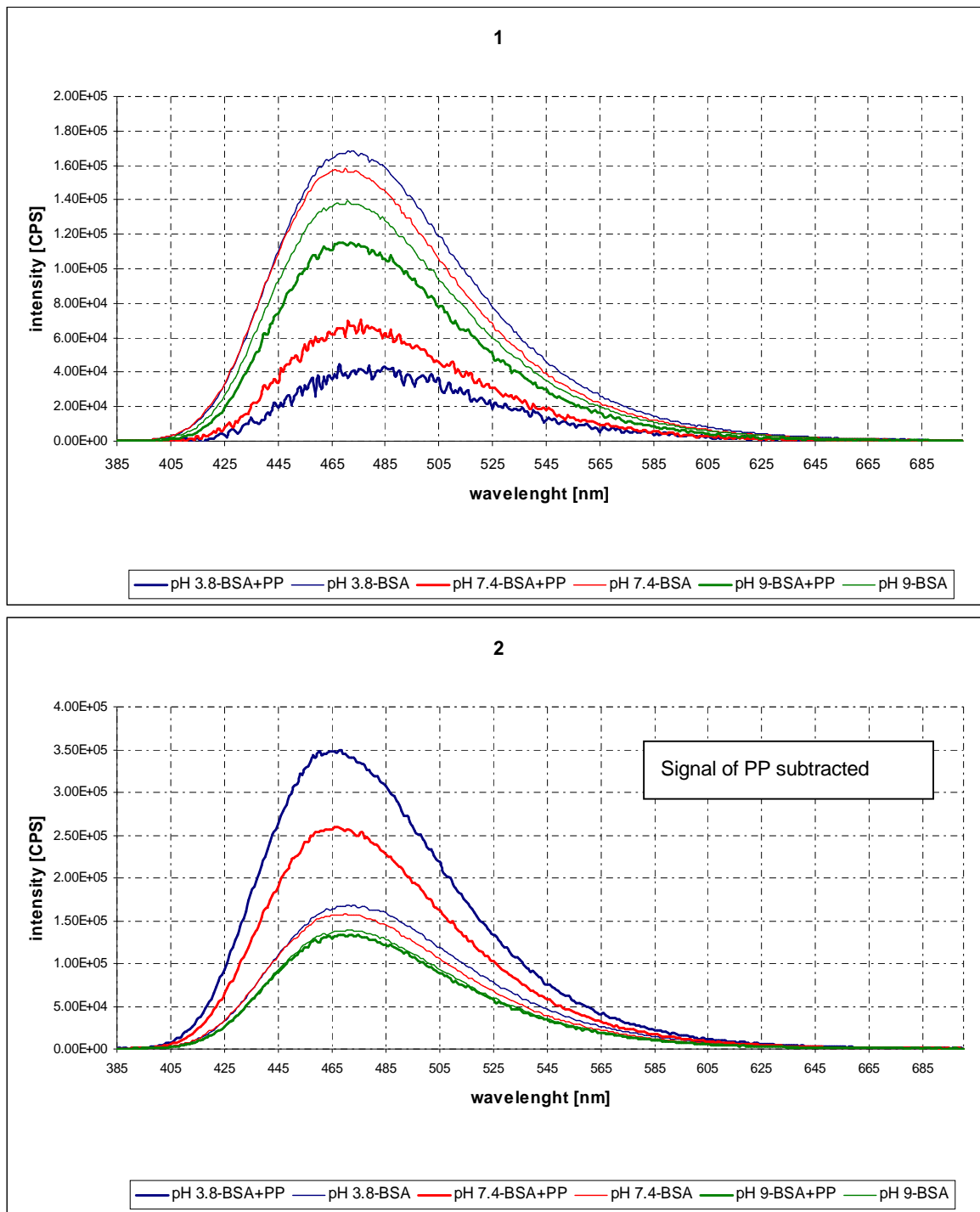


Figure. 5.20. Extrinsic ANS fluorescence emission spectra of BSA in the presence and absence of polymer nanoparticles at different pH. The concentrations used were: polymer nanoparticles 227 nm without epoxy groups 3.75 mg/ml (if it corresponds), BSA 3.6  $\mu$ M, ANS 17  $\mu$ M. Excitation wavelength 370 nm, slit 1, without polarization. Graphic 1 show the results with the constant spectra of polymer nanoparticles subtracted from the diminished spectra of the protein. Graphic 2 show the results without the constant spectra of polymer nanoparticles subtracted from the diminished spectra of the protein.



Extrinsic fluorescence spectra of polymer nanoparticles without epoxy groups differed considerably from the values of polymer nanoparticles with epoxy groups. Given only the graphics with the constant spectra of polymer nanoparticles subtracted (figure 6.16 graphic 1 and 3), the intensity of BSA-polymer nanoparticle constructs remained weaker than the intensity with only BSA protein. However, the sequence pH 7.4, pH 9 and pH 3.8 respects to the importance of changes was not followed. In this case interaction between BSA and polymer nanoparticles was purely electrostatic and this is the reason for the results. At pH 9 it was hardly any changes in emission intensity because the surface charge for both BSA and polymer nanoparticles was negative, and electrostatic repulsion occurred, while the most important variation was at pH 3.8 where proteins had positively surface charge and proteins negatively charge. There was no change in the emission maxima and only at pH 7.4 was it possible to identify some shifts, from 470 nm of BSA to 475 nm of BSA-polymer nanoparticle. For this reason it was possible that, although the immobilized amount of BSA on anionic polymer nanoparticles at pH 3.8 was highest, the protein was tightly packed and more likely to retain its native structure. The intensity and wavelength changes were not as pronounced as for polymer nanoparticles with epoxy groups, which means that covalent bonding induced more conformational changes. Compared to the other two graphics (Figure 7.16, graphics 2 and 4), which the baseline was extracted, there was no big difference in the emission from ANS at pH 9 whether the PP-baseline was subtracted or not. On the other hand, at pH 7.4 and pH 3.8 there was a big discrepancy in the intensity before and after the baseline extraction. Intensity increases a lot and the wavelength decrease slightly if baseline is not removed; these events could be related to the binding of ANS to the polymer nanoparticles instead of BSA, maybe because sulfonate group of ANS was strong attracted by positively surface charges of the nanoparticles.

Herein, it seems that polymer nanoparticle without epoxy groups induced less conformational changes to BSA protein. The most favourable conditions could be at pH 7.4 (as in the previous cases) while at pH 9 electrostatic repulsion was too strong and at pH 3.8 electrostatic binding was tightly and favourable to retain protein native structure. Thus, as a finally conclusions it appears that big polymer nanoparticles with epoxy groups are the best option and pH 7.4 the best conditions.

## **5.4. Unfolding studies of immobilized BSA using urea in combination with ANS**

The use of urea as denaturation agent induces to protein unfolding [116]. Thus by increasing the concentration of urea in a sample containing BSA it is possible to study the different intermediate state that following the complete denaturation of the protein. The present section aims to elucidate the conformational changes experimented by BSA-polymer nanoparticle constructs caused by varying denaturation conditions. Structural changes were detected by fluorescence spectroscopy using ANS as an external probe.

### **5.4.1. Extrinsic fluorescence of BSA-polymer nanoparticle constructs in urea solution.**

Polymer nanoparticles 227 nm and 153 nm with epoxy groups were used in the experiment. Figure 5.21 and 5.22 show the fluorescence emission spectra of BSA with polymer nanoparticles 227 nm and polymer nanoparticles 153 nm in different urea concentration and pH. Finally maximum intensity as a function of urea concentration in each case was plotted in Figure 5.23.

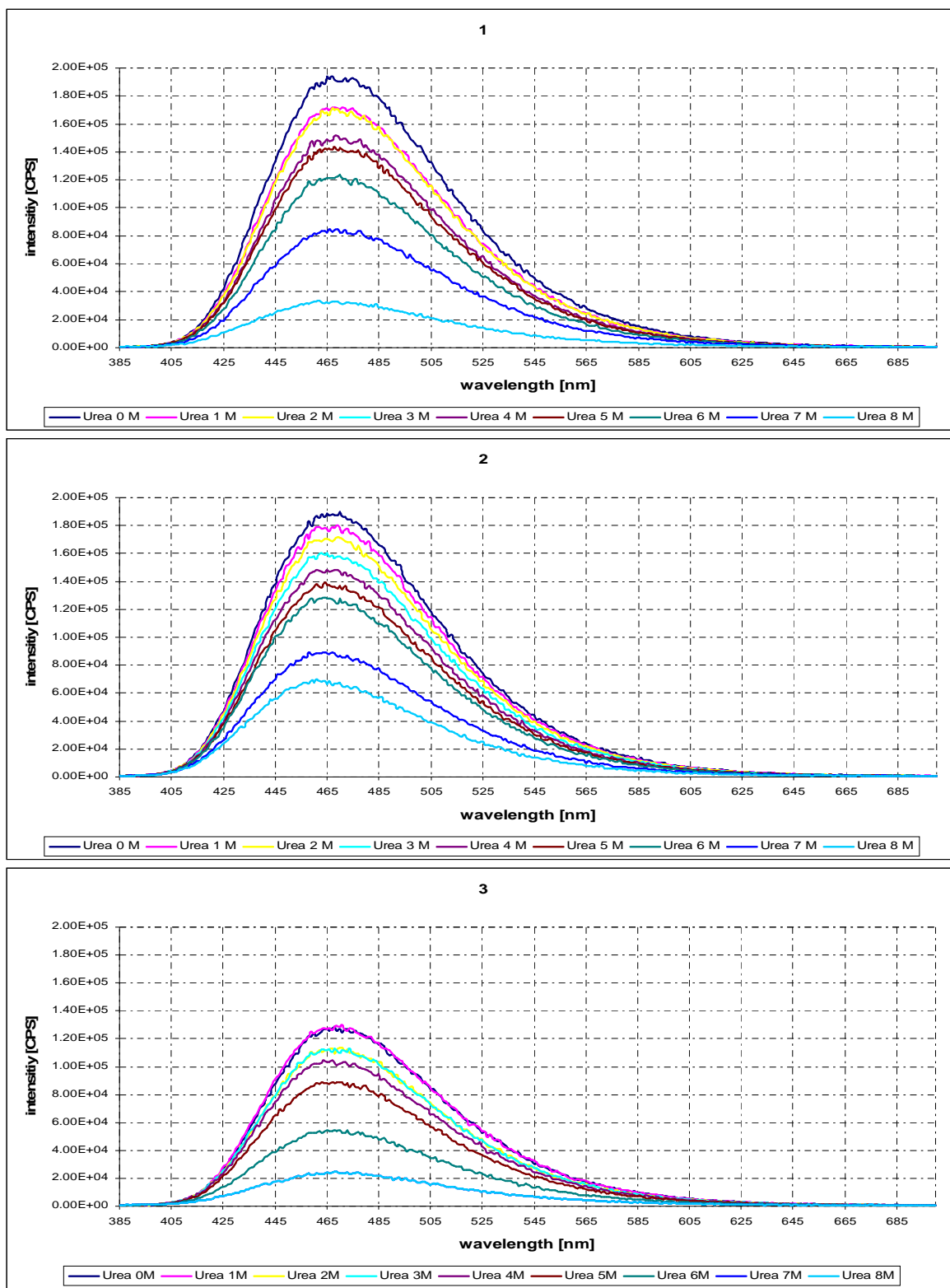


Figure 5.21. Extrinsic ANS fluorescence emission spectra of BSA in the presence of polymer nanoparticles 227 nm with epoxy groups and different urea concentrations. The concentrations used were: polymer nanoparticles 3.75 mg/ml, BSA 3.6  $\mu$ M, ANS 17  $\mu$ M, urea 0-8 M. Excitation wavelength 370 nm, slit 1, without polarization. Graphic 1 shows the results at pH 3.8. Graphic 2 shows the results at pH 7.4. Graphic 3 shows the results at pH 9.

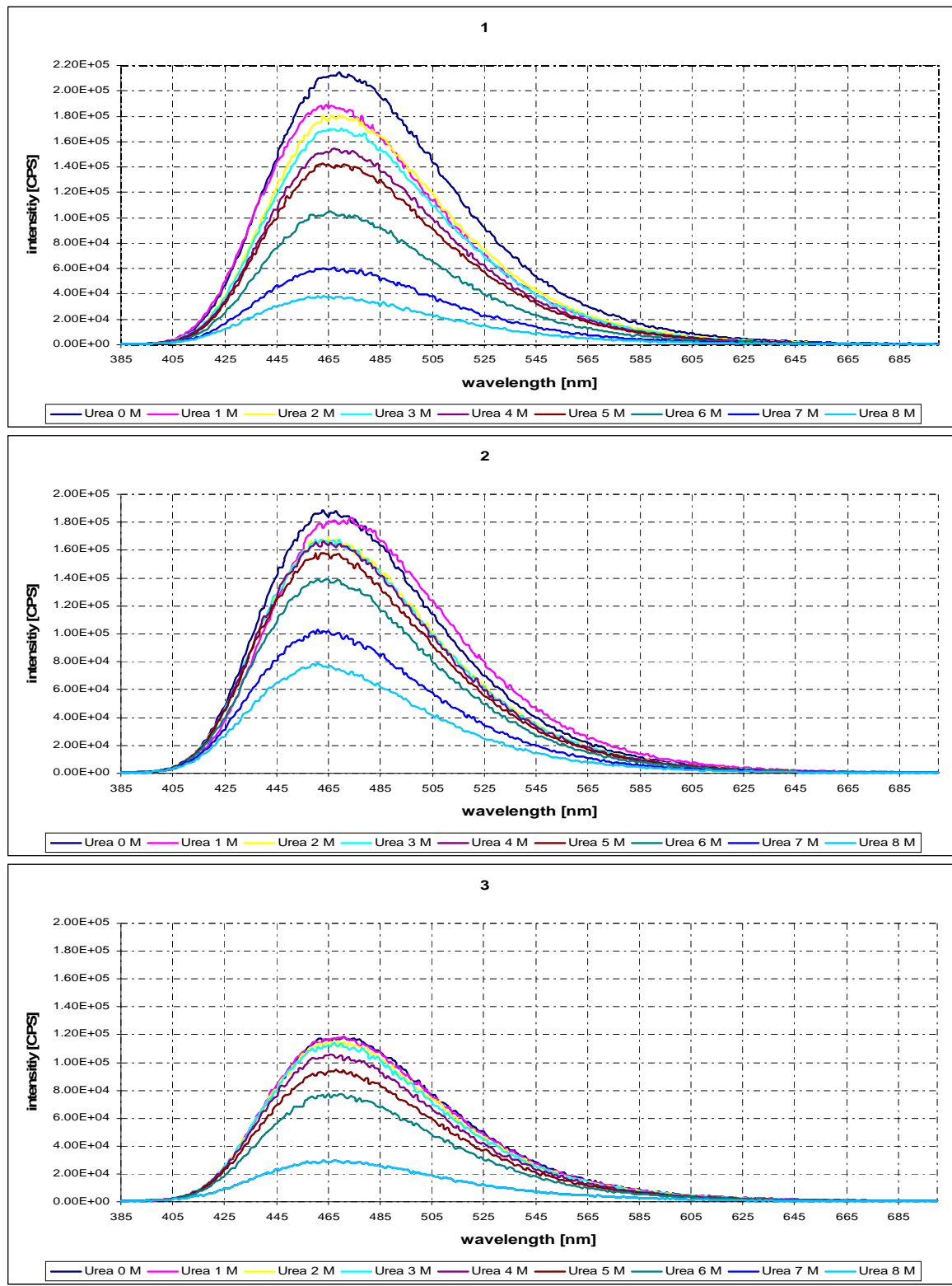


Figure 5.22. Extrinsic ANS fluorescence emission spectra of BSA in the presence of polymer nanoparticles 153 nm with epoxy groups and different urea concentrations. The concentrations used were: polymer nanoparticles 3.75 mg/ml, BSA 3.6  $\mu$ M, ANS 17  $\mu$ M, urea 0-8 M. Excitation wavelength 370 nm, slit 1, without polarization. Graphic 1 shows the results at pH 3.8. Graphic 2 shows the results at pH 7.4. Graphic 3 shows the results at pH 9.

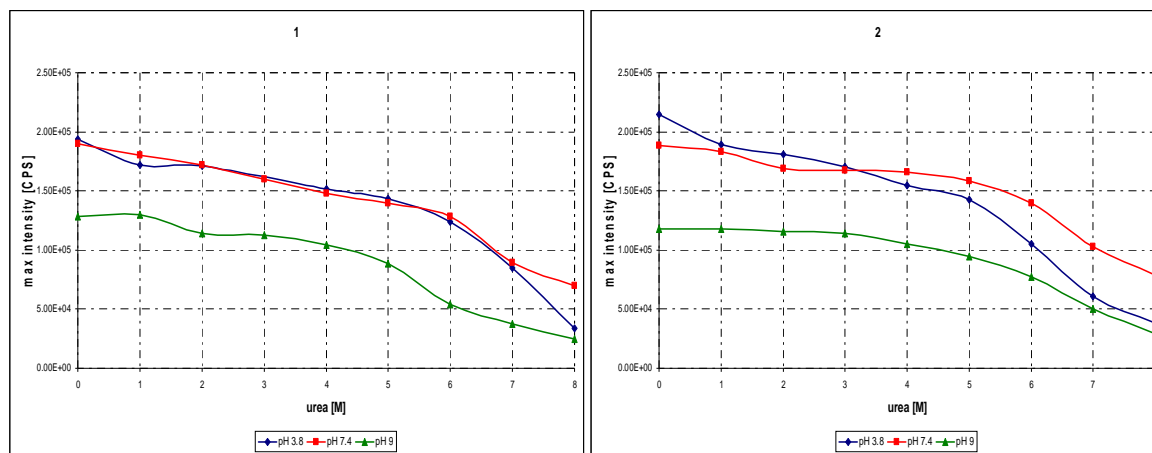


Figure 5.23. Changes in the ANS fluorescence intensity caused by increasing urea concentration. The concentrations used were: polymer nanoparticles 3.75 mg/ml, BSA 3.6  $\mu$ M, ANS 17  $\mu$ M, urea 0-8 M. Excitation wavelength 370 nm, slit 1, without polarization. Graphic 1 shows the results of polymer nanoparticles 227 nm with epoxy groups. Graphic 2 shows the results of polymer nanoparticles 153 nm with epoxy groups.

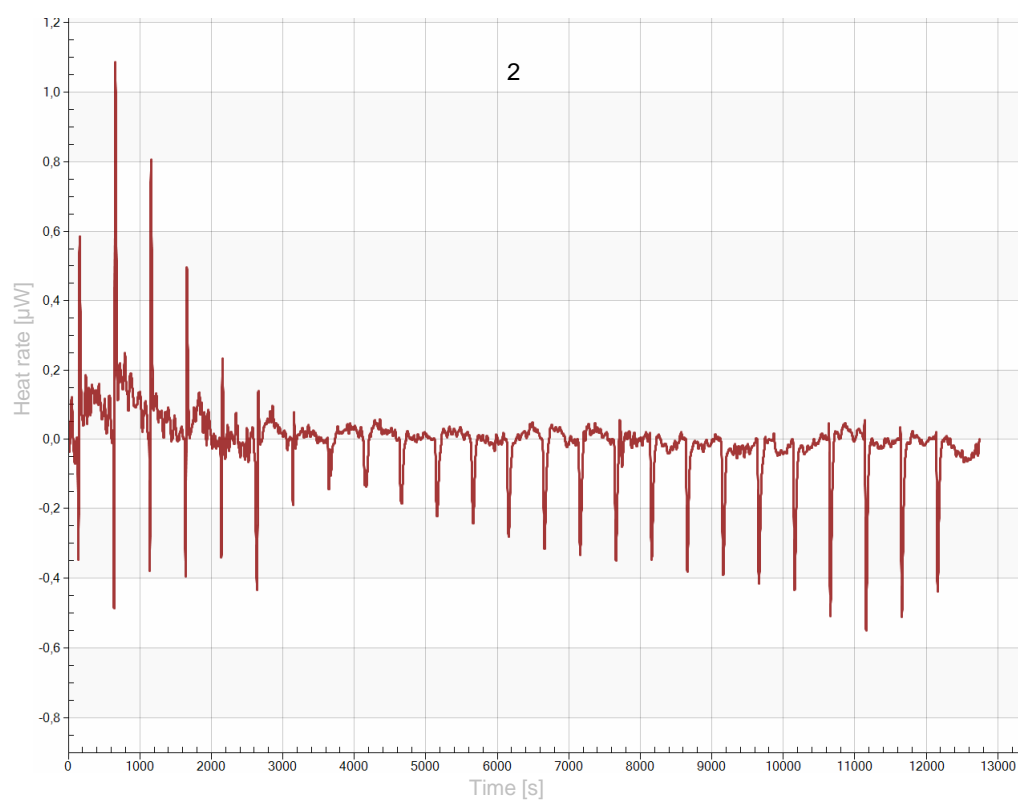
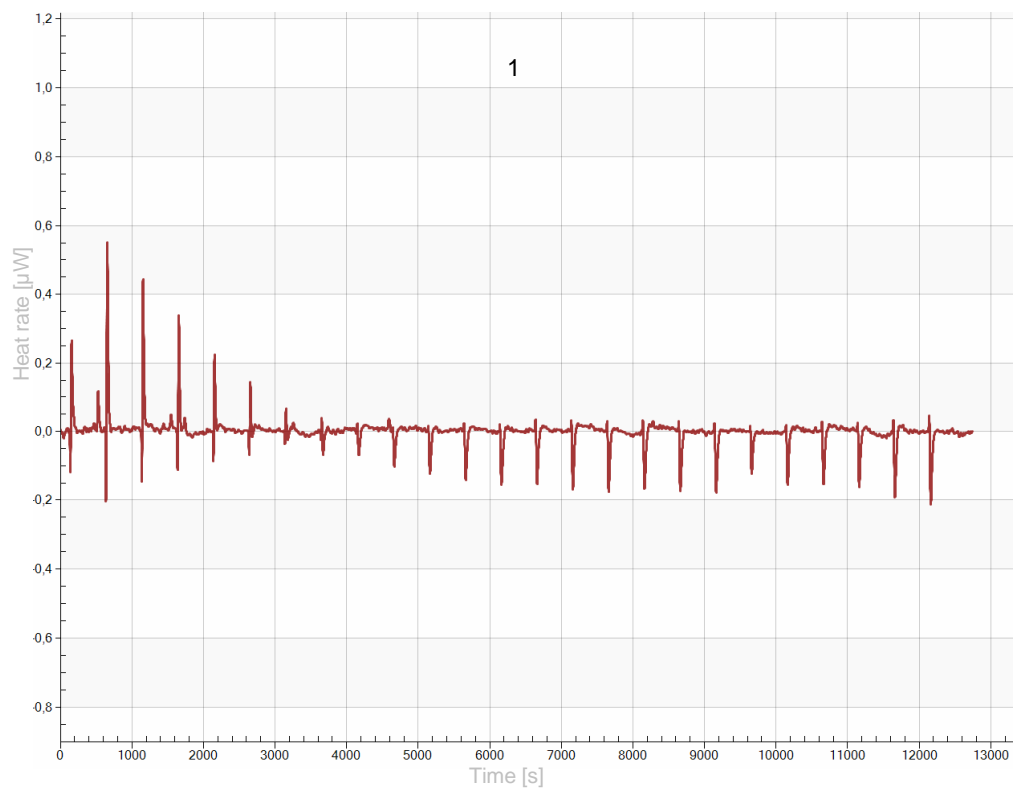
The intensity of emission decreased by increasing the urea concentration due to ANS got more access to the solvent. Regarding the results of BSA-polymer nanoparticle 227 nm and BSA-polymer nanoparticles 153 nm with epoxy groups there were no appreciated difference between them. Moreover it was not possible to identify any transition between conformations in the BSA. Thus it could be possible that urea affected the sample in such a way that the results did not represent the conformational changes of BSA. It would be recommended to find another procedure for the unfolding studies of the protein.

## 5.5. Studies of immobilized BSA by isothermal titration calorimetry

The adsorption of BSA on the surface of polymer nanoparticles was studied by isothermal titration calorimetry. As from the other sections it was deduced that at pH 7.4 the conditions were favourable for the attached followed conformational isomerisation of BSA, the experiments were carried out at this pH. Polymer nanoparticles 227 nm with epoxy groups were used as a model template. However since the use of this technique for the present purpose resides at the beginning, enthalpy, stoichiometry and equilibrium constant could not be deduced and it is necessary to do a more exhaustive experimentation for this purpose. Thus in the present section the results are treated qualitatively to identify the most relevant thermodynamics aspects of the adsorption process of BSA.

The results are shown in a graphic form where the heat rate [ $\mu$ W] released or absorbed from the reaction were plotted as a function of time [s] during the titrations. If the reaction is exothermic the heat rate should increase positively after each titration and if the reaction is endothermic the heat rate should increase negatively after each titration. During the first

titrations the absolute value of heat rate should be high since all BSA titrated reacts with the polymer nanoparticles. At the last titrations the absolute value of heat rate should be low since the solution has reached the equilibrium and there is no reaction. Figure 5.24 show the titration process at pH 7.4 of BSA 36  $\mu\text{M}$  in a sample cell of polymer nanoparticles 227 nm with epoxy groups at different concentrations (3.75 mg/ml, 7.5 mg/ml and 11.25 mg/ml).



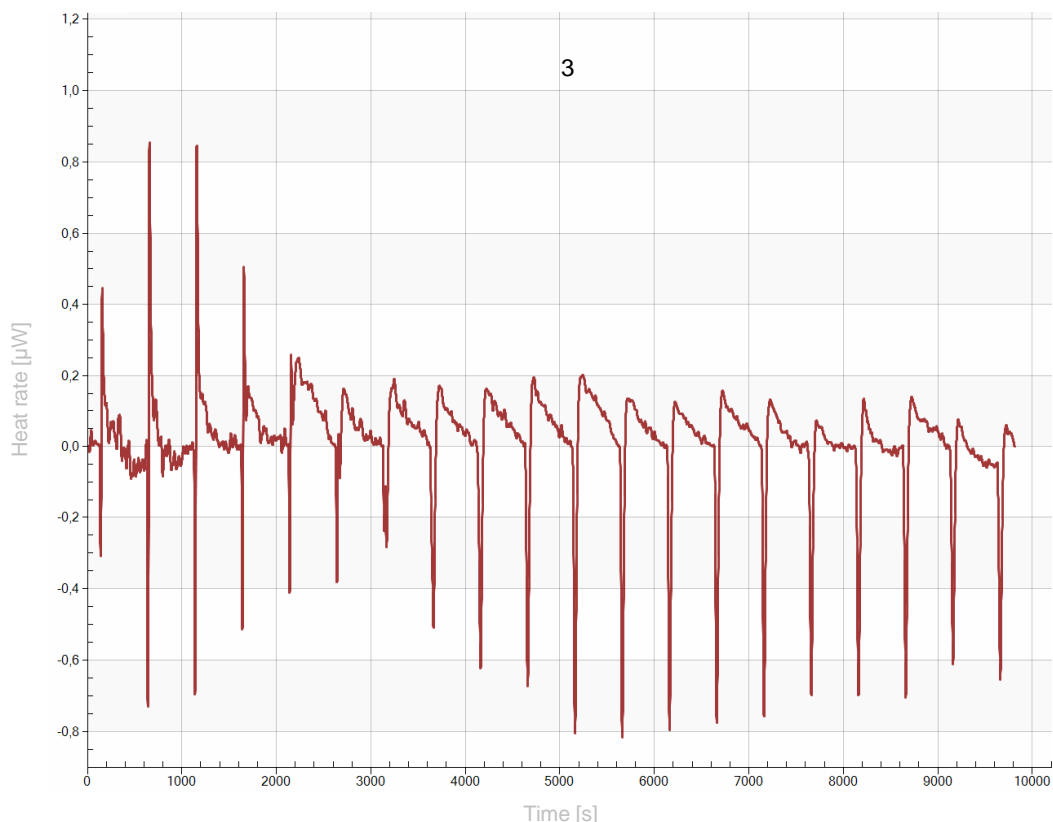


Figure 5.24. Syringe: 100  $\mu\text{l}$  of BSA 36  $\mu\text{M}$  adjusted at pH 7.4. Sample cell: Polymer nanoparticles 227 nm with epoxy groups adjusted at pH 7.4. Increasing concentration of polymer particles in the sample cell: 3.75 mg/ml (graphic 1), 7.5 mg/ml (graphic 2) and 11.25 mg/ml (graphic 3). Experiment consisting in 25 titrations (19 titrations graphic 3) of 4  $\mu\text{l}$  of BSA every 500 s. The first titration was at 120 s and the last measurement 120 s after the last titration.

According to graphic 1 of Figure 5.24 it seemed that some kind of reaction existed due to the fact that at the first titrations an exothermic peak could be observed. After four-six titrations this peak disappeared which means that all polymer particles 227 nm with epoxy groups had reacted. The adsorption process was exothermic but it was also possible to see an endothermic signal which could be derived from the mixture of the two samples. By increasing the concentration of polymer particles (graphics 2 and 3 of Figure 5.24) it would be expected to reach the equilibrium of the reaction after 10 or more titrations and see more exothermic peaks but it was not the case. After 4 titrations the reaction finished and it was only possible to see the endothermic peak from the mixture of the samples. However when the concentration of polymer particles was high (11.25 mg/ml) an exothermic behaviour was detected after the endothermic peak. Perhaps it was caused by a slow subprocess protein adsorption. Finally, although the graphics show a reaction process at the beginning of the titration, for the moment it is necessary with a more accurate experimental procedure to reach any conclusions. The results are not well defined enough to calculate the thermodynamic parameters of the adsorption.



## Conclusions

In the present project a set of experiments have been performed in order to develop and evaluate the use of polymer nanoparticles as a stable support for BSA immobilization.

Negatively charged monodisperse polymer nanoparticles functionalized with epoxy groups were synthesized by soap free emulsion polymerization. The samples showed a narrow polydispersity with the diameter of the particles inversely proportional to the stirring speed during the polymerization process. This fact indicated the validity of the method for the synthesizing of nanosized polymer particles and the possibility to obtain different diameters. The elimination of the epoxy groups did not result in physical alteration of the sample. Thus it was possible to functionalize the polymer nanoparticles with epoxy groups or remove them for purely electrostatic interaction. Polymer nanoparticles resided stable in the entire range of pH.

Immobilization of BSA was found to induce conformational changes in the protein. From zeta potential measurements, pI of BSA shifted to lower values when it was attached on the surface of the polymer nanoparticles and these shifts depended on the type used. By comparing the fluorescence emission spectra of different BSA-polymer nanoparticle constructs, it was determined that BSA immobilization and degree of unfolding was strongly affected by pH and surface groups. The results suggested that polymer nanoparticles with epoxy groups offered covalent binding and induced larger BSA conformational isomerisation than polymer nanoparticles without epoxy groups. These conformational alterations occurred to the largest degree at pH 7.4 since it was possible that at these conditions a high number of amino groups from BSA blended with epoxy groups of the nanoparticles. At pH 3.8 electrostatic attraction increased the number of adsorbed protein but no conformational changes were appreciated while at pH 9 adsorbed protein and induced conformational changes were in an intermediate level. Finally, there were no considerable discrepancies between polymer nanoparticles with different diameters.

Hence, the use of polymer nanoparticles as a stable support for BSA immobilization can be a good alternative in the monitoring of this protein. Nevertheless it is necessary to do an exhaustive research to understand the underlying of BSA adsorption and the conformational changes that are induced, as well as the total amount of attached protein on the polymer nanoparticles. ITC measurements could be a good choice for the study but at this moment it is necessary to realise further experiments.



# Bibliography

## Bibliographic referencing

- [1] Hornyak, G. L.; Moore, J. J.; Tibbals, H. F.; Dutta, J., *Fundamentals of nanotechnology*. CRC Press/Taylor & Francis Group, cop.: New York, 2009.
- [2] Feynman, R. P., *There is Plenty Room at the Bottom*. Lecture. American Physical Society, California Institute of Technology, 1959.
- [3] Brust, M.; Kiely, C. J., Some recent advances in nanostructure preparation from gold and silver particles: a short topical review. *Colloids and Surfaces, A: Physicochemical and Engineering Aspects* **2002**, 202(2-3), 175-186.
- [4] Kassing, R.; Petkov, P.; Kulisch, W.; Popov, C., *Functional Properties of Nanostructure Materials*. Springer: Berlin, 2006.
- [5] Fári, M. G., Kralovánszky, U. P., The founding father of biotechnology: Kárloy (Karl) Erky. *International Journal of Horticultural Science* **2006**, 12(1), 9-12.
- [6] Sobti, R. C.; Pachauri, S. S., *Essentials of Biotechnology*. Ane Books Pvt. Ltd.: Delhi, 2008.
- [7] Goodsell, D. S., *Bionanotechnology*. Wiley-Liss, cop.: Hoboken, 2004.
- [8] Niemeyer, C. M.; Mirikin, C. A., *Nanobiotechnology: concepts, applications and perspectives*. Wiley-VCH: Weinheim, 2004.
- [9] Sahoo, S. K.; Parveen, S.; MS, Panda, J. J., The present and the future of nanotechnology in human health care. *Nanomedicine: Nanotechnology, Biology, and Medicine* **2007**, 3(1), 20- 31.
- [10] Arrondo, J. L. R.; Goni, F. M., Structure and dynamics of membrane proteins as studied by infrared spectroscopy. *Progr. Biophys. Mol. Bio.* **1999**, 72, 367-405.
- [11] Baron M. H.; Revault M.; Servagent-Noinville S.; Abadie J.; Quiquampoix H., Baron, M. H.; Revault, M.; Servagent-Noinville, S.; Abadie, J.; Quiquampoix, H., Chymotrypsin Adsorption on Montmorillonite: Enzymatic Activity and Kinetic FTIR Structural Analysis. *J. Colloid Interf. Sci.* **1999**, 214(2), 319-332.
- [12] Brandes, N.; Welzel, P. B.; Werner, C.; Kroh, L. W., Adsorption-induced conformational changes of proteins onto ceramic particles: Differential scanning calorimetry and FTIR analysis. *Colloid Interf. Sci.* **2006**, 299(1), 56-69.
- [13] Bhardwaj, N.; Gerstein, M., Relating protein conformational changes to packing efficiency and disorder. *Protein Science* **2009**, 18(6), 1230-1240.
- [14] Engel, M. F. M.; Visser, A.; van Mierlo, C. P. M., Adsorption of bovine alpha-lactalbumin on suspended solid nanospheres and its subsequent displacement studied by NMR spectroscopy. *Langmuir* **2004**, 20(13), 5530-5538.
- [15] Engel, M. F. M.; Visser, A.; van Mierlo, C. P. M., Conformation and orientation of a protein folding intermediate trapped by adsorption. *Proc. Natl. Acad. Sci. U. S. A.* **2004**, 101(31), 11316-11321.
- [16] Glomm, W. R.; Halskau, O.; Hanneseth, A. M. D.; Volden, S., Adsorption behavior of acidic and basic proteins onto citrate-coated Au surfaces correlated to their native fold, stability, and pl. *J. Phys. Chem. B* **2007**, 111(51), 14329-14345.
- [17] Haynes, C. A.; Norde, W., Globular proteins at solid/liquid interfaces. *Colloids and Surfaces B: Biointerfaces* **1994**, 2, 517-566.

- [18] Kane, R. S.; Stroock, A. D., Nanobiotechnology: Protein-nanomaterial interactions. *Biotechnol. Prog.* **2007**, *23*(2), 316-319.
- [19] Hosokawa, M., *Nanoparticle technology handbook*. Elsevier: Amsterdam, 2007.
- [20] Glomm, W. R., Functionalized Gold Nanoparticles for Application in Bionanotechnology. *Journal of Dispersion Science and Technology* **2005**, *26*(3), 389-414.
- [21] Tkachenko, A. G.; Xie, H.; Coleman, D.; Glomm, W.; Ryan, J.; Anderson, M. F.; Franzen, S.; Feldheim, D. L., Multifunctional gold nanoparticle-peptide complexes for nuclear targeting. *Journal of the American Chemical Society* **2003**, *125*(16), 4700-4701.
- [22] Tkachenko, A. G.; Xie, H.; Liu, Y.; Coleman, D.; Ryan, J.; Glomm, W. R.; Shipton, M. K.; Franzen, S.; Feldheim, D. L., Cellular Trajectories of Peptide-Modified Gold Particle Complexes: Comparison of Nuclear Localization Signals and Peptide Transduction Domains. *Bioconjugate Chemistry* **2004**, *15*(3), 482-490.
- [23] Jahanshahi, M.; Babaei, Z., Protein nanoparticle: a unique system as drug delivery vehicles. *African Journal of Biotechnology* **2008**, *7*(25), 4926-4934.
- [24] Interface as two-dimensional folding templates for polypeptides. Dissertation. Institute for Biomedicine, 2009.
- [25] Pettersson, J.; Mossberg, A-K.; Svanborg, C.,  $\alpha$ -Lactalbumin species variation, HAMLET formation, and tumor cell death. *Biochemical and Biophysical Research Communications* **2006**, *345*(1), 260-270.
- [26] Casbarra, A.; Birolo, L.; Infusini, G.; Dal Piaz, F.; Svensson, M.; Pucci, P.; Svanborg, C.; Marino, G., Conformational analysis of HAMLET, the folding variant of human  $\alpha$ -lactalbumin associated with apoptosis. *Protein Science* **2004**, *13*(5), 1322-1330.
- [27] Greene, L. H.; Grobler, J. A.; Malinovskii, V. A.; Tian, J.; Acharya, K. Ravi; Brew, K., Stability, activity and flexibility in  $\alpha$ -lactalbumin. *Protein Engineering* **1999**, *12*(7), 581-587.
- [28] Svensson, M.; Hakansson, A.; Mossberg, A-K.; Linse, S.; Svanborg, C., Conversion of  $\alpha$ -lactalbumin to a protein inducing apoptosis. *Proceedings of the National Academy of Sciences of the United States of America* **2000**, *97*(8), 4221-4226.
- [29] Kane, R. S.; Stroock, A. D., Nanobiotechnology: Protein-nanomaterial interactions. *Biotechnol. Prog.* **2007**, *23*(2), 316-319.
- [30] Vertegel, A. A.; Siegel, R. W.; Dordick, J. S., Silica nanoparticle size influences the structure and enzymatic activity of adsorbed lysozyme. *Langmuir* **2004**, *20*(16), 6800-6807.
- [31] Lundqvist, M.; Sethson, I.; Jonsson, B. H., Protein adsorption onto silica nanoparticles: Conformational changes depend on the particles' curvature and protein stability. *Langmuir* **2004**, *20*(24), 10639-10647.
- [32] Griffin, C., "The Many Uses for Bovine serum albumin" in Article Resource, 2009, <<http://articleresource.org/business/customer-service/the-many-uses-for-bovine-serum-albumin-42655>> [10/09/2010].
- [33] Foster, J. F., *Albumin Structure, Function and Uses*. Pergamon press: New York, 1977.
- [34] Ribou, A-C.; Vigo, J.; Viallet, P.; Salmon, J-M.; Interaction of a protein, BSA, and a fluorescent probe, Mag-Indo-1, influence of EDTA and calcium on the equilibrium. *Biophysical Chemistry* **1999**, *81*(3), 179-189.
- [35] The Royal Society of Chemistry & The Royal Academy of Engineering, *Nanoscience and Nanotechnologies: Opportunities and uncertainties*. Clyvedon press: Cardiff, 2004.
- [36] Roco, M. C., Nanoparticles and nanotechnology research. *Journal of nanoparticle Research* **1999**, *1*(1), 1-6.

- [37] Lynch, I.; Dawson, K. A.; Linse, S., Detecting cryptic epitopes created by nanoparticles. *Science's STKE: signal transduction knowledge environment* **2006**, 2006(327).
- [38] Lundqvist, M.; Sethson, I.; Jonsson, B. H., Protein Adsorption onto Silica Nanoparticles: Conformational Changes Depend on the Particles' Curvature and the Protein Stability. *Langmuir* **2004**, 20(24), 10639-10647.
- [39] Roach, P.; Farrar, D.; Perry, C. C., Surface Tailoring for Controlled Protein Adsorption: Effect of Topography at the Nanometer Scale and Chemistry. *J. Am. Chem. Soc.* **2006**, 128(12), 3939-3945.
- [40] Lundqvist, M.; Sethson, I.; Jonsson, B. H., High-Resolution 2D 1H-15N NMR Characterization of Persistent Structural Alterations of Proteins Induced by Interactions with Silica Nanoparticles. *Langmuir* **2005**, 21(13), 5974-5979.
- [41] Kowalski, A.; Vogel, M.; Blankenship, R. M., European Patent 22633, 1981.
- [42] Nagao, Daisuke; Sakamoto, Tatsuro; Konno, Hiroyuki; Gu, Shunchao; Konno, Mikio Preparation of Micrometer-Sized Polymer Particles with Control of Initiator Dissociation during Soap-Free Emulsion Polymerization. *Langmuir* **2006**, 22(26), 10958-10962.
- [43] Lee, J. M.; Lee, D. G.; Lee, S. J.; Kim, J. H.; Cheong, I. W., One-Step Synthetic Route for Conducting Core-Shell Poly(styrene/pyrrole) Nanoparticles. *Macromolecules* **2009**, 42(13), 4511-4519.
- [44] Nagao, D.; Yokoyama, M.; Yamauchi, N.; Matsumoto, H.; Kobayashi, Y.; Konno, M., Synthesis of highly monodisperse particles composed of a magnetic core and fluorescent shell. *Langmuir* **2008**, 24(17), 9804-9808.
- [45] Deng, W.; Li, R.; Zhang, M.; Gong, L.; Kan, C., Influences of MAA on the porous morphology of P(St-MAA) latex particles produced by batch soap-free emulsion polymerization followed by stepwise alkali/acid post-treatment. *Journal of Colloid and Interface Science* **2010**, 349(1), 122-126.
- [46] McDonald, C. J.; Devon, M. J., Hollow latex particles: synthesis and applications. *Advances in Colloid and Interface Science* **2002**, 99(3), 181-213.
- [47] Okubo, M.; Ichikawa, K.; Fujimura, M., Studies on suspension and emulsion. CXXVIII. Production of multi-hollow polymer microspheres by stepwise alkali/acid method. II. Alkali treatment process. *Colloid Polym. Sci.* **1991**, 269(12), 1257-1262.
- [48] Okubo, M.; Ito, A.; Hashiba, A., Production of submicron-sized multihollow polymer particles having high transition temperatures by the stepwise alkali/acid method. *Colloid Polym. Sci.* **1996**, 274(5), 428-432.
- [49] Okubo, M.; Ito, A.; Kanenobu, T., Production of submicron-sized multihollow polymer particles by alkali/cooling method. *Colloid and Polymer Science* **1996**, 274(8), 801-804.
- [50] Yasuda, M.; Ono, K.; Hirabayashi, Y.; Aizawa, S.; Brewer, S. H.; Halskau, Ø. J.; Volden, S.; Glomm, W. R., pH-dependent Immobilization of Protein on Charged Monodisperse Polymer Particles. *Article in Preparation*.
- [51] Svensson, M.; Hakansson, A.; Mossberg, A.-K.; Linse, S.; Svanborg, C., Conversion of  $\alpha$ -lactalbumin to a protein inducing apoptosis. *Proceedings of the National Academy of Sciences of the United States of America* **2000**, 97(8), 4221-4226.
- [52] Berg, J. M. T.; John L.; Stryer, Lubert., *Biochemistry*. 5 ed.; W. H. Freeman and Company: New York, 2001.
- [53] Faber, K., *Biotransformations in Organic Chemistry*. 5 ed.; Springer-Verlag: Berlin, 2004.
- [54] Hinz, H. J.; Steif, C.; Vogl, T.; Meyer, R.; Renner, M.; Ledermueller, R., Fundamentals of protein stability. *Pure and Applied Chemistry* **1993**, 65(5), 947-952.
- [55] Jackson, S. E.; Fersht, A. R., Folding of chymotrypsin inhibitor 2. 1. Evidence for a two-state transition. *Biochemistry* **1991**, 30, 10428-10435.

- [56] Kuwajima, K, The molten globule state as a clue for understanding the folding and cooperativity of globular-protein structure. *Proteins: Structure, Function, and Genetics* **1989**, 6(2), 87-103.
- [57] Ptitsyn O. B., Molten globule and protein folding. *Adv. Protein Chem.* **1995**, 47, 83-229.
- [58] Arai, M.; Kuwajima, K., Role of the molten globule state in protein folding. *Adv. Protein Chem.* **2000**, 53(Protein Folding Mechanisms), 209-282.
- [59] Wright P. E.; Dyson H. J., Intrinsically Unstructured Proteins: Re-assessing the Protein Structure-Function Paradigm. *J. Mol. Biol.* **1999**, 293, 321-331.
- [60] Abkevich V. I.; Gutin A. M.; Shakhnovich E. I., Specific Nucleus as the Transition State for Protein Folding: Evidence from the Lattice Model. *Biochemistry* **1994**, 33(33), 10026-10036.
- [61] Ohgushi, M; Wada, A., 'Molten-globule state': a compact form of globular proteins with mobile side-chains. *FEBS Letters* **1983**, 164(1), 21-24.
- [62] Halskau, O. J.; Perez-Jimenez, R.; Ibarra-Molero, B.; Underhaug, J.; Munoz, V.; Martinez, A.; Sanchez-Ruiz, J. M., Large-scale modulation of thermodynamic protein folding barriers linked to electrostatics. *Proceedings of the National Academy of Sciences of the United States of America* **2008**, 105(25), 8625-8630.
- [63] Ptitsyn, O. B.; Uversky, V. N., The molten globule is a third thermodynamical state of protein molecules. *FEBS Letters* **1994**, 341(1), 15-18.
- [64] Demarest, S. J.; Boice, J. A.; Fairman, R.; Raleigh, D. P., Defining the Core Structure of the  $\alpha$ -Lactalbumin Molten Globule State. *Journal of Molecular Biology* **1999**, 294(1), 213-221.
- [65] Li S., Yizhe W., Junguang J., and Shaojun D., pH-Dependent Protein Conformational Changes in Albumin:Gold Nanoparticle Bioconjugates: A Spectroscopic Study. *Langmuir* **2007**, 23(5), 2714-2721.
- [66] Takeda, K.; Sasa, K.; Kawamoto, K.; Wada, A.; Aoki, K., Secondary structure changes of disulfide bridge-cleaved bovine serum albumin in solutions of urea, guanidine hydrochloride, and sodium dodecyl sulfate. *Journal of Colloid and Interface Science* **1988**, 124(1), 284-289
- [67] Takeda, K.; Shigeta, M.; Aoki, K., Secondary structures of bovine serum albumin in anionic and cationic surfactant solutions. *Journal of Colloid and Interface Science* **1987**, 117(1), 120-6.
- [68] Gerbanowski, A.; Rabiller, C.; Larre, C.; Gueguen, J., Grafting of Aliphatic and Aromatic Probes on Bovine. *Journal of Protein Chemistry* **1999**, 18(3), 325-336.
- [69] Hamandi, S.; Joly, D.; Carpentier, R.; Tajmir-Riahi, H. A., The effect of methylamine on the solution structures of human and bovine serum albumins. *Journal molecular structure* **2009**, 936, 80-86.
- [70] Friedli, G. L., Interaction of deamidated soluble wheat protein (SWP) with other food proteins and metals. *Ph.D. Thesis*. University of Surrey, England, 1996.
- [71] Glomm, W. R.; Halskau, O. J.; Hanneseth, A-M. D.; Volden, S., Adsorption Behavior of Acidic and Basic Proteins onto Citrate-Coated Au Surfaces Correlated to Their Native Fold, Stability, and pI. *Journal of Physical Chemistry B* **2007**, 111(51), 14329-14345.
- [72] Wright, A. K.; Thompson, M. R., Hydrodynamic structure of bovine serum albumin determined by transient electric birefringence. *Biophys. J.* **1975**, 15(2,Pt.1), 137-141.
- [73] Peters, T. Jr., Serum Albumin. *Adv. Protein Chem.* **1985**, 37, 161-245.
- [74] Carter, D. C.; Ho, J. X., Structure of Serum Albumin. *Adv. Protein Chem.* **1994**, 45, 153-203.
- [75] He, X. M.; Carter, D.C., Atomic structure and chemistry of human serum albumin. *Nature* **1992**, 358(6383) 209-215.
- [76] Shang, L.; Wang, Y.; Jiang, J.; Dong, S., pH-Dependent Protein Conformational Changes in Albumin:Gold Nanoparticle Bioconjugates: A Spectroscopic Study. *Langmuir* **2007**, 23(5), 2714-2721.

- [77] He, X. M.; Carter, D.C., Atomic structure and chemistry of human serum albumin. *Nature* **1992**, 358(6383), 209-215.
- [78] Hamdani, S.; Joly, D.; Carpentier, R.; Tajmir-Riahi, H. A., The effect of methylamine on the solution structures of human and bovine serum albumins. *Journal of Molecular Structure* **2009**, 936(1-3), 80-86.
- [79] Andrade, J. D.; Hlady, V.; Wei, A. P., Adsorption of complex proteins at interfaces. *Pure and Applied Chemistry* **1992**, 64(11), 1777-81.
- [80] Haynes, C. A.; Norde, W., Globular proteins at solid/liquid interfaces. *Colloids and Surfaces B-Biointerfaces* **1994**, 2, 517-566.
- [81] Norde, W.; Lyklema, J.; Thermodynamics of Protein Adsorption. Theory with special reference to the adsorption of human plasma albumin and bovine pancreas ribonuclease at polystyrene surfaces. *Journal of Colloid and Interface Science* **1979**, 71(2), 350-366.
- [82] Janin, J.; Wodak, S. J., Structural Domains in Proteins and their Role in the Dynamics of Protein Function. *Prog Biophys molec Biol* **1983**, 42, 21-78.
- [83] Glomm, W. R., Functionalized Gold Nanoparticles for Applications in Bionanotechnology. *Journal of Dispersion Science and Technology* **2005**, 26(3), 389-414.
- [84] Holmberg, K.; Jönsson, B.; Kronberg, B.; Lindeman, B., *Surfactants and polymers in aqueous solution*. 2 ed.; John Wiley & Sons: West Sussex, 2007.
- [85] Engel, M. F. M.; Visser, A. J. W. G.; van Mierlo, C. P. M., Conformation and orientation of a protein folding intermediate trapped by adsorption. *Proc. Natl. Acad. Sci. U. S. A.* **2004**, 101(31), 11316-11321.
- [86] Brown, W., *Light Scattering: Principles and development (Monographs on the Physics and Chemistry of Materials)*. Oxford University Press: New York, 1996.
- [87] Bohren, C.F.; Huffman, D.R., *Absorption and Scattering of Light by Small Particles*. John Wiley and Sons. Inc.: New York, 1983.
- [88] Sartor, M., *Dynamic Light Scattering to determinate the radius of small beads in Brownian motion in solution. Dissertation*. University of California.
- [89] "Chapter 7: Light Scattering", <[http://www.ias.ac.in/initiat/sci\\_ed/resources/chemistry/LightScat.pdf](http://www.ias.ac.in/initiat/sci_ed/resources/chemistry/LightScat.pdf)> [10/10/2010]
- [90] Singh, R., C. V. Raman and the Discovery of the Raman Effect. *Physics in Perspective (PIP)* **2002**, 4(4), 399-420.
- [91] Tschamner, W., Photon Correlation Spectroscopy in Particle Sizing. *Encyclopedia of Analytical Chemistry*, **2000**, 15, 5469-5485.
- [92] Finsy, R., Particle sizing by quasi-elastic light scattering. *Advances in Colloid and Interface Science* **1994**, 52, 79-143.
- [93] "Dynamic light scattering: An introduction in 30 minutes" in Malvern technical note, MRK656-01, 2010, <[http://www.malvern.com/LabEng/technology/dynamic\\_light\\_scattering/dynamic\\_light\\_scattering.htm](http://www.malvern.com/LabEng/technology/dynamic_light_scattering/dynamic_light_scattering.htm)> [22/9/2010].
- [94] Ravina, L., *Everything you want to know about Coagulation & Flocculation...* 4 ed. Zeta-Mater, Inc: Staunton, 1993.
- [95] Delgado, A. V.; González-Caballero, F.; Hunter, R. J.; Koopal, L. K.; Lyklema, J., Measurement and Interpretation of Electrokinetic Phenomena. *Pure Appl. Chem.* **2005**, 77(10), 1753-1805.
- [96] Derjaguin, B.; Landau, L., Theory of the stability of strongly charged lyophobic sols and of the adhesion of strongly charged particles in solutions of electrolytes. *Acta Physico Chemica URSS* **1941**, 14, 633.

- [97] Verwey, E. J. W.; Overbeek, J. Th. G., *Theory of the stability of lyophobic colloids*, Elsevier: Amsterdam, 1948.
- [98] Lyklema, J., *Fundamentals of Interface and Colloid Science Solid-Liquid Interfaces*. Academic Press: London, 1995; Vol. 2.
- [99] Yoval, L. S.; Palacios, L. M.; Soberanis, M. P.; Guzmán, L. O. S., Potencial zeta como una herramienta para determinar la aglomeración de las partículas en la reducción del volumen de lodo a disponer. Disertación. Instituto Mexicano de Tecnología del Agua.
- [100] Sattelle, D. B., Quasieastic laser light scattering and laser Doppler electrophoresis as probes of synaptic and spectroscopy terminal function. *J. exp. Boil.* **1988**, *139*, 233-252.
- [101] Ware, R.; Flygare, W.H., Light scattering in mixtures of BSA, BSA dimers, and fibrinogen under the influence of electric fields. *J. Colloid Interface Sci.* **1972**, *39*, 670-675.
- [102] "Z-potential: an introduction in 30 minutes" in Malvern technical note, MRK 654-01, 2010, <[http://www.malvern.com/LabEng/technology/zeta\\_potential/zeta\\_potential\\_LDE.htm](http://www.malvern.com/LabEng/technology/zeta_potential/zeta_potential_LDE.htm)> [22/9/2010].
- [103] Hilborn, R. C., Einstein coefficients, cross sections, f values, dipole moments, and all that. *Am. J. Phys.* **1982**, *50*(11), 982-986.
- [104] Lakowicz, J. R., *Principles of Fluorescence Spectroscopy*. 3 ed. Springer Science and Business Media, LLC: New York, 2006; Vol.1.
- [105] "Quantitation of Peptides and Amino Acids with a Synergy™ HT using UV Fluorescence" in BioTek application note, 2006, <[www.biotek.com](http://www.biotek.com)> [23/09/2010].
- [106] Moriyama, Y.; Ohta, D.; Hachiva, K.; Mitsui, Y.; Takeda, K., Fluorescence behaviour of tryptophan residues of bovine and human serum albumins in ionic surfactant solutions: a comparative study of the two and one tryptophan(s) of bovine and human albumins. *J. Protein* **1996**, *15*, 265-272.
- [107] Brukel, B. M.; von Dassow, G.; Bement, W.M., Versatile fluorescent probes for actin filaments based on the actin-binding domain of utrophin. *Cell Motil Cytoskeleton* **2007**, *64*(11), 822-832.
- [108] Cattoni, D. I.; Kaufman, S. B.; González Flecha, F.L., Kinetics and thermodynamics of the interaction of 1-anilino-naphthalene-8-sulfonate with proteins. *Biochimica et Biophysica Acta* **2009**, *1794*, 1700-1708.
- [109] Matulis, D.; Baumann, V. A.; Lovrien, R. E., 1-Anilino-8-Naphthalene Sulfonate as a Protein Conformational Tightening Agent. *Biopoly* **1999**, *49*, 451-458.
- [110] Celej, M. S.; Dassie, S. A.; Freire, E.; Bianconi, M. L.; Fidelio, G. D., Ligand-induced thermostability in proteins: Thermodynamic analysis of ANS-albumin interaction. *Biochimica et Biophysica Acta* **2005**, *1750*, 122-133.
- [111] Gasymov, O.K.; Glasgow, B.J., ANS fluorescence: Potential to augment the identification of the external binding sites of proteins. *Biochim. Biophys. Acta.*, **2007**, 403-411.
- [112] Demarse, N.; Hansen, L. D., "Analysis of Organic Compounds Binding to Nanoparticles by Isothermal Titration Calorimetry (ITC)" in TA instruments, MCAPN 2010-01, 2010, <<http://www.tainstruments.com>> [01/10/2010].
- [113] Pierce, M. M.; Raman, C. S.; Nall, B. T., Isothermal Titration Calorimetry of Protein-Protein Interactions. *Methods* **2009**, *19*, 213-221.
- [114] "Isothermal Titration Calorimetry (Nano ITC)" in TA instruments, Nano ITC Getting Started Guide, 2008. <<http://www.tainstruments.com>> [01/10/2010].
- [115] Colette, F. Q., "Analyzing ITC Data for the Enthalpy of Binding Metal Ions to Ligands" in TA instruments, MCAPN-2010-02. <<http://www.tainstruments.com>> [01/10/2010].



- [116] Malavasic, Mateja; Poklar, Natasa; Macek, Peter; Vesnaver, Gorazd, Fluorescence studies of the effect of pH, guanidine hydrochloride and urea on equinatoxin II conformation. *Biochimica et Biophysica Acta, Biomembranes* **1996**, 1280(1), 65-72.





# Appendices



# Index

HAZARDOUS ACTIVITY IDENTIFICATION PROCESS	_____	<b>A</b>
RISK ASSESSMENT	_____	<b>B</b>
HSE ACTION PLAN	_____	<b>C</b>



NTNU	Appendix A: Hazardous activity identification process	Prepared by	Number	Date	
		HSE section	HMSRV-26/01	01.12.2006	
HSE		Approved by	Page	Replaces	
		The Rector	1 out of 4	15.12.2003	



**Unit: Ugelstad Laboratory**

**Date: 14/02/11**

**Participants in the identification process (including their function): Jordi Piella Bagaria (Designer)**



**Short description of the main activity/main process: Experimentation with chemical reagents, laboratory scale.**

(Id.) Activity/process	Responsible person	Laws, regulations etc.	Existing documentation	Existing safety measures	Comment
<b>(1)</b> Divinylbenzene technical grade, 80% (handling and storage)	Jordi Piella Bagaria	Regulation (EC) No 1272/2008 [EU-GHS/CLP]. EU Directives 67/548/EEC or 1999/45/EC. Regulation (EC) No 1272/2008 [CLP]. European Directive 67/548/EEC as amended.	Material safe data sheet. HSE handbook. Lab handbook. Operation manual. Checklist.	Protective equipment and emergency procedures. Normal measures for preventive fire protection. Conditions for safe storage.	Use equipment for eye protection tested and approved under appropriate government standards such as NIOSH (US) or EN 166(EU). The selected protective gloves have to satisfy the specifications of EU Directive 89/686/EEC and the standard EN 374 derived from it. For nuisance exposures use type OV/AG (US) or type ABEK (EU EN 14387) respirator cartridges. Use respirators and components tested and approved under appropriate government standards such as NIOSH (US) or CEN (EU).



NTNU	Appendix A: Hazardous activity identification process	Prepared by	Number	Date	
		HSE section	HMSRV-26/01	01.12.2006	
HSE		Approved by	Page	Replaces	
		The Rector	2 out of 4	15.12.2003	

<p><b>(2)</b> Glycidyl methacrylate, 97% (handling and storage)</p>	<p>Jordi Piella Bagaria</p>	<p>Regulation (EC) No 1272/2008 [EU-GHS/CLP]. EU Directives 67/548/EEC or 1999/45/EC. Regulation (EC) No 1272/2008 [CLP]. European Directive 67/548/EEC as amended.</p>	<p>Material safe data sheet. HSE handbook. Lab handbook. Operation manual. Checklist.</p>	<p>Protective equipment and emergency procedures. Normal measures for preventive fire protection. Conditions for safe storage.</p>	<p>Face shield and safety glasses Use equipment for eye protection tested and approved under appropriate government standards such as NIOSH (US) or EN 166(EU). The selected protective gloves have to satisfy the specifications of EU Directive 89/686/EEC and the standard EN 374 derived from it. Where risk assessment shows air-purifying respirators are appropriate use a full-face respirator with multi-purpose combination (US) or type ABEK (EN 14387) respirator cartridges as a backup to engineering controls. If the respirator is the sole means of protection, use a full-face supplied air respirator. Use respirators and components tested and approved under appropriate government standards such as NIOSH (US) or CEN (EU).</p>
---	-----------------------------	---	---	--	---





NTNU	Appendix A: Hazardous activity identification process	Prepared by	Number	Date	
		HSE section	HMSRV-26/01	01.12.2006	
HSE		Approved by	Page	Replaces	
		The Rector	3 out of 4	15.12.2003	

<p><b>(3) Styrene RegeantPlus, 99%&gt;= (handling and storage)</b></p>	<p>Jordi Piella Bagaria</p>	<p>Regulation (EC) No 1272/2008 [EU-GHS/CLP]. EU Directives 67/548/EEC or 1999/45/EC. Regulation (EC) No 1272/2008 [CLP]. European Directive 67/548/EEC as amended.</p>	<p>Material safe data sheet. HSE handbook. Lab handbook. Operation manual. Checklist.</p>	<p>Protective equipment and emergency procedures. Normal measures for preventive fire protection. Conditions for safe storage.</p>	<p>Face shield and safety glasses. Use equipment for eye protection tested and approved under appropriate government standards such as NIOSH (US) or EN 166(EU). The selected protective gloves have to satisfy the specifications of EU Directive 89/686/EEC and the standard EN 374 derived from it. Where risk assessment shows air-purifying respirators are appropriate use a full-face respirator with multi-purpose combination (US) or type ABEK (EN 14387) respirator cartridges as a backup to engineering controls. If the respirator is the sole means of protection, use a full-face supplied air respirator. Use respirators and components tested and approved under appropriate government standards such as NIOSH (US) or CEN (EU).</p>
--	-----------------------------	---	---	--	--

NTNU	Appendix A: Hazardous activity identification process	Prepared by	Number	Date	
		HSE section	HMSRV-26/01	01.12.2006	
HSE		Approved by	Page	Replaces	
		The Rector	4 out of 4	15.12.2003	

<p><b>(4) Ammonium persulfat (handling and storage)</b></p>	<p>Jordi Piella Bagaria</p>	<p>Regulation (EC) No1272/2008 European Directive 67/548/EEC as amended</p>	<p>Material safe data sheet. HSE handbook. Lab handbook. Operation manual. Checklist.</p>	<p>Protective equipment and emergency procedures. Normal measures for preventive fire protection. Conditions for safe storage.</p>	<p>Where risk assessment shows air-purifying respirators are appropriate use a full-face particle respirator type N100 (US) or type P3 (EN 143) respirator cartridges as a backup to engineering controls. If the respirator is the sole means of protection, use a full-face supplied air respirator. Use respirators and components tested and approved under appropriate government standards such as NIOSH (US) or CEN (EU). The selected protective gloves have to satisfy the specifications of EU Directive 89/686/EEC and the standard EN 374 derived from it.</p>
---	-----------------------------	---	---	--	--

NTNU	Appendix B: Risk assessment	Prepared by	Number	Date	
		HSE section	HMSRV-26/03	01.12.2006	
HSE/KS		Approved by	Page	Replaces	
		The Rector	1 out of 7	15.12.2003	



Unit: Ugelstad Laboratory

Date: 14/02/11



Line manager: Wilhelm Robert Glomm

Participants in the risk assessment (including their function): Jordi Piella Bagaria (*Designer*)



(Id.) Activity from the identification process form	Potential undesirable incident/strain	Likelihood:	Consequence:			Risk value	Comments/status Suggested measures
		Likelihood (1-4)	Human (1-4)	Environment (1-4)	Economy/materiel (1-4)		
(1) Divinylbenzene technical grade, 80% (handling and storage)	Accidental release	1	2	1	1	2+1+1	<b>Preventive:</b> Store in cool place. Keep container tightly closed in a dry and well-ventilated place. Containers which are opened must be carefully resealed and kept upright to prevent leakage. <b>Corrective:</b> Avoid breathing vapours, mist or gas. Use personal protective equipment: Eye/face protection, skin protection, body protection, respiratory protection. Do not let product enter drains. Keep in suitable, closed containers for disposal.
(1) Divinylbenzene technical grade, 80% (handling and storage)	Fire	1	2	1	2	2+1+2	<b>Corrective:</b> Use water spray, alcohol-resistant foam, dry chemical or carbon dioxide as extinguishing media.
(2) Glycidyl methacrylate, 97% (handling and storage)	Accidental release	1	2	1	1	2+1+1	<b>Preventive:</b> Store in cool place. Keep container tightly closed in a dry and well-ventilated place. Containers which are

NTNU	Appendix B: Risk assessment	Prepared by	Number	Date	
		HSE section	HMSRV-26/03	01.12.2006	
HSE/KS		Approved by	Page	Replaces	
		The Rector	2 out of 7	15.12.2003	

							<p>opened must be carefully resealed and kept upright to prevent leakage. Avoid contact with skin and eyes. Avoid inhalation of vapour or mist.</p> <p><b>Corrective:</b> Avoid breathing vapours, mist or gas. Ensure adequate ventilation. Remove all sources of ignition. Evacuate personnel to safe areas. Beware of vapours accumulating to form explosive concentrations. Vapours can accumulate in low areas. Keep away from sources of ignition - No smoking. Take measures to prevent the build up of electrostatic charge. Use personal protective equipment: Eye/face protection, skin protection, body protection, respiratory protection. Prevent further leakage or spillage if safe to do so. Do not let product enter drains. Contain spillage, and then collect with an electrically protected vacuum cleaner or by wet-brushing and place in container for disposal according to local regulations. Keep in suitable, closed containers for disposal.</p>

NTNU	Appendix B: Risk assessment	Prepared by	Number	Date	
		HSE section	HMSRV-26/03	01.12.2006	
HSE/KS		Approved by	Page	Replaces	
		The Rector	3 out of 7	15.12.2003	

(2) Glycidyl methacrylate, 97% (handling and storage)	Fire	1	2	1	2	2+1+1	<b>Corrective:</b> Use water spray, alcohol-resistant foam, dry chemical or carbon dioxide as extinguishing media.
(3) Styrene RegeantPlus, 99%>= (handling and storage)	Accidental release	1	2	1	1	2+1+1	<b>Preventive:</b> Store in cool place. Keep container tightly closed in a dry and well-ventilated place. Containers which are opened must be carefully resealed and kept upright to prevent leakage. Handle in accordance with good industrial hygiene and safety practice. Wash hands before breaks and at the end of workday. <b>Corrective:</b> Avoid contact with skin and eyes. Avoid inhalation of vapour or mist. Keep away from sources of ignition - No smoking. Take measures to prevent the build up of electrostatic charge. Use personal protective equipment: Eye/face protection, skin protection, body protection, respiratory protection. Use personal protective equipment. Avoid breathing vapours, mist or gas. Ensure adequate ventilation. Remove all sources of ignition. Beware of vapours accumulating to form explosive concentrations. Vapours can accumulate in low areas. Prevent further leakage or

NTNU	Appendix B: Risk assessment	Prepared by	Number	Date	
		HSE section	HMSRV-26/03	01.12.2006	
HSE/KS		Approved by	Page	Replaces	
		The Rector	4 out of 7	15.12.2003	

							spillage if safe to do so. Do not let product enter drains. Discharge into the environment must be avoided. Contain spillage, and then collect with an electrically protected vacuum cleaner or by wet-brushing and place in container for disposal according to local regulations.
(3) Styrene, RegeantPlus, 99%>= (handling and storage)	Fire	1	2	1	2	2+1+2	<b>Corrective:</b> Use water spray, alcohol-resistant foam, dry chemical or carbon dioxide as extinguishing media. Use water spray to cool unopened containers.
(4) Ammonium persulfat (handling and storage)	Accidental release	1	2	1	1	2+1+1	<b>Preventive:</b> Store in cool place. Keep container tightly closed in a dry and well-ventilated place. <b>Corrective:</b> Avoid contact with skin and eyes. Avoid formation of dust and aerosols. Provide appropriate exhaust ventilation at places where dust is formed. Keep away from sources of ignition - No smoking. Keep away from combustible material. Moisture sensitive. Use personal protective equipment. Avoid dust formation. Avoid breathing dust. Ensure adequate ventilation. Evacuate personnel to safe areas. Do

NTNU	Appendix B: Risk assessment	Prepared by	Number	Date	
		HSE section	HMSRV-26/03	01.12.2006	
HSE/KS		Approved by	Page	Replaces	
		The Rector	5 out of 7	15.12.2003	

							not let product enter drains. Pick up and arrange disposal without creating dust. Keep in suitable, closed containers for disposal.
(4) Ammonium persulfate 98+%, A.C.S. reagent (handling and storage)	Fire	1	2	1	2	2+1+2	<b>Corrective:</b> Use water spray, alcohol-resistant foam, dry chemical or carbon dioxide as extinguishing media. May intensify fire; oxidiser. Use water spray to cool unopened containers.

**Likelihood, e.g.:**

1. Minimal
2. Low
3. High
4. Very high

**Consequence, e.g.:**



1. Relatively safe
2. Dangerous
3. Critical
4. Very critical

**Risk value (each one to be estimated separately):**

**Human = Likelihood x Human Consequence**

**Environmental = Likelihood x Environmental consequence**

**Financial/material = Likelihood x Consequence for Economy/materiel**

NTNU	Appendix B: Risk assessment	Prepared by	Number	Date	
		HSE section	HMSRV-26/03	01.12.2006	
HSE/KS		Approved by	Page	Replaces	
	The Rector	6 out of 7	15.12.2003		

### Potential undesirable incident/strain



Identify possible incidents and conditions that may lead to situations that pose a hazard to people, the environment and any materiel/equipment involved.

### Criteria for the assessment of likelihood and consequence in relation to fieldwork

Each activity is assessed according to a worst-case scenario. Likelihood and consequence are to be assessed separately for each potential undesirable incident. Before starting on the quantification, the participants should agree what they understand by the assessment criteria:

<p>The likelihood of something going wrong is to be assessed according to the following criteria:</p> <ol style="list-style-type: none"> <li><b>1 Minimal</b> Once every 10 years or less</li> <li><b>2 Low</b> Once a year</li> <li><b>3 High</b> Once a month</li> <li><b>4 Very high</b> Once a week or more often</li> </ol>	<p><b>Human</b> consequence is to be assessed according to the following criteria:</p> <ol style="list-style-type: none"> <li><b>1 Relatively safe</b> Injury that does not involve absence from work; insignificant health risk</li> <li><b>2 Dangerous</b> Injury that involves absence from work; may produce acute sickness</li> <li><b>3 Critical</b> Permanent injury; may produce serious health damage/sickness</li> <li><b>4 Very critical</b> Injury that may produce fatality/ies</li> </ol>	<p><b>Environmental</b> consequences are assessed according to the following criteria:</p> <ol style="list-style-type: none"> <li><b>1 Relatively safe</b> Insignificant impact on the environment</li> <li><b>2 Dangerous</b> Possibility of undesirable long term effects; some cleanup is to be expected</li> <li><b>3 Critical</b> Undesirable long term effects; cleanup to be expected</li> <li><b>4 Very critical</b> Damaging to living organisms; irreversible impact on the environment; cleanup must be undertaken</li> </ol>
--	---	--



NTNU	Appendix B: Risk assessment	Prepared by	Number	Date	
		HSE section	HMSRV-26/03	01.12.2006	
HSE/KS		Approved by	Page	Replaces	
		The Rector	7 out of 7	15.12.2003	

The unit makes its own decision as to whether opting to fill in or not consequences for economy/materiel, for example if the unit is going to use particularly valuable equipment. It is up to the individual unit to choose the assessment criteria for this column.



### **Risk = Likelihood x Consequence**

Please calculate the risk value for “Human”, “Environment” and, if chosen, “Economy/materiel”, separately. For activities with a risk value of 16 or 12, or a single value of 4, safety measures (designed to both reduce the likelihood and to limit the consequences) must be documented with descriptions of measures and allocation of responsibility.

### **About the column “Comments/status, suggested preventative and corrective measures”:**

Measures can impact on both likelihood and consequences. Prioritise measures that can prevent the incident from occurring; in other words, likelihood-reducing measures are to be prioritised above greater emergency preparedness, i.e. consequence-reducing measures.



NTNU	Appendix C: HSE action plan	Prepared by	Number	Date	
		The HSE section	HMSRV-12/24	01.12.2006	
HSE		Approved by	Page	Replaces	
		The Rector	1 of 1	20.08.1999	

Unit: Ugelstad Laboratory \_\_\_\_\_

What	Measure	Unit responsible	Priority	Cost	Current status
(1) Divinylbenzene technical grade, 80% (handling and storage)	Safe storage of the substance. Availability of protective clothing.	Jordi Piella Bagaria	Human		OK
(2) Glycidyl methacrylate, 97% (handling and storage)	Safe storage of the substance. Availability of protective clothing.	Jordi Piella Bagaria	Human		Ok
(3) Styrene RegeantPlus, 99%>= (handling and storage)	Safe storage of the substance. Availability of protective clothing.	Jordi Piella Bagaria	Human		OK
(4) Ammonium persulfat (handling and storage)	Safe storage of the substance. Availability of protective clothing.	Jordi Piella Bagaria	Human		OK

Date: 15/02/11 \_\_\_\_\_ Line manager: Wilhelm Robert Glomm \_\_\_\_\_

